A MICROMECHANICAL APPROACH TO MODELING PARTLY

SATURATED SOILS

A Thesis

by

MARK JACKSON LAMBORN

Submitted to the Graduate College of
Texas A&M University
in partial fulfillment of the requirements for the degree of
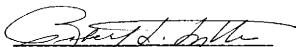
MASTER OF SCIENCE

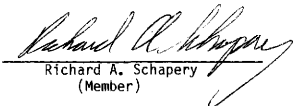December 1986

Major Subject: Civil Engineering

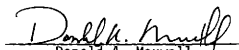A MICROMECHANICAL APPROACH TO MODELING PARTLY

SATURATED SOILS

A Thesis

by

MARK JACKSON LAMBORN

Approved as to style and content by:

_____   _____
      Robert L. Lytton   David Allen
    (Chair of Committee)   (Member)

_____   _____
      Richard A. Schapery   Donald A. Maxwell
         (Member)   (Head of Department)

December 1986

ABSTRACT

A Micromechanical Approach to Modeling

Partly Saturated Soils. (December 1986)

Mark Jackson Lamborn, A.A., Montgomery College;

B.S., Texas A&M University

Chairman of Advisory Committee: Dr. Robert L. Lytton

Constitutive equations are given which seek to represent the load-deformation behavior of soils. The soil is viewed as a two phase system. One phase represents the soil particles as a collection of equal spheres in contact. The other phase, representing an air-water mixture, is contained in the void space surrounding the equal spheres. Both phases are modeled as homogeneous, isotropic, linear elastic materials. The constitutive equations are developed through thermodynamic considerations and attempt to recognize actual deformation mechanisms which are present on the microscale. In their final form, the constitutive equations are in terms of material properties, particle size, degree of saturation, some dimensionless quantities, and the loads transmitted by the individual particles. The determination of the dimensionless quantities, required for the evaluation of the constitutive equations is discussed. Values for these dimensionless quantities are not available at present. Approximations for the loads transmitted by individual particles are given.

ACKNOWLEDGEMENTS

TABLE OF CONTENTS

LIST OF TABLES

LIST OF FIGURES

CHAPTER I

INTRODUCTION

BACKGROUND

Recently much work has been directed towards developing constitutive models to represent the complex load-deformation behavior of soils. The models developed to date have primarily been for the special cases of dry and completely saturated soils. The use of these constitutive models in representing the behavior of partly saturated soils has resulted in inaccurate predictions of soil response. It is the intent of this research to formulate a constitutive model describing the behavior of partly saturated soils.

There are essentially two approaches which have been used by those attempting to develop constitutive laws for soils. The first approach is termed phenomenological modeling. Phenominological models may be defined as those concerned with describing material behavior on the size scale of the experiment. For soils, thousands to millions of soil grains and pores would be included in a model representation of this type. Phenomenological methods or theories include empirical curve fitting, elastic theories, elastic-plastic theories, and viscoelastic theories. These methods and continuum theories are concerned with describing the overall observable behavior of the soil

---

The citations on these pages follow the style of the Journal of Geotechnical Engineering Division, ASCE.

mass. They are not concerned with describing the actual deformation mechanisms, which act on the level of the grains and pores which comprise the soil mass. The second type of approach is termed micromechanical modeling. This approach attempts to derive constitutive laws by considering the deformation mechanisms acting on a very small but representative sample of the material. For soils, a micromechanical model description might include one to hundreds of grains and pores in the model description.

The primary problem with constitutive models representing soils, is a failure to describe all aspects of their load-deformation behavior. While a model may give reasonable predictions under one set of input, it may fail to predict the soil response under another set of input. With the present knowledge it appears that a constitutive model representing all aspects of soil behavior may not be obtainable. This is due partly to a lack of understanding of the mechanisms causing soil deformation and partly due to the mathematical complexities one may encounter when modeling soils. A micromechanical approach to the constitutive modeling of soils may provide a better means to understand the soil load-deformation mechanisms.

SCOPE OF WORK

The purpose of the research studies contained in this report is to develop a constitutive model representing the load-deformation behavior of soils. The following types of investigations are contained in this report:

a) Review of the available literature on previously developed
   constitutive models describing the load-deformation behavior
   of soils.

b) Development of constitutive equations to represent the
   load-deformation behavior of partly saturated soils, under
   idealized conditions. The constitutive equations will be
   developed using a micromechanical approach, and will attempt
   to recognize some of the deformation mechanisms present on
   the microscale.

METHOD OF APPROACH AND ORGANIZATION

The studies undertaken to achieve the stated objectives are
described in the subsequent chapters.

Chapter II contains a brief description of experimentally observed
load-deformation behavior of soils and a review of the approaches
taken in the development of constitutive equations to describe this
behavior.

Chapter III reviews the development of constitutive equations to
predict the load-deformation behavior of an idealized partly saturated
soil system.

Chapter IV contains some simple examples of predicting soil
response with the newly developed constitutive equations for the
idealized partly saturated soil system.

Chapter V contains conclusions and recommendations.

CHAPTER II

PREVIOUS WORK

LOAD DEFORMATION BEHAVIOR OF SOILS

When a soil mass is subjected to any arbitrary set of surface
tractions, the result will be a volume deformation of the soil mass.
The resulting displacement and stress fields within the soil mass will
depend on a number of variables. These variables include the type of
loads applied, the stress history, and the chemical and physical
properties of the soil mass.

Experimental observations of the response of a soil mass to
various applied loads has provided a great deal of information
concerning the load-deformation behavior of soils. The information
provided by experimental work will be discussed briefly.

Shown in Figure 2.1 is a typical pressure vs. volumetric strain
curve. This curve would be obtained by performing a lab test on a
soil sample. The arrows appearing on the curve shown in Figure 2.1
indicate the load path taken. Initial loading of a soil mass results
in a state of stress within the soil, which the soil experiences for
the first time. In Figure 2.1, initial loading curves correspond to
those lying between points 1 and 5, and points 7 and 8. When the soil
particles are initially in a loose state, a small change in pressure
may result in a large volume deformation. This is due to grain
movement resulting in densification of the soil mass. Behavior of
this type is shown as that portion of the curve connecting points 1
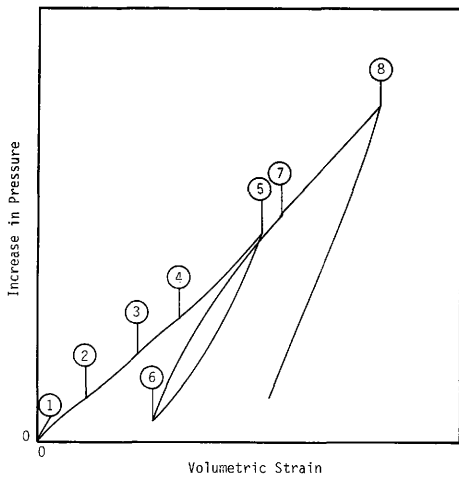
Figure 2.1. -- Pressure Versus Volumetric Strain Curve for a
Typical Soil.

and 2 in Figure 2.1. As the stress is increased past point 2 in
Figure 2.1, the soil will stiffen as repacking of the soil grains
continues. At some intermediate stress level the soil may again soften
as a result of fracturing and yielding of the soil grains. This
behavior is illustrated by the portion of the curve lying between
points 3 and 4 of Figure 2.1. As the soil mass is loaded past point 4
of Figure 2.1, the soil will stiffen. When the minimum void ratio is
reached, continued loading of the soil mass will result in failure.

When an applied load is removed from a soil mass, rebound will
normally occur resulting in an increase in soil volume. The stress
path taken by the soil mass during unloading will typically be
different from that taken for initial loading. A typical unloading
curve is shown in Figure 2.1 as that between points 5 and 6. It is
shown in Figure 2.1 that the stress occurring within the soil mass is
not a single valued function of strain. Instead the stress at a
particular value of strain may be multi-valued and its magnitude at a
particular time will depend on the load-deformation history of the
soil.

The term reloading refers to the addition of a load to the soil
mass which results in a stress state which the soil has previously
experienced. A typical reload curve is shown in Figure 2.1 as that
portion of the curve connecting points 6 and 7. When a soil
experiences an unload-reload cycle, there will in general be a volume
change associated with this cycle. As shown in Figure 2.1, the
unload-reload cycle begins at point 5 and ends at point 7. The volume

change which occurs during this cycle is proportional to the
difference in the volumetric strains corresponding to points 5 and 7.
When the reload path reaches point 7 of Figure 2.1, continued loading
will follow a path similar to that for initial loading.

Soils also exhibit interesting behavior when loaded in simple
shear. The behavior of soils when loaded in simple shear will depend
on the initial void ratio of the soil. When a soil of an initially
high void ratio is loaded in simple shear, a densification of the soil
will result. This decrease in volume is due to particle
rearrangement, yielding, and fracture. Densification continues with
increased loading until a minimum void ratio is reached. Upon
obtaining this minimum void ratio, continued loading will cause the
soil to fail, with a dilation of the soil mass usually associated with
failure. The dilation of the soil mass occurs because, in order for
the soil to fail, grains must ride over one another. Soils which
exhibit the behavior just described are loose granular materials and
normally consolidated clays. For soils of an initially low void
ratio, the application of a simple shear loading will result in
dilation of the soil mass. This is because the void ratio of the soil
mass will be near its minimum value and for deformation to take place,
the soil grains will have to slide over each other. Soils which show
this type of behavior are dense sands and overconsolidated clays.
Some typical stress-strain curves for different soils loaded in pure
shear are shown in Figure 2.2.
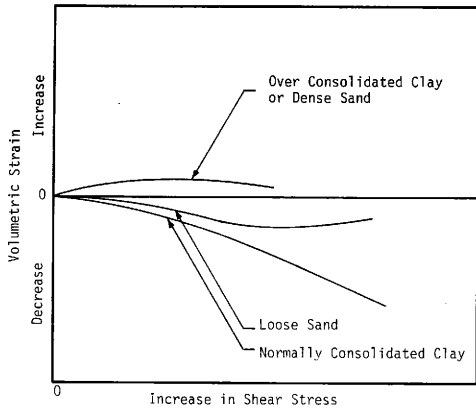
Figure 2.2. -- Volumetric Strain Versus Shear Stress Curves
for Some Typical Soils.

For some soils, the total deformation resulting from the application of a load will not occur instantaneously, but rather it will occur over a period of time. This type of deformation is referred to as consolidation and is found to occur in silts and clays. Theories which predict the amount and rate of consolidation usually consider the soil to be saturated. The common assumption is that when a load is applied to the soil, it is initially transferred to the liquid phase present in the pores of the soil mass. This results in an increase in the pore pressure so that steady-state conditions in the pores no longer exist. Over a period of time, steady-state conditions will be obtained, requiring a flow of the liquid from the pores. This causes a dissipation of the pore pressures until hydrostatic pressure is achieved. As the pressure is dissipated from the pores, the load will be transferred to the soil grains resulting in consolidation of the soil mass. The permeability of the soil controls the rate at which liquid may flow from the pores thus controlling the rate at which consolidation takes place. The behavior described above is termed primary consolidation and is shown in Figure 2.3.

Secondary consolidation, or creep is also shown in Figure 2.3. Secondary consolidation is defined as the deformation which takes place after the pore pressures have reached steady state conditions. Theories exist for the prediction of secondary consolidation but to date, none have found general acceptance.
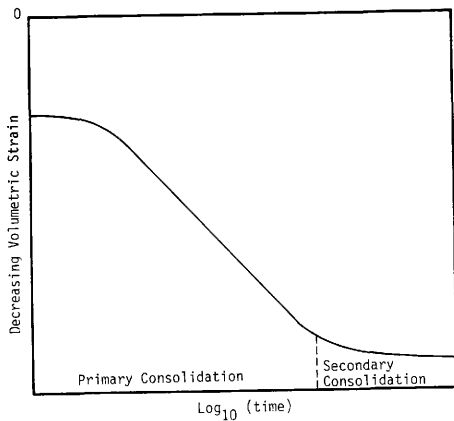
Figure 2.3. -- Volumetric Strain Versus Log_{10} (time) for a
Silt or Clay Under Constant Load.

CONSTITUTIVE MODELS REPRESENTING SOIL BEHAVIOR

Over the last two decades much work has been done to develop a constitutive model to represent the load-deformation behavior of soils. Thus far, most of these models are used to represent the behavior of dry or completely saturated soils. When these models have been used to represent the behavior of partly saturated soils, they yielded poor predictions of the soil response. However, these models are worthy of some attention, since they provide some insight to the approaches which have been taken to develop constitutive laws describing soil behavior.

The problem of developing a constitutive model for soils has followed one of two approaches. These two approaches are termed phenomenological and micromechanical modeling. The following subsections will discuss the soil models obtained from these two approaches.

Phenomenological Models

Phenomenological models may be defined as those concerned with describing behavior on the size scale of the experiment. These models treat the soil as a continuum including thousands to millions of soil grains and pores in the model representation. Phenomenological methods or theories include mathematical curve fitting, elasticity theory, plasticity theory, and viscoelasticity theory. Some soil

constitutive models developed from these methods or theories will be discussed.

    Empirical Models. A great many models representing soil behavior have been developed using empirical curve fitting methods. This approach entails making a mathematical fit to experimental data. In this manner the response of the soil due to some specific input may be predicted.

    Many workers have taken the empirical approach to model the pressure-volume behavior of soils. Herrmann (12) has taken such an approach in introducing the "P- " description. In this model, the pressure was assumed to be a function of the specific volume, internal energy, and the porosity of the soil. The relationship Herrmann proposed is

$$P = f \ (v/\alpha, u) \tag{2.1}$$

where

    P = the pressure,

    u = the specific internal energy,

    v = the specific volume of the soil, and

    α = the porosity.

The function f appearing in Equation 2.1 was assumed to be that which relates pressure and volume for the soil particles. Carrol and Holt

(4) proposed that it is more reasonable to represent the
pressure-volume relationship for soils by

$$P = \frac{1}{\alpha} \ f(v/\alpha, u) \tag{2.2}$$

When the pressure-volume relationship for the soil particles is known,
the problem reduces to determining the function

$$\alpha = g(P) \tag{2.3}$$

which gives the porosity as a function of pressure. The approach taken
for this model was to use the Mie-Gruneisen equation of state (4) to
relate the pressure to the specific internal energy and the specific
volume. This equation is given by

$$P = P_0 + (u-u_0) \ \frac{T_g}{v} \tag{2.4}$$

where

T_g = the Gruneisen ratio,

P_0 = a reference pressure, and

u_0 = a reference value of the specific internal energy.

A polynomial fit was then used to determine the function q.
Butkovich (3) developed a model relating the porosity to the applied
pressure. The expression that was obtained is given by

$$\frac{1}{\alpha} = \frac{1 - (1 - \frac{1}{\alpha_0}) \log_e (\frac{P}{P_c})}{\log_e (\frac{P_e}{P_c})} \qquad (2.5)$$

where

α_0 = the initial porosity,

P_c = the pressure required for pore closure to be complete, and

P_e = the pressure required for the onset of pore closure.

Equation 2.5 is applicable for pressures within the range between P_e and P_c. For pressure less than P_e, the soil is assumed to behave elastically. For pressures greater than P_c, the pressure-volume relationship for the matrix material is used. In Butkovich's work, the pressure-volume relationship for the matrix material is assumed to be given by soil unloading data. A polynominal fit to initial loading data is used to determine the pressure volume relationship for pressures lying between P_e and P_c. Other empirical models describing the pressure-volume relationship of soils have been developed, but the models cited above are representative of this work.

Other models have been developed which make mathematical fits to deviator stress-axial strain data, obtained from triaxial tests. The simplest model of this type is obtained by approximating the deviator stress versus axial strain curve by a series of piecewise linear curves. This type of approximation is shown in Figure 2.4. More sophisticated mathematical fits such as hyperbolas and cubic splines have been made to deviator stress versus axial strain data. The most
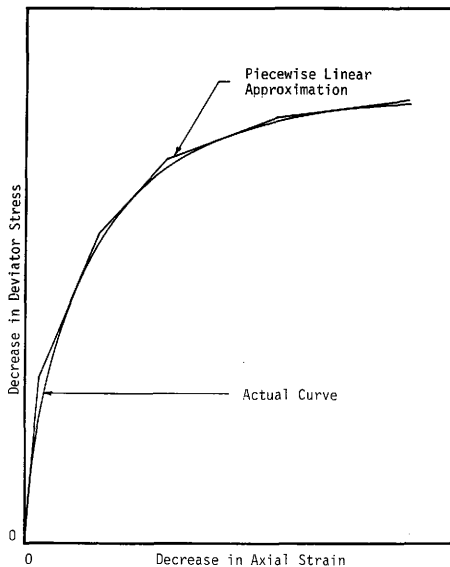
Figure 2.4. -- Piecewise Linear Approximation of Deviator Stress Versus Axial Strain Curve Obtained from Triaxial Test.

popular of these methods has been the hyperbolic stress-strain model
used in finite element representations of soil by Duncan and Chang
(8). This model is based on the discovery that the deviator stress
versus axial strain curves for a number of soils could be approximated
with sufficient accuracy by hyperbolas like that shown in Figure 2.5.
This hyperbola may be represented by

$$(\sigma_{11}-\sigma_{33}) = \frac{\varepsilon_{11}}{\frac{1}{E_i} + \frac{1}{(\sigma_{11} - \sigma_{33})_{ult}}} \qquad (2.6)$$

where

$(\sigma_{11}-\sigma_{33})$ = the deviator stress,

ε_{11} = the axial strain, and

E_i = the initial tangent modulus.

Equation 2.6 is the basis of the hyperbolic stress-strain model.
Other empirical relations are used to account for the variation in
soil stiffness strength with depth and different modulus values for
loading and unloading. Because of these relationships, the hyperbolic
model requires a large number of parameters for its use.

There are some basic problems associated with soil models
developed from empirical methods. First, an empirical model cannot be
expected to provide reasonable predictions of soil behavior when the
soil and–site conditions being modeled deviate greatly from those used
to calibrate the model. Second, this type of model cannot be expected
to provide any insight as to the actual physical deformation
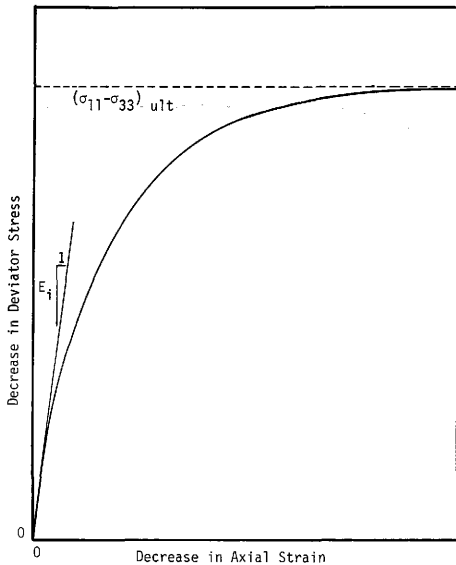
Figure 2.5. -- Hyperbolic Approximation of Deviator Stress Versus
Axial Strain Curve Obtained From Triaxial Test.

mechanisms acting within the soil mass. Despite these shortcomings, empirical models are frequently used due to their simplicity.

   Nonlinear Elastic Models. Some models representing soil behavior have been developed using non-linear elasticity theories. These theories have not found widespread use since their predictions of unload behavior will not represent actual soil behavior. For cases where initial loading is of interest, nonlinear elasticity theories may provide reasonable predictions of soil response.

   Hyperelastic constitutive laws have been used to represent soil behavior. These models employ constitutive laws obtained by the differentiation of a strain energy function. Different orders of hyperelastic models are obtained by retaining the higher order derivatives obtained from the strain energy function.

   Truesdell (30) has proposed a rate theory which states that the rate of change of stress is a function of the rate of change of strain. This is known as the hypoelastic formulation. At present this formulation has not found much use in representing the load-deformation behavior of soils.

   Elastic-Plastic Models. The use of elastic-plastic continuum theory has found widespread use in soil modeling. Recently, many constitutive models for soils have been presented which use these theories. Generally this type of model assumes a yield criterion of the form

$$F(\sigma_{ij}, \varepsilon^P_{ij}, \chi) = 0 \qquad\qquad (2.7)$$

in which σ_{ij} and ε_{ij}^{p} (i,j = 1,2,3) are the components of the stress

and plastic strain tensors, respectively, referred to an orthogonal

set of Cartesian axes (x_i), and χ is a work hardening parameter.

When the above equation is not satisfied $[F (\sigma_{ij}, \varepsilon_{ij}^{p}, \chi) < 0]$,

the material is said to behave elastically. When Equation 2.7 is

satisfied, the behavior is said to be elastic-plastic. Deformation

when Equation 2.7 is satisfied occurs as a combination of elastic and

plastic strains, prescribed by an assumed flow rule. The yield

surface is typically described in principal stress space as shown in

Figure 2.6. The area contained by the yield surface is the region of

elastic behavior. For a known stress point inside this region, the

strains are found using elastic constitutive laws. When the stress

point lies on the yield surface, the total strain is a combination of

elastic and plastic strains. For a stress point lying on the yield

surface, further loading may cause the surface to expand, translate,

or both according to the work hardening rule assumed. Unloading may

be elastic, or elastic-plastic.

A well known elastic-plastic soil model is that developed by

Schofield and Wroth (26), and has been termed "Cam-clay." This model

accounts for the volume deformation and strain-hardening of soils.

The basis of their model is an incremental flow rule which balances

the irreversible work occurring during deformation against a mechanism

for the frictional loss. Their flow rule is
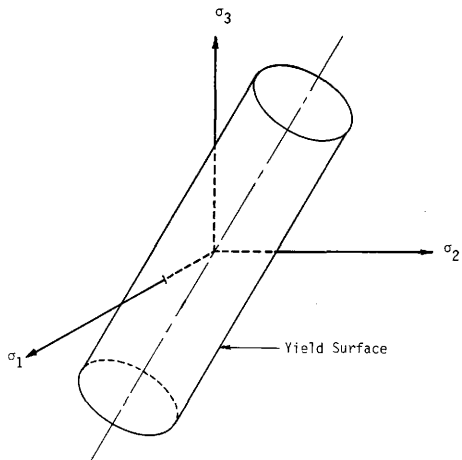
Figure 2.6. -- Typical Yield Surface in Principal Stress Space.

$$\overline{\tau} \, \Delta\overline{\gamma}^P - P(\frac{\Delta v}{v})^P = k_f \, P |\Delta\gamma^P|$$

(2.8)

where

P = pressure,

V = volume,

k_f = friction parameter, and

$\overline{\tau}\,\overline{\gamma}$ = measures of shear stress and shear strain, respectively.

In Equation 2.8 the superscript, P, denotes plastic portions of the quantities indicated.

The elastic volume deformation during hydrostatic deformation is given by

$$\Delta(\frac{V}{V_s})^e = -A_1 \, \frac{\Delta P}{P}$$

(2.9)

where

V_s = the volume of solids contained in the soil,

A_1 = a constant, and

the superscript e is used to denote the elastic portion of the quantity indicated. As yielding takes place, the total volume change is

$$\Delta(\frac{V}{V_s}) = -A_2 \, \frac{\Delta P}{P}$$

(2.10)

where A_2 is a constant. The assumption of an associated flow rule
gives the following equation of the yield surface.

$$\frac{\overline{\tau}}{k_f p} = \log_e \left(\frac{P*}{P}\right) \qquad (2.11)$$

Here $P*$ is the intercept of the yield surface with the P axis as shown
in Figure 2.7. An important assumption of the "Cam-clay" model is
that the plastic volume deformation during non-hydrostatic stress
states is the same as for hydrostatic, but with the P replaced by $P*$.
Thus the plastic volume deformation is given by

$$\Delta\left(\frac{V}{V_s}\right)^P = -(A_2 - A_1)\frac{\Delta P*}{P*} \qquad (2.12)$$

The Equations 2.8, 2.9 and 2.10 form a system of equations from
which strain increments may be determined from stress increments, or
vice versa. The constants A_1 and A_2 are determined experimentally.
Hydrostatic loading corresponds to a movement along the P axis shown
in Figure 2.7. When yielding occurs, a non-hydrostatic loading will
cause the yield surface to change in accordance with Equation 2.8.
Movement of the yield surface is shown in Figure 2.7. The critical
state line is shown in Figure 2.7 as the line connecting points of
zero slope for all possible yield surfaces. This separates yielding
into densification and dilation. Densification with strain hardening
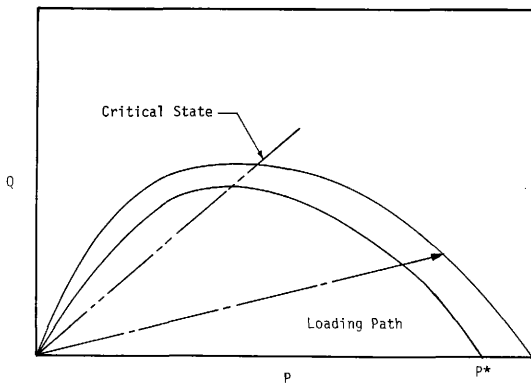
Figure 2.7 -- Typical Yield Surfaces for "Cam Clay" Model.

occurs to the right of the critical state line while dilation with strain softening occurs to the left.

The "Cam-clay" model has proved useful in representing soil behavior. However, in this model, elastic shear stresses and soil cohesion are completely neglected. The assumption of an associated flow rule is also made. This assumption results in a plastic strain vector normal to the yield surface. Works such as Mandl and Luque (17) and Frydman, et al. (9) have shown that normality of plastic flow is neither a mathematical necessity nor supported by experimental evidence. The "Cam-clay" model predicts no non-recoverable deformations for hydrostatic loadings. This is not representative of soils. Unloading is elastic, which is not descriptive of actual soil behavior.

Sandler and Baron (21) have introduced the "cap" model to describe the behavior of soils. This model is based on a classical plasticity model, defined by a yield surface and a strain rate vector. The yield surface of this model is shown in Figure 2.8. Inspection of this yield surface shows that three modes of soil behavior are possible. These being elastic, failure, and cap behavior. Elastic behavior occurs when the stress point lies in the region contained by the coordinate axes, the failure envelope, and the cap surface. The behavior in this region is considered to be linearly elastic. The failure mode of behavior occurs when the stress point lies on the failure envelope. The failure envelope is assumed to be fixed. The equation of the failure envelope is
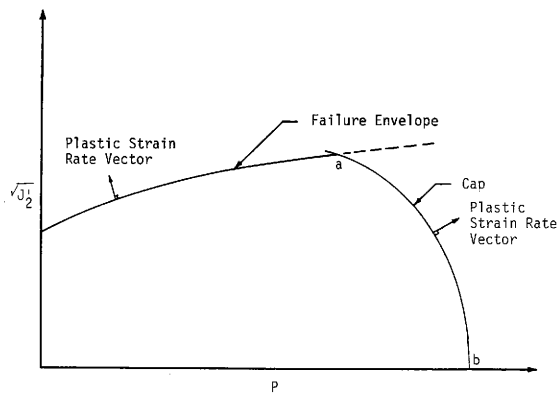
Figure 2.8. -- Yield Surface for "Cap" Model.

$$\sqrt{J_2'} = B_1 - B_2 \exp(-3 B_3 P)$$

(2.13)

where

J_2' = the second invariant of the deviatoric stress tensor,

and

B_1, B_2, B_3 = material constants.

The model assumes an associated flow rule so that the plastic strain during the failure mode of behavior is composed of a shear component and a dilatant component. The cap mode of behavior occurs when the stress point lies on the cap surface, and moves it outward. The motion of the cap is related to the plastic strain by a hardening rule. The equation for the cap surface is

$$(P - Pa) + \frac{1}{9} B_4 I_1 J_2' = (P_b - P_a)^2$$

(2.14)

where

I_1 = the first invariant of the stress tensor,

B_4 = a constant, and

P_a, P_b = the pressures at points a and b of Figure 2.8, respectively.

The cap is related to the strain history of the material through a strain hardening rule given by

$$\bar{\varepsilon}\, _y^P = B_5\, (1 - \exp\, (-3\, B_6\, P_b))$$

$$(2.15)$$

where

B₅ and B₆ are material constants.

Here $\bar{\varepsilon}\, _y^P$ is related to the past strain history of the soil in the following manner. When the stress point lies on either the failure envelope or the cap surface, the value of $\bar{\varepsilon}\, _y^P$ changes exactly as the plastic volumetric strain. For a stress point on the cap surface, the plastic strain rate vector will be directed as shown in Figure 2.8. The position of the plastic strain rate vector implies that it consists of an irreversible decrease in volume in conjunction with an irreversible shear strain. This decrease in volume represents volumetric hysteresis observed in soil during compaction. As the cap moves outward, the compaction resulting from the associated flow will lead to an increase in the cap parameter $\bar{\varepsilon}\, _y^P$. By Equation 2.15 this leads to an increase in P_b, resulting in a movement of the cap to the right. When the stress point lies on the failure surface, the plastic strain rate vector will be directed upwards and to the left as shown in Figure 2.8. The plastic strain rate vector indicates an increase in volume associated with the movement along the failure surface. The dilatancy will lead to a decrease in the cap parameter $\bar{\varepsilon}_y^P$ resulting in a leftward movement of the cap by Equation 2.15. The backward

movement of the cap is limited to the point where it intersects the stress point lying on the failure surface.

The soil model just described is the basic cap model. Modifications to this basic cap model have been made to include viscous damping and strain hardening. The viscous cap model is used to represent materials which exhibit hystersis during cyclic loading. This model was formulated by introducing linear viscous damping into the elastic portion of the cap model. This model is shown in Figure 2.9. The parameters which define the non-plastic portion of the model are an instantaneous modulus G_f, a long term modulus G_s, and a relaxation time t_r. The parameters G_s and t_r are related to those shown in Figure 2.9 by

$$G_s = \frac{G_f G_v}{G_f + G_v}$$ (2.16)

$$t_r = \frac{\mu_d (G_f - G_s)}{G_f^2}$$ (2.17)

where

G_v, G_f = the spring moduli for the model appearing in Figure 2.9, and

μ_d = a damping constant.

The deviatoric stress-strain relationship for the viscous cap model is

$$\overset{\circ}{s}_{ij} = 2G_f \; \overset{\circ}{e}_{ij}^v + \frac{2G_s \; e_{ij}^v - s_{ij}}{t_r}$$ (2.18)
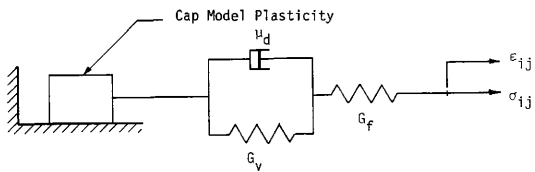
Figure 2.9. -- Viscous Cap Model.

where

s_{ij}, e_{ij}^v = components of the deviatoric stress tensor and viscoelastic deviatoric strain tensor, respectively.

$\overset{\circ}{s}_{ij}$, $\overset{v}{e}_{ij}$ = rate of change of the components of the deviatoric stress tensor and viscoelastic deviatoric strain tensor, respectively.

The parameters G_f, G_s, and t_r appearing in the viscous cap model are determined from cyclic triaxial data.

A kinematically hardening failure envelope has been added to the basic cap model by replacing the stress tensor σ_{ij} by $(\sigma_{ij} - \alpha_{ij})$. Here α_{ij} is a tensor whose components are memory parameters defining the translation of the failure surface in stress space. In the model it is assumed that kinematic hardening occurs only in shear, yielding the relation

$$\alpha_{kk} = 0 \qquad\qquad (2.19)$$

In Equation 2.19 and henceforth, a repeated index implies summation unless otherwise indicated.

The kinematic hardening rule which governs the memory parameters α_{ij} is of the form

$$\alpha_{ij} = f_{ijkl} (\sigma_{ij}, \alpha_{ij}, \chi, \varepsilon_{ij}) \dot{e}_{kl}^p \qquad\qquad (2.20)$$

where e^P_{ij} are the components of the deviatoric plastic strain tensor.

In order to represent the non-linear behavior of soils at or near failure, it is necessary to assume a non-linear hardening rule. A simple rule of this type which gives reasonable behavior at all stress levels is

$$\alpha_{ij} = C_\alpha F_\alpha e^P_{ij} \qquad (2.21)$$

where

$$F_\alpha = \text{maximum} \left[0, \ 1 - \frac{(\sigma_{ij} - \alpha_{ij})\alpha_{ij}}{2 N_y(\sqrt{J'_2} - N_y)}\right] \qquad (2.22)$$

and

C_α = a constant,

N_y = a constant defining the size of the yield surface, and

J'_2 = is given by Equation 2.13.

Here F_α is related to the proximity of the yield surface to the failure surface, and the location of the stress point of the yield surface. For $\alpha_{ij} = 0$, F_α will be equal to 1.0. Therefore from Equation 2.21 it is found that C_α is the inelastic slope for the initial yielding of the material in shear. F_α will decrease for continued yielding and is equal to zero when the stress point reaches

the failure surface. Upon unloading from the failure surface, the value of F_α will increase, reaching a value of 2 upon reyielding.

As a final note, the cap model has been modified to represent the behavior of saturated soils using the effective stress approach. This modification is straightforward and is achieved by replacing the stress tensor, σ_{ij}, by the effective stress, σ'_{ij}. The effective stress tensor is determined as

$$\sigma'_{ij} = \sigma_{ij} - P_w \delta_{ij} \qquad (2.23)$$

in which P_w is the pore water pressure, and δ_{ij} is the Kronecker delta.

Although the cap model has been used successfully to model several soils, there are some difficulties associated with it. A major problem is that a large number of parameters must be determined from experimental data and their determination may require special tests. Another problem is the assumption of an associated flow rule. This assumption is not necessarily correct for soils.

Other elastic-plastic constitutive models for soils have been developed. The models may use different yield surfaces or a non-associated flow rule, but the methodology used to formulate these models is the same as those already described.

Viscoelastic Models. Soils exhibit viscoelastic behavior in that the response of a soil to some specific input is dependent on the

entire past history of input to the soil system. Viscoelastic theory can be used to include rate and history effects in soil constitutive models.

Nonlinear viscoelastic theory was used by Schapery and Riggins (23) in the development of cyclic constitutive equations for marine sediment. Only simple shear of the marine sediment was considered. The shear strain, ε_{12}, was assumed to be related to the shear stress, a_{12}, through a modified superposition integral given by

$$\varepsilon_{12} = G_R \int_0^t J(t-s) \frac{df}{ds} \, ds \qquad (2.24)$$

where

$$f = f(\sigma_{12}, S_d) \qquad (2.25)$$

G_R = an arbritary constant,

J = the linear viscoelastic creep compliance,

S_d = a damage parameter, and

t = time.

The damage parameter, S_d, is used to account for the effect of damage growth in the marine sediment. The damage parameter, S_d, depends on stress history. One form derived by Schapery (22) is

$$S_d = \int_0^t \left| \sigma_{12} \right|^q f_1 \, dt' \qquad (2.26)$$

in which q is a positive constant, and the coefficient f_1 comes from
the expression

$$\overset{\circ}{a} = cf_1|\sigma_{12}|^q \tag{2.27}$$

where $\overset{\circ}{a}$ is the damage growth rate and c is a positive constant. The
term f_1 is positive and serves to define the ease at which defects
will grow at a certain stress level. Predictions of the response of
marine sediments undergoing simple shear were made using this theory.
It was reported that the theory predicted the essential
characteristics of the soil data under monotonic and periodic
straining.

Micromechanical Models

Mechanistic modeling of soils has been approached from two
different viewpoints. One approach has been to treat the soil as an
assembleage of particles in contact as shown in Figure 2.10. The
particles within a soil mass are random in shape and size and to use
this approach some assumptions as to size and shape must usually be
made. Once a model representing the soil mass has been chosen, the
solution consists of representing the deformed geometry of the
particles in contact. The other approach to mechanistic modeling has
been to consider the soil to be composed of a matrix material
containing voids as shown in Figure 2.11. Here a solution to the
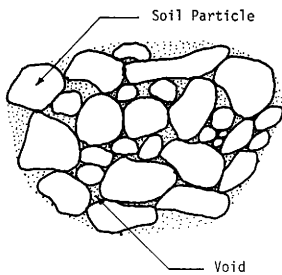
Figure 2.10. -- Soil Viewed as an Assemblage of Particles in Contact.
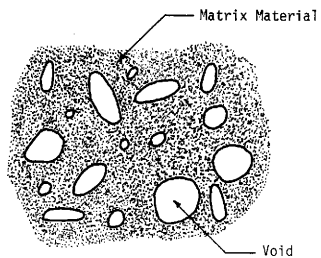
Figure 2.11. -- Soil Viewed as a Collection of Voids Contained in a Matrix Material.

problem consists of modeling the deformation of the voids contained in the matrix material.

Mechanistic models have been formulated on two scales. One scale has been intermediate to that of the experiment and the grains and pores within the soil mass. While this scale may be very small compared to the scale of the experiment, it may be quite large in comparison to the size scale of the grains and pores. On this size scale the use of phenomenological theories may be necessary. This is because the behavior observed on this level may be that of many grains and pores and may best be described by the use of a phenomenological theory. The other scale which is used in mechanistic modeling is termed the micro-scale. On this level, models are formulated at the size scale of the grains and pores, and are concerned with describing the actual deformation mechanisms present at this level.

The void deformation models have been formulated using both the intermediate and micro size scales. Modeling of objects in contact has usually been done on the microscale.

Contact Models. When a mass composed of a number of particles in contact is subjected to an externally applied load, the deformation resulting from the load is due to grain movement and grain deformation. The movement of the grains will be controlled by interparticle friction, cohesion between adjacent particles, and the initial porosity of the mass. The grain deformation will be greatest at areas of contact between adjacent grains, and may be elastic or elastic-plastic, depending on the stress level present in the grains.

In addition to that already mentioned, the grains may fracture thus increasing the number and shape of grains, and the number of contacts.

Models seeking to describe this behavior usually consider the soil grains to be spherical in shape. The load-deformation behavior of the spheres themselves is considered to be that of an elastic material. Further simplifications are obtained by neglecting friction, cohesion, and tangential forces acting on the contacts between grains. With all these simplifications, a logical step is to use Hertzian contact theory by which the movement of adjacent spheres relative to one another may be determined. Consider the two spheres in contact as shown in Figure 2.12. The x axis is positioned at the centerline of the contact. The solid lines represent the deformed configuration of the spheres while the dashed line represents the undeformed spheres. From Hertzian contact theory, the deformation along the centerline of contact for each sphere is given by

$$u_3^1 = \frac{3\pi(1-\nu_1^2)F_c}{8R_cE_1} \qquad\qquad (2.28a)$$

$$u_3^2 = \frac{3\pi(1-\nu_2^2)F_c}{8R_cE_2} \qquad\qquad (2.28b)$$

where

u_3 = the centerline displacement along the x_3 axis,

ν = Poisson's ratio,

E = Young's modulus,
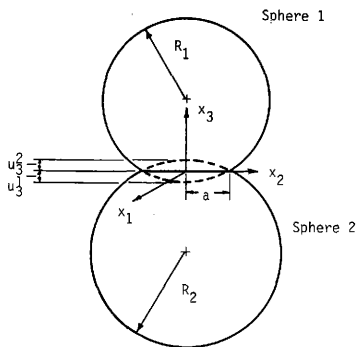
Figure 2.12. -- Geometry Considered in Hertz Problem
of Contact Between Two Spheres.

R_c = the radius of the contact surface, and

F_c = the force transmitted across the contact.

The superscripts appearing on the displacement components and the subscripts on the Poisson's ratio and Young's moduli are used to denote quantities for spheres 1 and 2. The radius of the contact area between the spheres is given by

$$R_c = \left[\frac{3\pi}{4} \ P \ \frac{R_1 R_2}{R_1 + R_2} \left(\frac{(1-\nu_1^2)}{E_1} + \frac{(1-\nu_2^2)}{E_2} \right) \right]^{1/3} \qquad (2.29)$$

where R_1 and R_2 are the radii of spheres 1 and 2, respectively.

Using Equations 2.28 and 2.29, the deformation of an assemblage of spheres may be determined when the force transmitted across each contact is known. Ko and Scott (14) have solved this problem for assemblies of spheres in ideal packing configurations, under conditions of hydrostatic loading. Here all the spheres were considered to have equal radii and the same material properties. They solved this problem for simple cubic (sc) and face centered cubic (fcc) packing configurations. Their solution is

$$\frac{\Delta V}{V} = 3 \left[\frac{3 \ c_p \ (1-\nu^2) \ P}{E} \right]^{2/3} \qquad (2.30)$$

where c_p is a constant equal to 1 for sc packing and equal to $1/\sqrt{2}$ for fcc packing.

As seen from Equation 2.30, the term c_p accounts for the initial density of the mass giving smaller volumetric strains for the denser packing configuration. However, this model predicts larger than actual deformations for the sc configuration while predicting smaller than actual deformations for the fcc packing configuration. To correct this, Ko and Scott used a combination of sc and fcc blocks to achieve the initial porosity of the soil. By assuming a distribution of grain contact pressures and an effective contact radius, they generated pressure-volume relationships for sands of three initial porosities. The results they obtained are shown in Figure 2.13 along with the limiting cases of sc and fcc packing configurations. A major shortcoming of Ko and Scott's model is that it is elastic and the path the soil takes during unloading will be the same as that for loading. Because of this fact, this model is incapable of accurately representing the load-deformation behavior of soils. Warren and Anderson (31) have formulated a contact model in which initially some of the spheres are not in contact. The pressure-volume relationship they obtained is

$$\frac{\Delta V}{V} = 3 \left[\left(\frac{Ng}{Nc} \right)^2 \frac{3 \ (1-\nu^2) \ P}{E} \right]^{2/3} \tag{2.31}$$
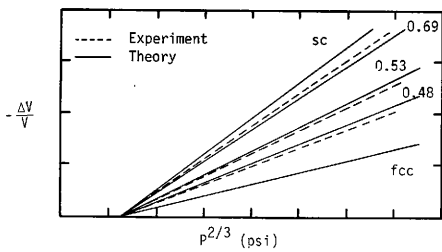
Figure 2.13. -- Pressure-Volume Relationships for
Sands of Different Initial Porosities.

where

    N_g = the number of grains in a typical cross section, and

    N_c = the number of contacts transmitting force across a

        typical cross section.

    Initially all the grains are not in contact. As loading

progresses, more grains come into contact. At some critical pressure,

all grains make contact thus approaching a fcc packing configuration.

It is apparent from Equation 2.31 that as the number of contacts is

increased, the amount of volume deformation resulting from an increase

in pressure, will decrease. The model will predict unloading along a

path different from that of loading as long as the grains were not all

initially in contact. The difficulty with this model is the

determination of the value of N_c. The variation in the value of N_c

which occurs during loading, corresponds to the rigid body motion of

the particles within the soil mass. This model does not attempt to

describe the actual grain motion within the soil mass but rather the

variation in the parameter N_c would have to be chosen so as to fit

experimental data.

    Some models of granular media include friction of the contacts

between grains. Rowe (20) has considered the shearing of various

assemblages of spheres. Using a minimum energy criterion, he arrived

at the stress-dilatancy equation

$$\frac{\sigma_1}{\sigma_3} = \left(\frac{1 + \epsilon_{kk}}{\Delta\epsilon_1}\right) \tan \left(45° + \frac{\phi u}{2}\right)$$

(2.32)

where

σ_1 = the maximum principal stress,

σ_3 = the minimum principal stress,

ϵ_1 = the maximum principal strain, and

ϕ_u = the undrained angle of shearing resistance.

The above equation holds only for the case when the intermediate principal stress is equal to the least principal stress. Rowe states that the angle ϕ_u must be replaced by an effective angle of shearing resistance, ϕ_u', to match experimental data. Test conditions may be created so that many values of the undrained angle of shearing resistance, ϕ_u, may be obtained for the same soil sample. However, with pore pressure measurements during the test, the value of the effective angle of shearing resistance may be determined. This value has been found not to vary with test conditions. Equation 2.32 does not account for compaction during non-hydrostatic loading. Therefore, it is not general enough to adequately represent actual soil behavior. Barden, et al. (1) used Equation 2.32 to formulate a plastic flow rule and a set of yield surfaces. They tested the behavior of sand in plane strain and found that the yield criterion and plastic potential did not coincide. This implies non-associativity of flow. However, it was found that the volumetric strain was suitably predicted by this

model. Nemat-Nasser (18) formulated a model to represent the behavior
of granular material undergoing shear loading. This model is found to
model dilation as well as densification which occurs during shear.
This is done by defining the dilatancy angle $\hat{\phi}$. The dilatancy angle
defines the position of a microscopic shear plane, as shown in Figure
2.14. In this model it is assumed that the actual shearing takes
place on many microscopic shear planes rather than on one macroscopic
shear plane. From Figure 2.14 it is clear that positive value of the
dilatancy angle corresponds to an upward movement of the grains along
the microscopic shear plane thus representing dilation. A negative
value of the dilatancy angle will therefore represent densification.
To formulate the model, Nemat-Nasser considers a sample of soil for
which failure takes place along one microscopic shear plane.

   The relationship between the shear and normal stresses acting on
the macroscopic and microscopic shear planes was assumed to be that of
a Mohr-Coulomb material with no cohesion. These relationships are

$$\bar{\tau} = \bar{\sigma} \ \tan \bar{\phi} \tag{2.33a}$$

$$\tau^* = \ \sigma^* \tan \phi^* \tag{2.33b}$$

where

   $\bar{\tau}$ = the shear stress acting on the macroscopic shear plane,
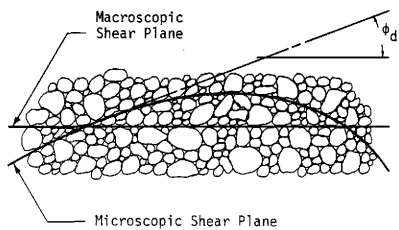
Figure 2.14. -- Relationship Between Macroscopic Shear Plane,
Microscopic Shear Plane, and the Dilatancy
Angle, ϕ_d.

$\overline{\sigma}$ = the normal stress acting on the macroscopic shear plane,

$\overline{\phi}$ = the angle of shearing resistance for the macroscopic shear plane,

τ^* = the shear stress acting on the microscopic shear plane,

σ^* = the normal stress acting on the microscopic shear plane, and

ϕ^* = the angle of shearing resistance for the microscopic shear plane.

$$F^* = \frac{\overline{F} \tan \phi^* (\cos(\overline{\phi}-\phi^*))}{\sin\overline{\phi}} \qquad (2.34a)$$

$$\tan \phi^* = \tan (\overline{\phi}-\phi) \qquad (2.34b)$$

where

F^* = the frictional force acting on the microscopic shear plane, and

$\overline{F}$ = the total shear force acting on the macroscopic sample.

The rate of energy dissipation per unit volume, which occurs as slippage takes place along a microscopic shear plane is

$$\overset{\circ}{W} = \frac{\overline{\tau} \tan \phi^* \cos(\overline{\phi}-\hat{\phi})}{\sin\overline{\phi} \sin\hat{\phi}} \frac{\overset{\circ}{V}}{V} \qquad (2.35)$$

$\overset{\circ}{W}$ = the rate of energy dissipation per unit volume;

$\overset{\circ}{V}$ = rate of volume change.

The following approximations were made concerning $\overset{\circ}{W}$

$$\overset{\circ}{W} = \overset{\circ}{W}' + \overset{\circ}{W}''$$ (2.36a)

$$W' = \overset{-}{\tau}\,\overset{\circ}{\gamma}$$ (2.36b)

$$\overset{\circ}{W}'' = \frac{\overset{-}{\tau}}{\sin\overline{\phi}\,\cos\overline{\phi}}\,\frac{\overset{\circ}{V}}{V}$$ (2.36c)

where $\overset{\circ}{\gamma}$ is the rate of shear deformation on the macroscopic sample.
Combining Equation 2.36 with Equation 2.35 yields the following
equation for the microscopic shear plane i.

$$\frac{1}{V_i}\frac{\overset{\circ}{V}_i}{\overset{\circ}{\gamma}} = \frac{\cos(\phi* + \hat{\phi})\,\sin\hat{\phi}}{\cos\,\phi*}$$ (2.37)

The volume fraction, V_i, of the family of particles having a
dilatancy angle, $\hat{\phi}_i$, is defined by

$$p_i'\,(\hat{\phi}) = \frac{V_i}{V}$$ (2.38)

where p_i is the volume fraction of family of particles having
dilatancy angle ϕ_i. The restriction on p_i is the following

$$\int_{\hat{\phi}-}^{\hat{\phi}+} p_i(s)ds = 1$$ (2.39)

In Equation 2.39, $\hat{\phi}+$ and $\hat{\phi}-$ form the range of variation of the

dilatancy angle ϕ. Using Equations 2.38 and 2.39 in Equation 2.37,

Nemat-Nasser arrives at the final result.

$$\frac{1}{V}\overset{\circ}{\frac{V}{\overset{\circ}{V}}} = \cos\phi^* \int\limits_{\hat{\phi}-}^{\hat{\phi}+} p(s) \cos(\phi^*+s) \sin(s) \, ds \qquad (2.40)$$

Equation 2.40 contains all experimentally observed behavior of

granular material in simple shear. However, the accuracy of the

predictions made by Equation 2.40 will depend on the chosen form of

the distribution function, $p(\hat{\phi})$. This distribution function may be

very difficult to determine for an actual soil sample. Another

shortcoming of this model is that the individual particles within the

sample mass are considered to be rigid. Wilkins (31) has taken a

somewhat different approach to develop a theory for the shear strength

of a granular medium. He used an empirical curve fitting method and

Rowes Equation 2.32 to predict the number of unstable contacts in a

granular assemblage as a function of the stress ratio. According to

this approach, when all the contacts on a grain become unstable, the

grain is no longer considered to contribute to the system and it

effectively becomes a void. When the number of voids not supporting

any stresses is equal in number to the particles which continue to

carry loads, the medium is assumed to fail. Although this attempt is

interesting, it becomes unattractive due to its empirical nature.

Volume changes and stress-strain relations are neglected in Wilkin's formulation.

Other contact models have been developed for which the plastic flow of the bodies in contact was considered to be important. Kakar and Chaklader (13) have solved this problem for spheres in a variety of packing configurations. In this model it is assumed that the particle surfaces which are not in contact remain spherical. They solved this problem for the case of a simple cubic packing. Assumptions made were that the volume of the spheres remains constant, the contacts transmit the load applied to the assembly, and that the material near the contact is in a state of uniaxial stress. The material of the contacts was allowed to yield until the stress developed at the contacts was balanced by the applied pressure. The relationship that Kakar and Chaklader obtained is

$$\frac{\Delta V}{V} = 3\left[\frac{6P}{\pi Y}\right] - 2\left[\frac{4P}{\pi Y} + 1\right]^{3/2} - 1 \qquad (2.41)$$

where Y = a yield parameter.

Equation 2.41 is valid until the contact areas touch thus forming a new geometry. Figure 2.15 shows the results obtained from this model along with those obtained from a Hertzian contact model for a simple cubic packing configuration. Figure 2.15 shows that the yielding model predicts larger strains for a given load than that obtained from the elastic Hertzian contact model. The actual
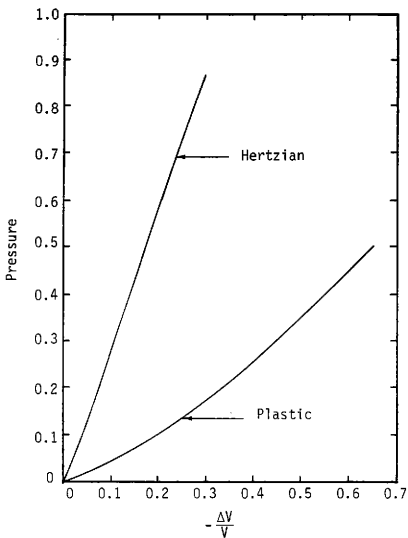
Figure 2.15. -- Results of Plastic Contact Model of Soils.

stress-strain curve will likely fall in between those shown since not all points within a sphere will yield at once. The actual behavior will be stiffer than that predicted by the complete yielding model as formulated by Kakar and Chaklader.

Void Deformation Models. One approach to modeling soils has been to consider the soil as a mass composed of a matrix material and voids. The deformation resulting from the application of loads to a material of this type will depend on the materials making up the matrix and voids, the size and shape of the voids, and the volume fraction of the voids. A common assumption in using this approach to model soils is that the voids are either spherical or flat in shape. O'Connel and Budiansky (19) have considered the effect that flat cracks would have on the moduli of a material. The equation they obtained for the bulk modulus of such a material is

$$\frac{K}{K_m} = 1 - \frac{16}{9} \left(\frac{1-\nu^2}{1-2\nu} \right) d \qquad (2.42a)$$

$$\nu = \nu_m \left[1 - \frac{16}{9} d \right] \qquad (2.42b)$$

$$d = \frac{1}{V} \Sigma a^3 \qquad (2.42c)$$

where

    K = the bulk modulus of the material,

    d = the crack density, and

    a = the crack length.

The subscript m appearing in Equations 2.42 is used to denote matrix
properties.

Equations 2.42 were developed by considering the cracks to contain
only air. Equations 2.42 indicate that a sufficiently large crack
density would have a considerable effect on the material properties,
while the cracks themselves may be of negligible volume. As the
pressure is increased on such a material, the cracks would close and
their effect would disappear.

Other workers have considered the effects of spherical voids on
material behavior. MacKenzie (16) has determined the effective bulk
modulus for a material represented by a matrix containing spherical
voids. Henceforth the term effective will be used to precede material
properties which are descriptive of the entire mass being considered.
The geometry which MacKenzie considers is shown in Figure 2.16. The
porous material is modeled as a collection of spheres of matrix
material, each containing a spherical void. Under this geometrical
assumption, the problem reduces to that of determining the solution
for one of these composite spheres with a uniform radial pressure
acting on its boundary. The term composite refers to the material
composed of both matrix and voids. The expression MacKenzie obtained
for the effective bulk modulus of such a material is given by

$$\frac{1}{K} = \frac{V}{V_m K_m} + \frac{3 V_m}{4 G_m (V - V_m)} \qquad (2.43)$$
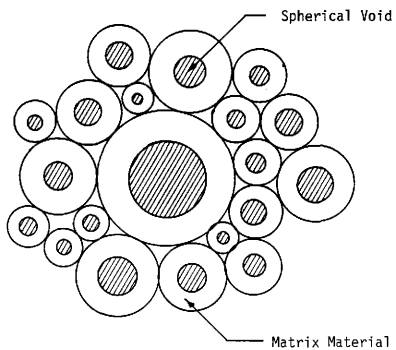
Figure 2.16. -- Geometry Used in Spherical Void Models.

where

G = the shear modulus and the subscript m is used to denote
properties of the matrix material.

Equation 2.43 was developed under the assumption that air was
contained in the voids. Hashin (10,11) has determined upper and lower
bounds for the effective bulk and shear moduli of an elastic matrix
material which contains spherical inclusions of another elastic
material. The geometry that is considered is that shown in Figure
2.16. The upper and lower bounds were determined from the theorems of
minimum potential energy and minimum Complementary energy. The upper
and lower bounds that were determined for the effective bulk modulus
coincided. This result is given by

$$K = K_m + \frac{(K_p - K_m) \ (4G_m + 3 \ K_m) \ C_p}{4G_m + 3 \ K_p + 3 \ (K_m - K_p) \ C_p} \qquad (2.44)$$

where C_p = the volume fraction of the inclusions and the subscript p
is used to denote properties of the inclusions.

The upper and lower bounds which Hashin obtained for the effective
shear modulus were not equal. However, the expression for the
effective shear modulus can be regarded as a good approximation
whenever the bounds are close together. The expression is

$$G = \frac{15 \ (1 - \nu_m) \ G_m \ (G_p - G_m) \ C_p}{7 - 5\nu_m + 2 \ (4 - 5\nu_m) \ [G_p - G_m) \ C_p]} \qquad . \qquad (2.45)$$

The bounds determined by Hashin have found success in approximating the effective elastic moduli of composite materials. As seen in these results, the effect of a material other than air present within the voids may be accounted for.

Some spherical void models have been developed which account for the plastic yielding of the matrix material. Torre (29) has developed such a model. The result which he obtained is

$$P = \frac{2}{3} Y \log_e \left(\frac{\alpha}{\alpha-1} \right) \qquad (2.46)$$

where

$$\alpha = \frac{V}{V_m} \qquad (2.47)$$

Y = the yield stress of the matrix material.

A problem with Equation 2.46 is that the matrix material is considered to be fully plastic. A model should be able to describe elastic as well as plastic phases, which occur for both loading and unloading. A step toward including both elastic and plastic phases is to prescribe a work-hardening rule for the matrix material. Chadwick (6) has developed such a model. Certain essential parts of this model remain in integral form making it difficult to use. Carrol and Holt (5) as well as Chu and Hashin (7) have taken a different approach which simplifies the results. Considering the same spherical pore

geometry, they derive the pressure-volume relationship for the
composite material by temporarily assuming that the matrix material is
incompressible. Carrol and Holt then go on to use an empirical
relationship to describe the pressure volume relationship for the
matrix material. The empirical relationship for the matrix material
is that given by Equation 2.2. The results Carrol and Holt obtain for
the pressure-volume relationship of a mass composed of an ideally
elastic-plastic matrix material containing voids is given by

$$P = \frac{4G_m (\alpha_0 - \alpha)}{3 (\alpha - 1)} \ , \ (\alpha_0 > \ \alpha > \alpha_1) \tag{2.48a}$$

$$P = \frac{2G_m}{3} + Y - \frac{2G_m \alpha_0}{\alpha} + Y \log_e \left[\frac{2G_m(\alpha_0 - \alpha)}{Y(\alpha - 1)} \right] \ , \ (\alpha_1 > \ \alpha > \alpha_2) \tag{2.48b}$$

$$P = \frac{2Y}{3} \log_e \left(\frac{\alpha}{\alpha - 1} \right) \ , \ (\alpha_2 > \ \alpha > 1) \tag{2.48c}$$

$$\alpha_0 = \frac{V_{mo}}{V_m} \tag{2.48d}$$

$$\alpha_1 = \frac{2G_m \alpha_0 + Y}{2G + \nu} \tag{2.48e}$$

$$\alpha_2 = \frac{2G_m \alpha_0}{2G_m + Y} \tag{2.48f}$$

$$\alpha = \frac{V}{V_m}$$
(2.48g)

where V_{mo} = the initial volume of the matrix material.

There are two problems associated with using Equations 2.48 to represent soil behavior. First, the parameters obtained by using Equations 2.42 to describe the pressure-volume relationship of the matrix material have very little to do with the actual behavior of the soils grains. Second, soils exhibit a pronounced reverse yielding during unloading which is not predicted by Equations 2.48. Bhatt, et al. (2) attempted to remove these difficulties by making the matrix a Mohr-Coulomb material. The yield criterion for the matrix material is given by

$$(1 + D)\ \sigma_1 - \sigma_3 - Y = 0$$
(2.49)

where D = a constant.

Using the yield criterion given by Equation 2.49, the results obtained by Bhatt, et al. are given by

$$P = \frac{4G_m\ (\alpha_0 - \alpha)}{3\alpha(\alpha - 1)}\ ,\ (\alpha_0 > \alpha > \alpha)$$
(2.50a)

$$P = \frac{4G_m (\alpha_0 - \alpha)}{3 (\alpha - \alpha_1)} \left\{ \alpha \left[\frac{2G_m (\alpha_0 - \alpha)}{\gamma (\alpha - 1)} \right]^{\frac{3}{2D + 3}} - \alpha + 1 \right\}$$

$$+ \frac{\gamma}{D} \left[\frac{2G_m (\alpha_0 - \alpha)}{\gamma (\alpha - 1)} \right]^{\frac{2D}{2D + 3}} - 1 \right] \quad , (\alpha_1 > \alpha > \alpha_2)$$

$$\tag{2.50b}$$

$$P = \left[\frac{\gamma}{D} \left(\frac{\alpha}{\alpha - 1} \right)^{\frac{2D}{3}} - 1 \right] \quad , (\alpha_2 > \alpha > 1)$$

$$\tag{2.50c}$$

$$\alpha_1 = \frac{2G_m \alpha_0 + \gamma}{2G_m + \gamma}$$

$$\tag{2.50d}$$

The parameter α_2 is determined from the equation below.

$$\frac{2G_m (\alpha_0 - \alpha_2)}{\gamma (\alpha_2 - 1)} = \left[\frac{\alpha_2}{\alpha_2 - 1} \right]^{1 + \frac{2D}{3}}$$

$$\tag{2.51}$$

Defining the value of α when unloading is initiated as α^*, the following relationships hold when unloading takes place in the fully plastic state.

$$P = \frac{\gamma}{P} \left[\left(\frac{\alpha}{\alpha - 1} \right)^{\frac{2D}{3}} - 1 \right] - \frac{\gamma (2 + D)}{D} \left(\frac{c}{a} \right)^{2D}$$

$$+ \frac{2G_m (\alpha - \alpha^*)}{3} \left[\frac{3 + D}{D(\alpha - 1)} \left(\frac{a}{c} \right)^3 + \frac{2}{\alpha} \right]$$

$$\tag{2.52a}$$

$$\alpha = \frac{2G_m \, \alpha^* - Y'}{2G_m - Y}$$ (2.52b)

$$Y' = Y \left[(\frac{c}{a})^{2D+3} + \frac{1}{(1+D)} (\frac{c}{a})^{\frac{3+D}{1+D}} \right]$$ (2.52c)

Equations 2.52 must be solved numerically to obtain the pressure-volume relationship during unloading. There was good agreement between Bhatt's model and experimental results. Some problems with the model just described have been recognized. The predicted high pressure compressibility is often too low and low pressure behavior is not adequately represented. Schatz, et al. (25) has modified Bhatt's model to allow for the curvature of the Mohr-Coulomb failure surface. The failure criterion which Schatz, et al. incorporates into Bhatt's model is

$$\sigma_1 - \sigma_3 - \sigma_{ult} + (\sigma_{ult} - Y_o) \, exp \, (\sigma_1/\sigma_o)$$ (2.53)

where σ_{ult} = the ultimate strength of the matrix material, and

Y_o = the yield stress for a $\sigma_1=0$ condition.

Another modification which Schatz, et al. incorporated into Bhatt's model was to include the effect of flat cracks on the bulk modulus of the matrix material. This modification of the bulk modulus is given by

$$\frac{K}{K_m} = 1 - P\left[1 - \frac{P}{P_a}\right] , \quad P < P_{c1} \qquad (2.54a)$$

$$K = K_m, \quad P \geq P_{c1} \qquad (2.54b)$$

where

    D   = a constant, and

    P_{c1} = pressure required for complete crack closure.

The modification given in Equation 2.54 has the effect of dividing the

voids into two populations. These being spherical voids which deform

according to Equation 2.53, and flat cracks which deform according to

Equations 2.54. The modifications just described have served to

improve the predictions made by Bhatt's model. One problem with

Bhatt's and Schatz's models are that neither allows for a distribution

of pore sizes. An approach to account for the pore size variation in

an actual material is to start with the ideally plastic spherical pore

model and then allow for each sphere to have a different porosity,

with the requirement that the total porosity be equal to that of the

material being modeled. Kreher and Schopt (15) have developed such a

model which considers only an ideally plastic matrix material. Their

results for the pressure volume relationship of one pore is given by

$$P = \frac{4G_m}{3} \left[\alpha(1 - \frac{V_p}{V_{Po}}) - \bar{\alpha}(1 - \frac{\bar{V}_p}{V_{Po}}) \right] +$$

$$\frac{2Y}{3} \log_e \left[1 + (\frac{1-\alpha}{\alpha}) \frac{V_{Po}}{V_p} \right] \tag{2.55a}$$

$$\alpha = \frac{V}{V_m} \tag{2.55b}$$

where

  V_p = the current pore volume, and

  V_{Po} = the initial pore volume.

The overbars in Equations 2.55 denote averages taken over the entire volume of material being considered. The pressure-volume relationship for the entire material is determined by evaluating Equations 2.55 for all pores present in the material. A problem which is apparent for this model is the determination of the pore size distribution.

Other spherical void deformation models have been developed; however, it would be too lengthy to give a description of all of these models here. The models thus far described in this section are representative of the work which has been done in this area.

SUMMARY OF SOILS MODELS

The soil models reviewed in the previous sections, with few exceptions, have only considered the pores within the soil mass to contain air. The modification of many of these models to represent saturated soil conditions is straightforward through the effective stress principle. However, many situations exist when the soil is

partly saturated. This condition presents a problem due to the complexity of having an air-water mixture present in the pores. One problem is that, as the pressure is increased, some of the air will be driven into solution. Due to this and the compressibility of the air phase, it is difficult to predict the pore pressure resulting from the application of a load. If the pore pressures could be predicted, the principle of effective stress could be used to model the partly saturated system.

Phenomenological models have been used a great deal to model soil behavior. It would seem that empirical models obtained from curve fitting methods are undesirable for use as a constitutive model representing soil behavior. These models should not be expected to yield reasonable results when used to represent conditions which deviate greatly from those by which the model was calibrated. They also provide no understanding as to the actual deformation mechanisms acting within the soil mass. Elastic models are poor representations of soil behavior primarily due to their inability to predict unloading behavior. Elastic-plastic models have been used a great deal and provide reasonable results for many situations. While these models may work well, they often require a great many parameters and may be difficult to use in practice. There has been little work using viscoelastic models for soils.

Micromechanical models attempt to derive constitutive laws from observing the actual mechanisms causing deformation of the microstructure. These models are favorable because of this reason.

As these deformation mechanisms are more fully understood, a better understanding of the complex behavior of soils will be achieved.

CHAPTER III

MICROMECHANICAL MODEL FOR AN ELASTIC SOIL SYSTEM

MODELING APPROACH

A model to be used to represent the load-deformation behavior of a
partly saturated soil, will be presented. The model views the soil as
an assemblage of soil particles in contact. The soil particles are
surrounded by an air-water mixture. The model views the soil
particles and the air-water mixture as two different elastic phases.
A micromechanical approach is used to derive constitutive equations
describing the load deformation behavior of the two phase system. The
micromechanical approach seeks to derive constitutive laws by
observing the actual deformation mechanisums acting on a small
representative volume of the material. The representative volume is
chosen as the smallest volume of material which exhibits the
load-deformation behavior of the material as a whole. If a sample
volume, larger than the representative volume is considered, the
load-deformation behavior of this volume will be the same as that for
the representative volume. The material as a whole will contain of a
large number of samples of representative volume size. Macroscopic
quantities referenced to a representative volume are those which are
observable on the size scale of the experiment. These macroscopic
quantities will be assumed to be spacewise constant within the
representative volume. If gradient fields are present in the sample
as a whole, it is reasonable to assume that these fields are spacewise

constant within the representative volume, provided this volume is very small in comparison to the sample volume. Microscopic quantities referenced to a representative volume are those present in the different phases contained in this volume. These microscopic quantities may vary appreciably between the different phases contained in the representative volume. The macroscopic quantities referenced to a representative volume, will be viewed as volume averages of the microscopic quantities present in this volume. These ideas will be used to develop consitutive equations describing the load-deformation behavior of a two phase elastic system.

The laws of thermodynamics provide a means of determining constitutive equations to describe the load-deformation behavior of a representative volume of a two phase elastic system. These constitutive equations will be determined in terms of the actual load-deformation behavior of the elastic phases. Use of thermodynamics will also provide a means of properly handling the nonlinearities arising from the load-displacement behavior of particles in contact.

MODEL GEOMETRY AND MATERIALS

The elastic soil system will be modeled as a two phase elastic material. It will be assumed that both phases of the system are homogeneous, linear elastic materials. The two phases will have different material properties.

The soil particles will be represented as a collection of spheres of equal radii, in contact. All spheres will have the same material properties and constitute one phase of the system. This phase will be referred to as the particulate phase. The position of the spheres relative to one another will be restricted so that they are arranged in ideal packing configurations. The four ideal packing configurations to be considered are cubic, orthorhombic, tetrogonal-spheroidal, and rhombohedral. These packing configurations appear in Figure 3.1 through Figure 3.4.

The air-water mixture will be represented by another elastic phase with different material properties than that of the particulate phase. This phase will be contained in the void space around the spheres and will be referred to as the mixture phase. Only changes in the mean stress of the mixture phase will be considered. This represents a pressure change which might occur in an air-water mixture contained in the voids of an actual soil mass. Micromechanics will be used to determine the pressure-volume relationship of the air-water mixture. The model used to represent the soil is shown in Figure 3.5.

The representative volume of the elastic soil system is taken to be the smallest volume which exhibits the load-deformation behavior of the system as a whole. As a result of the assumed geometry, the representative volume is a single sphere surrounded by a proportionate volume of the elastic mixture material. Due to the restriction that the spheres in the system are arranged in ideal packing configurations, each sphere will experience the same number of contacts with adjacent spheres. Each sphere will also be surrounded by
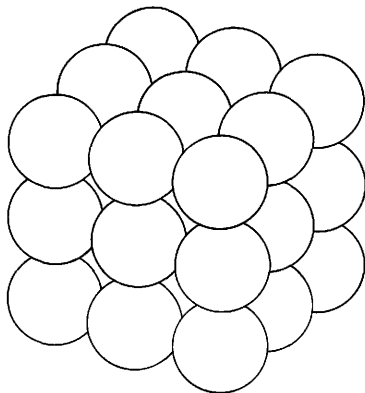
Figure 3.1 -- Simple Cubic Packing Configuration.
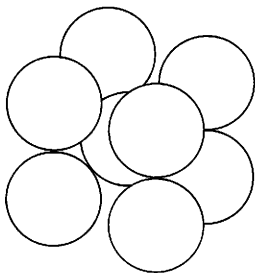
Figure 3.2 -- Orthorhombic Packing Configuration.
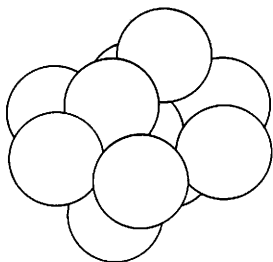
Figure 3.3 -- Tetragonal - Spheroidal Packing
          Configuration.
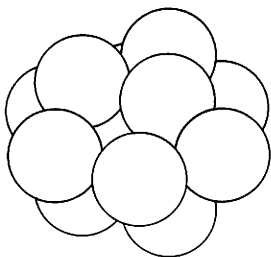
Figure 3.4 -- Rhombohedral Packing Configuration.
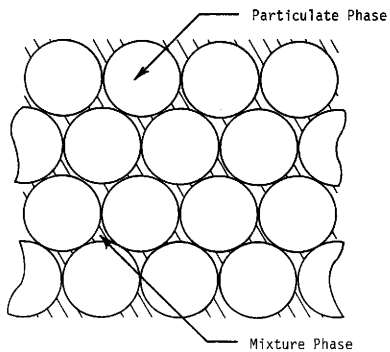
Figure 3.5 -- Elastic Soil System

an equal amount of the mixture phase. Because of this symmetry, the load-deformation behavior of a single sphere and its surrounding mixture phase will be characteristic of the system as a whole. The volume fraction of the mixture phase contained in the representative volume will be equal to the volume fraction of the mixture phase contained in the system as a whole.

THERMODYNAMICS OF ELASTIC SYSTEMS

Constitutive equations describing the load-deformation behavior of a two phase elastic system will be developed. The constitutive equations will relate macroscopic quantities in terms of the actual deformation mechanisms acting on the microscale, and the material properties of the two different elastic phases. These relationships will be based on the load-deformation behavior of the representative volume, which is characteristic of the load deformation behavior of the system as a whole. The representative volume will constitute a closed thermodynamic system.

The first and second laws of thermodynamics provide a means of determining the constitutive equations. The first law of thermodynamics is stated as follows:

> There exists a function of state, U_T, called the internal energy, with the property that

$$\overset{\circ}{W}_T + \overset{\circ}{H}_T = \overset{\circ}{U}_T \tag{3.1}$$

where

$\overset{\circ}{W}_T$ = the rate of total work done on the system, and

$\overset{\circ}{H}_T$ = the rate of heat addition to the system.

The dot is used to denote derivatives with respect to time. The second law of thermodynamics is stated as follows:

There exist two functions of state, S_T, called the entropy, and T, called the absolute temperature, with the property that

$$\overset{\circ}{S}_T \geq \frac{\overset{\circ}{H}_T}{T} \tag{3.2}$$

The second law of thermodynamics given by Equation 3.2, may be written in a more convenient form by letting the entropy production, $S_T{}'$, be defined by

$$\overset{\circ}{S}_T' = \overset{\circ}{S}_T - \frac{\overset{\circ}{H}_T}{T} \tag{3.3}$$

Use of Equations 3.2 and 3.3 allows the second law of thermodynamics to be stated as

$$\overset{\circ}{S}_T' \geq 0 \tag{3.4}$$

It is Equations 3.1 through 3.4 which are used to derive the constitutive equations for a two phase elastic system.

Single Phase Elastic System

The first and second laws of thermodynamics, stated by Equations 3.1 through 3.4, will be applied to a closed system containing a single elastic phase. This will provide information useful in the development of the constitutive equations describing the load-deformation behavior of the two phase elastic system.

Elastic materials are known to undergo reversible processes. A reversible process is one which at any time during the process, the system and the surrounding environment may be returned to their initial states. This will require that the entropy production given by Equation 3.3, equal zero. In reality, the reversible process is an idealization which can never be realized by experiment. However, it can be approximated very closely in some cases. Elastic materials undergo processes which are very closely approximated by reversible processes.

The approach taken in using the first and second laws of thermodynamics to determine constitutive relationships for an elastic material is like that of the inverse method of elasticity theory. Constitutive assumptions are made concerning the independent and dependent variables and then checked to see if the desired solution is obtained. For an elastic material it is desired to check if the constitutive assumptions result in a entropy production equal to zero.

For the single phase elastic material under consideration, it will be assumed that the independent variables are the absolute

temperature, T, and the strain tensor, ε_{ij}. The constitutive
assumptions are

$$U = U(\varepsilon_{ij}, T) \tag{3.5}$$

$$S = S(\varepsilon_{ij}, T) \tag{3.6}$$

$$\sigma_{kl} = \sigma_{kl}(\varepsilon_{ij}, T) \tag{3.7}$$

where

    U = the internal energy per unit initial volume,

    S = the entropy per unit initial volume, and

  σ_{ij} = the components of the stress tensor.

It is further assumed that these quantities are spacewise constant
within the system. The first and second laws of thermodynamics may be
written on a per unit initial volume basis. In this form the first law
is given by

$$\overset{\circ}{W} + \overset{\circ}{H} = \overset{\circ}{U} \tag{3.8}$$

and the second law is given by

$$\overset{\circ}{S}{}' \geq 0 \tag{3.9}$$

where

$$\overset{\circ}{S}{}' = \overset{\circ}{S} - \frac{\overset{\circ}{H}}{T} \qquad\qquad (3.10)$$

and

$\overset{\circ}{W}$ = the rate of work per unit initial volume done on the system, and

$\overset{\circ}{H}$ = the rate of heat addition per unit initial volume.

It will be assumed that only mechanical work is done on the system and that inertial forces are negligible. The rate of work per unit initial volume, done on the system is

$$\overset{\circ}{W} = \sigma_{ij}\, \overset{\circ}{\epsilon}_{ij} \qquad\qquad (3.11)$$

Combining Equations 3.8 through 3.11 yields the following equation.

$$T\overset{\circ}{S}{}' = T\overset{\circ}{S} - \overset{\circ}{U} + \sigma_{ij}\, \overset{\circ}{\epsilon}_{ij} \qquad\qquad (3.12)$$

The Helmholtz free energy per unit initial volume, F, is defined by

$$F = U - TS \qquad\qquad (3.13)$$

According to Equations 3.5 and 3.6, the Helmholtz free energy per unit initial volume is of the form

$$F = F\,(\epsilon_{ij},\, T) \qquad\qquad (3.14)$$

Equations 3.12, 3.13 and 3.14 may be combined to yield

$$T\overset{\circ}{S}{}' = [\sigma_{ij} - \frac{\partial F}{\partial \epsilon_{ij}}] \overset{\circ}{\epsilon}_{ij} - [S + \frac{\partial F}{\partial T}] \overset{\circ}{T} \tag{3.15}$$

Equation 3.15 can be used to determine constitutive relationships for the thermodynamic system characterized by Equations 3.5, 3.6, and 3.7. Consider a process where $\overset{\circ}{T} > 0$ and $\overset{\circ}{\epsilon}_{ij} = 0$ for all i and j. Combining Equations 3.9 and 3.15 for this process yields

$$- [S + \frac{\partial F}{\partial T}] \geq 0 \tag{3.16}$$

As a second process, consider the case where $\overset{\circ}{T} < 0$ and $\overset{\circ}{\epsilon}_{ij} = 0$ for all i and j. Combining Equations 3.9 and 3.15 yields

$$[S + \frac{\partial F}{\partial T}] \geq 0 \tag{3.17}$$

In order for Equations 3.16 and 3.17 to both be satisfied, the following condition must hold.

$$S = - \frac{\partial F}{\partial T} \tag{3.18}$$

Other special processes can be considered in which $\overset{\circ}{T} = 0$ and the components of the strain rate tensor, $\overset{\circ}{\epsilon}_{ij}$, are varied one at a time. Consideration of these processes by Equations 3.9 and 3.15 will show that the following conditions must hold.

$$\sigma_{ij} = \frac{\partial F}{\partial \varepsilon_{ij}} \qquad\qquad (3.19)$$

Combining Equations 3.15, 3.18, and 3.19 yields the following

expression for the entropy production rate per unit initial volume.

$$S' = 0 \qquad\qquad (3.20)$$

Equation 3.20 is true for all processes involving the independent

variables of the absolute temperature, T, and the strain tensor, ε_{ij}.

Processes which obey Equation 3.20 are reversible. As stated

previously, elastic materials undergo reversible processes.

Therefore, the constitutive assumptions given by Equations 3.5, 3.6,

and 3.7 are valid for an elastic material.

The components of the compliance tensor give the change in a

component of the stress tensor due to a unit change in a component of

the strain tensor. The compliance tensor is defined as

$$C_{ijkl} = \frac{\partial \sigma_{ij}}{\partial \varepsilon_{kl}} \qquad\qquad (3.21)$$

where

C_{ijkl} = the components of the compliance tensor.

As a result of the constitutive assumption given in Equation 3.7, the

compliance tensor will be a function of the absolute temperature, T,

and the strain tensor, ε_{ij}. The use of Equation 3.19 in Equation 3.21

gives the following alternate expression for the compliance tensor.

$$C_{ijkl} = \frac{\partial^2 F}{\partial \varepsilon_{ij} \partial \varepsilon_{ij}}$$ (3.22)

The entropy, stress tensor, and compliance tensor of a single phase elastic material may be determined by Equations 3.18, 3.19, and 3.22, respectively. These quantities are expressed in terms of the Helmholtz free energy per unit initial volume, F, the absolute temperature, T, and the strain tensor, ε_{ij}. Cases may arise where the stress tensor is known as an independent variable rather than the strain tensor. For these cases, expressions for quantities in terms of the stress tensor are desired. Toward this end, the Complementary free energy per unit initial volume, F_c, is defined to be

$$F_c = \sigma_{ij} \varepsilon_{ij} - F$$ (3.23)

It is allowed that Equation 3.8 be inverted and solved for the strain tensor in terms of the absolute temperature, T, and the stress tensor, σ_{ij}. This permits the following forms of the internal energy per unit initial volume, U, the entropy per unit initial volume, S, and the strain tensor, ε_{ij}.

$$U = U (\sigma_{ij}, T)$$ (3.24)

$$S = S (\sigma_{ij}, T)$$ (3.25)

$$\varepsilon_{kl} = \varepsilon_{kl} (\sigma_{ij}, T)$$ (3.26)

Equations 3.24, 3.25 and 3.26 are to be viewed as constitutive assumptions in which the absolute temperature, T, and the stress tensor, σ_{ij}, have been chosen as the independent variables. In view of Equation 3.14, the Complementary free energy per unit initial volume is of the form

$$F_c = F_c (\sigma_{ij}, T) \tag{3.27}$$

Combining Equations 3.12, 3.13, and 3.23 yields

$$T\overset{\circ}{S}{}' = \overset{\circ}{F}_c - \overset{\circ}{\sigma}_{ij} \, \epsilon_{ij} - T\overset{\circ}{S} \tag{3.28}$$

Due to the form of the Complementary free energy given by Equation 3.27, Equation 3.28 may be rewritten as

$$T\overset{\circ}{S}{}' = [\frac{\partial F_c}{\partial \sigma_{ij}} - \epsilon_{ij}] \, \overset{\circ}{\sigma}_{ij} + [\frac{\partial F_c}{\partial T} - S] \, \overset{\circ}{T} \tag{3.29}$$

By considering special processes similar to those already mentioned, it can be shown that Equation 3.29 is satisfied for all processes when the following two conditions are true.

$$S = \frac{\partial F_c}{\partial T} \tag{3.30}$$

$$\epsilon_{ij} = \frac{\partial F_c}{\partial \sigma_{ij}} \tag{3.31}$$

Substitution of Equations 3.30 and 3.31 into Equation 3.29 results in
the following

$$\overset{\circ}{S}{}' = 0 \qquad\qquad (3.32)$$

For the constitutive assumptions given by Equations 3.24, 3.25, and
3.26, it was determined that the entropy production per unit initial
volume is zero. Therefore, these assumptions are valid for an elastic
material.

The components of the stiffness tensor give the change in a
component of the strain tensor, due to a unit change in a component of
the stress tensor. The stiffness tensor is defined to be

$$S_{ijkl} = \frac{\partial \varepsilon_{ij}}{\partial \sigma_{kl}} \qquad\qquad (3.33)$$

where

S_{ijkl} = the components of the stiffness tensor.

In accordance with Equation 3.26, the stiffness tensor will be a
function of the absolute temperature, T, and the stress tensor, σ_{ij}.
Combining Equations 3.31 and 3.33 given the following alternate
expression for the stiffness tensor.

$$S_{ijkl} = \frac{\partial^2 F_c}{\partial \sigma_{ij} \partial \sigma_{kl}} \qquad\qquad (3.34)$$

The results have shown that for an elastic material, for which the absolute temperature and strain tensor are known, the entropy, stress tensor, and compliance tensor may be determined when the Helmholtz free energy is known. Similarly, for an elastic material for which the absolute temperature and the stress tensor are known, the entropy, strain tensor, and stiffness tensor may be determined when the Complementary free energy is known. The Helmholtz free energy and the Complementary free energy will be determined for an initially unstrained and unstressed elastic material under isothermal conditions.

The Helmholtz free energy will be considered first. According to Equation 3.19, the following may be obtained

$$\int_0^t \frac{\partial F}{\partial \varepsilon_{ij}} \, \overset{\circ}{\varepsilon}_{ij} \, d\bar{t} = \int_0^t \sigma_{ij} \, \overset{\circ}{\varepsilon}_{ij} \, d\bar{t} \tag{3.35}$$

where

$\bar{t}$ = the dummy variable of integration.

Under isothermal conditions, Equation 3.14 may be used to obtain

$$\overset{\circ}{F} = \frac{F}{\varepsilon_{ij}} \, \overset{\circ}{\varepsilon}_{ij} \tag{3.36}$$

Substitution of Equation 3.36 into Equation 3.35, and integration of the left hand side of the equation yields

$$F(t) - F(0) = \int_0^t \sigma_{ij} \, \overset{\circ}{\varepsilon}_{ij} \, d\bar{t} \tag{3.37}$$

For an elastic body initially unstrained and unstressed the initial

value of the Helmholtz free energy per unit volume, $F(0)$, is equal to

zero. Therefore, for these conditions Equation 3.37 becomes

$$F(t) = \int_0^t \sigma_{ij} \; \overset{o}{\epsilon}_{ij} \; d\bar{t} \qquad (3.38)$$

The result given by Equation 3.38 is that for an initially unstrained

and unstressed elastic material under isothermal conditions, the

Helmholtz free energy per unit volume is equal to the total mechanical

work input to the elastic system.

The Complementary free energy for the conditions previously stated

may be determined in a similar manner. According to Equation 3.31,

the following may be obtained

$$\int_0^t \frac{\partial F_c}{\partial \sigma_{ij}} \; \overset{o}{\sigma}_{ij} \; d\bar{t} = \int_0^t \overset{o}{\sigma}_{ij} \epsilon_{ij} \; d\bar{t} \qquad (3.39)$$

Under isothermal conditions, Equation 3.27 reduces to

$$F_c = \frac{\partial F_c}{\partial \sigma_{ij}} \overset{o}{\sigma}_{ij} \qquad (3.40)$$

Substitution of Equation 3.40 into Equation 3.39 and integration of

the left hand side of the equation gives

$$F_c(t) - F_c(0) = \int_0^t \overset{\partial}{\sigma}_{ij} \; \epsilon_{ij} \; d\bar{t} \qquad\qquad (3.41)$$

For an initially unstrained and unstressed elastic material, the initial value of the complementary free energy per unit initial volume, $F_c(0)$, is equal to zero. Therefore, Equation 3.41 becomes

$$F_c(t) = \int_0^t \overset{\circ}{\sigma}_{ij} \, \epsilon_{ij} \; d\bar{t} \qquad\qquad (3.42)$$

The right hand side of Equation 3.42 is called the Complementary work. As seen by Equation 3.42, for an initially unstrained or unstressed elastic material under isothermal conditions, the Complementary free energy per unit initial volume is equal to the total Complementary work input to the system.

If the material is linear elastic, the components of the compliance tensor, C_{ijkl}, and the stiffness tensor, S_{ijkl}, are constants. For this case it is easy to verify that the Helmholtz free energy per unit initial volume given by Equation 3.38, and the Complimentary free energy per unit initial volume given by Equation 3.42, are equal.

Two Phase Elastic System

The results of the previous subsection will be used to determine relationships for a two phase elastic system. The system to be considered will consist of a representative volume of a two phase
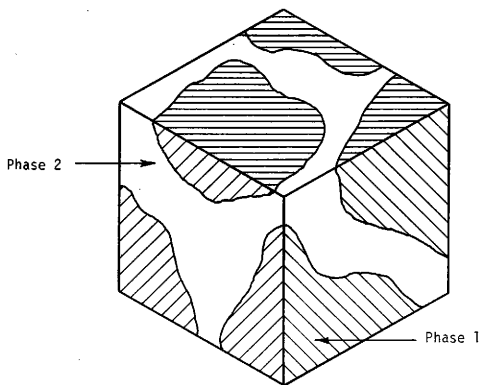
Figure 3.6 -- Representative Volume of Two Phase
Elastic Material

elastic material. The system is shown in Figure 3.6. The
representative volume will constitute a closed system.

In dealing with the two phase system, effective or average values
of quantities will be expressed in terms of the actual values of these
quantities occurring in the two different elastic phases. These
effective quantities are to be viewed as those which would be
observable on the size scale of the experiment. When the
representative volume is small in comparison to the size scale of the
experiment, effective quantities will appear spacewise constant
throughout the volume. As an example of effective quantities consider
a soil sample subjected to a triaxial test. If a small representative
volume of the soil sample was examined, the experimentally observable
stresses would appear constant throughout the volume. In the present
terminology, the experimentally observable stress field would be the
effective stress field. If the representative volume was viewed on
the microscale, the stress field would be seen to vary throughout the
different phases comprising the sample. It will be shown that under
specific conditions, the effective quantities may be viewed as average
values of these quantities, taken over the representative volume. In
the work to follow, effective quantities for the representative volume
will be denoted by an overbar.

To develop relationships for the two phase elastic system, the
effective strain tensor, $\overline{\varepsilon_{ij}}$, and the absolute temperature, T, will
first be chosen as the independent variables. It is assumed that no
temperature gradients exist in the system. The effective quantities

will be assumed to be spacewise constant throughout the system. The constitutive assumptions are

$$\overline{U} = \overline{U} \, (\overline{\varepsilon_{ij}}, \, T) \tag{3.43}$$

$$\overline{S} = \overline{S} \, (\overline{\varepsilon_{ij}}, \, T) \tag{3.44}$$

$$\overline{\sigma_{kl}} = \overline{\sigma_{kl}} \, (\overline{\varepsilon_{ij}}, \, T) \tag{3.45}$$

where

$\overline{U}$ = the effective internal energy per unit initial volume,

$\overline{S}$ = the effective entropy per unit initial volume, and

$\overline{\sigma_{ij}}$ = the effective stress tensor.

The constitutive assumptions given by Equations 3.43, 3.44, and 3.45 are of the same form as those given by Equations 3.5, 3.6, and 3.7. The system under consideration is elastic. The results of the previous subsection may be applied to the system to yield constitutive relationships for the effective quantities. The relationships which are of interest are

$$\overline{S} = -\frac{\partial \overline{F}}{\partial T} \tag{3.46}$$

$$\overline{\sigma}_{ij} = \frac{\partial \overline{F}}{\partial \overline{\varepsilon}_{ij}} \tag{3.47}$$

$$\overline{C}_{ijkl} = \frac{\partial^2 \overline{F}}{\partial \overline{\varepsilon}_{ij} \partial \overline{\varepsilon}_{kl}} \tag{3.48}$$

where

$\overline{F}$ = the effective Helmholtz free energy per unit initial volume,

and

$\overline{C_{ijkl}}$ = the effective compliance tensor.

It is desired to relate these effective quantities for the representative volume to the phase quantities. The two phases are elastic. The constitutive relationships for each phase are

$$U = U \ (\varepsilon_{ij}, \ T) \tag{3.49}$$

$$S = S \ (\varepsilon_{ij}, \ T) \tag{3.50}$$

$$\sigma_{kl} = \sigma_{kl} \ (\varepsilon_{ij}, \ T) \tag{3.51}$$

where

U = the internal energy per unit initial volume for either phase,

S = the entropy per unit initial volume for either phase,

σ_{ij} = the stress tensor for either phase, and

ε_{ij} = the strain tensor for either phase.

It will be assumed that the strain tensor for each phase, ε_{ij}, is expressible as

$$\varepsilon_{kl} = \varepsilon_{kl} \ (\overline{\varepsilon_{ij}}, \ T) \tag{3.52}$$

Expressions for the effective quantities appearing in Equations 3.46 to 3.48 may be obtained through a balance of the total internal energy of the system. The internal energy balance is given by

$$\overline{U}V = \overline{U}_1 V_1 + \overline{U}_2 V_2 \qquad (3.53)$$

where
$$\overline{U}_1 = \frac{1}{V_1} \int_{V_1} U \, dV \qquad (3.54)$$

$$\overline{U}_2 = \frac{1}{V_2} \int_{V_2} U \, dV \qquad (3.55)$$

and U = the effective internal energy per unit initial volume,

   V = the initial volume of the system,

   V_1 = the initial volume of phase 1,

   V_2 = the initial volume of phase 2, and

   U = the internal energy per unit initial volume.

Equation 3.53 relates the total internal energy of the two phase system expressed in terms of the effective internal energy, to the same expressed in terms of the internal energies of the two phases. Solving Equation 3.53 for $\overline{U}$ yields

$$\overline{U} = C_1 \overline{U}_1 + C_2 \overline{U}_2 \qquad (3.56)$$

where

$$C_1 = \frac{V_1}{V} \qquad (3.57)$$

$$C_2 = \frac{V_2}{V} \qquad (3.58)$$

The quantities C_1 and C_2 appearing in Equations 3.57 and 3.58 are the initial volume fractions of phases 1 and 2, respectively. The Helmholtz free energy per unit initial volume for phase n (n = 1,2) is given by

$$\overline{F}_n = \overline{U}_n - T\,\overline{S}_n \tag{3.59}$$

where

$$\overline{S}_n = \frac{1}{V_n} \int_{V_n} S_n \, dV \tag{3.60}$$

and $\overline{S}_n$ = the entropy per unit initial volume for phase n.

Combining Equations 3.56 and 3.59 with Equations 3.12 and 3.20 written in terms of effective quantities yields

$$T\overset{\circ}{S} + \overline{\sigma}_{ij}\,\overset{\circ}{\overline{\epsilon}}_{ij} - C_1\,[\overset{\circ}{\overline{F}}_1 + T\overset{\circ}{\overline{S}}_1 + T\overset{\circ}{\overline{S}}_1] - C_2\,[\overset{\circ}{\overline{F}}_2 +$$

$$T\overset{\circ}{S}_2 + T\,\overset{\circ}{\overline{S}}_2] = 0 \tag{3.61}$$

According to Equations 3.49, 3.50, and 3.52, the Helmholtz free energy per unit initial volume for phase n (n = 1,2) is expressible as

$$\overline{F}_n = \overline{F}_n\,(\overline{\epsilon_{ij}},\ T) \tag{3.62}$$

Substitution of Equation 3.62 into Equation 3.61 while applying the condition given by Equation 3.18 to the entropies of the two phases yields

$$[\overline{\sigma}_{ij} - C_1\,\frac{\partial \overline{F}_1}{\partial \overline{\epsilon}_{ij}} - C_2\,\frac{\partial \overline{F}_2}{\partial \overline{\epsilon}_{ij}}]\,\overset{\circ}{\overline{\epsilon}}_{ij} + [\overline{S} - C_1\,\overset{\circ}{\overline{S}}_1 -$$

$$C_2\,\overset{\circ}{\overline{S}_2}]\,T = 0 \tag{3.63}$$

Special processes may now be considered to determine relationships between effective and phase quantities. As a special process consider

the case where $\overset{\circ}{\overline{\varepsilon}}_{ij}=0$ for all i and j. For this process, Equation 3.63 yields the condition

$$\overset{\circ}{\overline{S}} - C_1 \overset{\circ}{\overline{S}}_1 - C_2 \overset{\circ}{\overline{S}}_2 = 0 \qquad (3.64)$$

In view of Equation 3.64, the following condition must be true for Equation 3.63 to be satisfied for all processes.

$$\overline{\sigma}_{ij} = C_1 \frac{\partial \overline{F}_1}{\partial \overline{\varepsilon}_{ij}} + C_2 \frac{\partial \overline{F}_2}{\partial \overline{\varepsilon}_{ij}} \qquad (3.65)$$

Equation 3.65 relates the effective stress tensor to the Helmholtz free energies per unit initial volume of the two phases, and the effective strain tensor. Equations 3.47 and 3.65 may be used to determine the relationship between the effective and phase, Helmholtz free energies per unit initial volume. This relationship is

$$\overline{F} = C_1 \overline{F}_1 + C_2 \overline{F}_2 \qquad (3.66)$$

Equation 3.66 states that the effective Helmholtz free energy per unit initial volume is equal to an average of this quantity taken over the representative volume. The same type of relationship may be obtained for S by integrating Equation 3.64 with respect to time. The relationship between the effective entropy per unit initial volume, and the phase entropies per unit initial volumes is

$$\overline{S} = C_1 \overline{S}_1 + C_2 \overline{S}_2 \qquad (3.67)$$

The forms of the effective quantities, $\overline{F}$ and $\overline{S}$, given by Equations
3.66 and 3.67 might have been defined as such from the assumption that
the effective quantities are spacewise constant throughout the system.
However, Equations 3.66 and 3.67 were arrived at through an energy
equivalence and the assumption that no temperature gradients existed
in the system as a whole. The resulting relationships given by
Equations 3.66 and 3.67, correspond to the rule of mixtures. The
effective compliance of the system, $\overline{C}_{ijkl}$, may be determined from
Equations 3.48 and 3.66. Substitution of Equation 3.66 into Equation
3.48 yields the following expression for the effective compliance.

$$\overline{C}_{ijkl} = C_1 \frac{\partial^2 \overline{F}_1}{\partial \overline{\epsilon}_{ij} \partial \overline{\epsilon}_{kl}} + C_2 \frac{\partial^2 \overline{F}_2}{\partial \overline{\epsilon}_{ij} \partial \overline{\epsilon}_{kl}} \tag{3.68}$$

Relationships for effective quantities have been determined for
the case when the effective strain tensor, $\overline{\epsilon}_{ij}$, and the absolute
temperature T, are the independent variables. Cases will arise when
the effective stress tensor, $\overline{\sigma}_{ij}$, is the independent variable rather
than the effective strain tensor, $\overline{\epsilon}_{ij}$. Assuming that Equation 3.45
may be inverted to express $\overline{\sigma}_{ij}$ in terms of $\overline{\epsilon}_{ij}$, Equations 3.43, 3.44
and 3.45 may be rewritten as

$$\overline{U} = \overline{U}(\overline{\sigma}_{ij}, T) \tag{3.69}$$

$$\overline{S} = \overline{S}(\overline{\sigma}_{ij}, T) \tag{3.70}$$

$$\bar{\epsilon}_{kl} = \bar{\epsilon}_{kl} \, (\bar{\sigma}_{ij}, \, T) \tag{3.71}$$

The constitutive assumptions given by Equations 3.69, 3.70, and 3.71
are of the same form as those given by Equations 3.24, 3.25 and 3.26.
The relationships determined for the constitutive assumptions given by
Equations 3.24, 3.25, and 3.26 will apply to the two phase elastic
system under consideration. The relationships which are of interest
are

$$\bar{S} = \frac{\partial \bar{F}_c}{\partial T} \tag{3.72}$$

$$\bar{\epsilon}_{ij} = \frac{\bar{F}_c}{\partial \bar{\sigma}_{ij}} \tag{3.73}$$

$$\bar{S}_{ijkl} = \frac{\partial^2 \bar{F}_c}{\partial \bar{\sigma}_{ij} \, \partial \bar{\sigma}_{kl}} \tag{3.74}$$

where

$\bar{F}_c$ = the effective Complementary free energy per unit initial
volume and,

$\bar{S}_{ijkl}$ = the effective compliance tensor.

The relationship between F_c and F is given by

$$\bar{F}_c = \bar{\sigma}_{ij} \, \bar{\epsilon}_{ij} - \bar{F} \tag{3.75}$$

For the effective stress tensor, $\bar{\sigma}_{ij}$, and the absolute temperature, T,
chosen as the independent variables, the constitutive assumptions for
each phase of the system are

$$U = U \, (\sigma_{ij}, \, T) \tag{3.76}$$

$$S = S \, (\sigma_{ij}, \, T) \tag{3.77}$$

$$\epsilon_{kl} = \epsilon_{kl} (\sigma_{ij}, T) \tag{3.78}$$

It is further assumed that the stress tensor for each phase is expressible as

$$\sigma_{kl} = \sigma_{kl} (\bar{\sigma}_{ij}, T) \tag{3.79}$$

The Complementary free energy per unit initial volume for phase n of the system is given by

$$\bar{F}_{cn} = (\overline{\sigma_{ij} \epsilon_{ij}})_n - \bar{F}_n \tag{3.80}$$

where

$$(\overline{\sigma_{ij} \epsilon_{ij}})_n = \frac{1}{V_n} \int_{V_n} \sigma_{ij} \epsilon_{ij} \, dV \tag{3.81}$$

and

F_{cn} = the Complementary free energy per unit initial volume for phase n,

σ_{ij} = the stress tensor, and

ϵ_{ij} = the strain tensor.

Substitution of Equation 3.80 into Equation 3.61 yields

$$T\overset{\circ}{S} - \overset{\circ}{\sigma}_{ij} \bar{\epsilon}_{ij} + C_1 [\overset{\circ}{F}_{c1} - T\overset{\circ}{S}_1 - T\overset{\circ}{S}_1] +$$

$$C_2 [\overset{\circ}{F}_{c2} - T \overset{\circ}{S}_2 - T \overset{\circ}{S}_2] = 0 \tag{3.82}$$

By virtue of Equations 3.62, 3.78, 3.79, and 3.80, the Complementary free energy per unit initial volume for phase n is of the form

$$\bar{F}_{cn} = \bar{F}_{cn} (\bar{\sigma}_{ij}, T) \tag{3.83}$$

Use of Equation 3.83 in Equation 3.82 yields

$$[\overset{\circ}{S} - C_1 \overset{\circ}{S}_1 - C_2 \overset{\circ}{S}_2] T - [\bar{\epsilon}_{ij} - C_1 \frac{\partial \bar{F}_{c1}}{\partial \bar{\sigma}_{ij}} - C_2 \frac{\partial \bar{F}_{c2}}{\partial \bar{\sigma}_{ij}}] \overset{\circ}{\bar{\sigma}}_{ij} = 0 \tag{3.84}$$

where the condition given by Equation 3.30 has been applied to both phases of the system. By virtue of Equation 3.64, for Equation 3.84 to be satisfied for all processes, the following condition must be true.

$$\bar{\epsilon}_{ij} = C_1 \frac{\partial \bar{F}_{c1}}{\partial \bar{\sigma}_{ij}} + C_2 \frac{\partial \bar{F}_{c2}}{\partial \bar{\sigma}_{ij}} \tag{3.85}$$

An alternate expression for the effective strain tensor is given by Equation 3.73. Substitution of Equation 3.73 in Equation 3.85 will yield the following relationship.

$$\bar{F}_c = C_1 \bar{F}_{c1} + C_2 \bar{F}_{c2} \tag{3.86}$$

Equation 3.86 shows that the effective Complementary free energy for the system is equal to an average value of this quantity taken over the volume of the system. Substitution of Equation 3.86 into Equation 3.74 yields the following expression for the effective stiffness of the system.

$$\overline{S_{ijkl}} = C_1 \frac{\partial^2 \overline{F}_{c1}}{\partial \overline{\sigma}_{ij} \partial \overline{\sigma}_{kl}} + C_2 \frac{\partial^2 \overline{F}_{c2}}{\partial \overline{\sigma}_{ij} \partial \overline{\sigma}_{kl}} \tag{3.87}$$

Expressions have been obtained for effective quantities of a two phase elastic system with a spacewise constant temperature. These quantities are expressed in terms of the Helmhotz and Complementary free energies of the two elastic phases, and their initial volume fractions. Evaluation of the effective quantities also requires that the relationships given by Equations 3.52 and 3.78 be known. The evaluation of the effective quantities is simplified when the two phases are homogeneous linear elastic materials and the system undergoes only isothermal processes. If the system is initially unstrained or unstressed, the Helmholtz and Complementary free energies per unit initial volume for phase n are given by

$$\overline{F}_n = \overline{F}_{cn} = 1/2 \, (\overline{\sigma_{ij} \, \epsilon_{ij}})_n \tag{3.88}$$

This simplification will be used to evaluate the effective quantities for the elastic soil system.

CONSTITUTIVE EQUATIONS FOR ELASTIC SOIL SYSTEM

Constitutive equations describing the load-deformation behavior of the idealized elastic soil system will be developed. The system consists of a particulate phase modeled by equal spheres in contact, and a mixture phase representing an air-water mixture. The elastic

soil system is shown in Figure 3.5. In the work to follow both phases of the system will be modeled by homogeneous, linear elastic materials. It will further be assumed that the temperature is spacewise constant in the system and the system undergoes only isothermal processes.

The results provided by the thermodynamics of the previous section can be used to relate macroscopic quantities for the two phase elastic soil system, to the phase quantities. In the development of these relationships, a representative volume of the two phase system is considered. For the elastic soil system, the representative volume consists of a single sphere surrounded by a volume of the air-water mixture. The representative volume of the elastic soil system is shown in Figure 3.7. The macroscopic quantities which are of interest are the effective stress, effective strain, effective compliance, and effective stiffness tensors. The results of the previous section provide the following expressions for these quantities.

$$\overline{\sigma}_{ij} = C_p \frac{\partial \overline{F}_p}{\partial \overline{\epsilon}_{ij}} + C_m \frac{\partial \overline{F}_m}{\partial \overline{\epsilon}_{ij}} \tag{3.89}$$

$$\overline{\epsilon}_{ij} = C_p \frac{\partial \overline{F}_{cp}}{\partial \overline{\sigma}_{ij}} + C_m \frac{\partial \overline{F}_{cm}}{\partial \overline{\sigma}_{ij}} \tag{3.90}$$

$$\overline{C}_{ijkl} = C_p \frac{\partial^2 \overline{F}_p}{\partial \overline{\epsilon}_{ij} \partial \overline{\epsilon}_{kl}} + C_m \frac{\partial^2 \overline{F}_m}{\partial \overline{\epsilon}_{ij} \partial \overline{\epsilon}_{kl}} \tag{3.91}$$

$$\overline{S}_{ijkl} = C_p \frac{\partial^2 \overline{F}_{cp}}{\partial \overline{\epsilon}_{ij} \partial \overline{\epsilon}_{kl}} + C_m \frac{\partial^2 \overline{F}_{cm}}{\partial \overline{\epsilon}_{ij} \partial \overline{\epsilon}_{kl}} \tag{3.92}$$
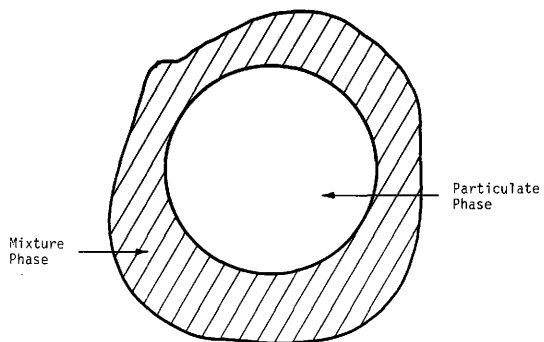
Figure 3.7 -- Representative Volume for Elastic Soil System.

In Equations 3.89 through 3.92, the subscript p has been used to
denote the particulate phase represented by the equal spheres and the
subscript m is used to denote the phase representing the air-water
mixture. In order to evaluate Equations 3.89 through 3.92, it is
necessary to evaluate the Helmholtz and Complementary free energies
for the particulate and mixture phases. Since both phases are being
modeled as homogeneous, linear elastic materials and the system
undergoes only isothermal processes, Equation 3.88 can be used to
evaluate the Helmholtz and Complementary free energies for the phases.
Equation 3.88 yields

$$\bar{F}_p = \bar{F}_{cp} = \tfrac{1}{2}\,(\overline{\sigma_{ij}\epsilon_{ij}})_p \tag{3.93}$$

$$\bar{F}_m = \bar{F}_{cm} = \tfrac{1}{2}\,(\overline{\sigma_{ij}\epsilon_{ij}})_m \tag{3.94}$$

where

$$(\overline{\sigma_{ij}\epsilon_{ij}})_p = \frac{1}{V_p} \int_{V_p} \sigma_{ij}\epsilon_{ij}\ dV \tag{3.95}$$

$$(\overline{\sigma_{ij}\epsilon_{ij}})_m = \frac{1}{V_m} \int_{V_m} \sigma_{ij}\epsilon_{ij}\,dV \qquad . \tag{3.96}$$

and V_p = the initial volume of the particulate phase contained in
the representative volume, and

V_m = the initial volume of the mixture phase contained in the
representative volume.

The quantities expressed by Equations 3.93 and 3.94 are the strain
energy densities of the particulate and mixture phases, respectively.
To evaluate these expressions it will be necessary to relate these
quantities to either the effective stress tensor, σ_{ij}, or the
effective strain tensor, ε_{ij}. In the work to follow it will be
assumed that these relationships are known and Equations 3.93 through
3.96 may be evaluated. In a later subsection the relationship between
the effective stress or strain tensors and the strain energy density
of the phases will be evaluated.

Strain Energy Density of the Particulate Phase

The strain energy density of the particulate phase as well as the
derivatives of this quantity required to determine the effective
quantities of interest, will be determined. As previously mentioned,
the particulate phase of the system consists of spheres of equal
radii, arranged in ideal packing configurations. All spheres in the
system will be modeled by isotropic, homogeneous, linear elastic
materials. All spheres will be of the same material type.

Due to the symmetry of the idealized elastic soil system, the
representative volume consists of a single sphere surrounded by a
specific amount of the material modeling the air-water mixture.
Therefore the strain energy density of a single sphere is required.
Calculation of the strain energy density requires an elastic solution
for the displacement and stress fields occurring in the sphere due to

applied surface tractions or surface displacements. Sternberg, Eubanks, and Sadowsky (27) determined the solution for a sphere with torsion-free rotational symmetry about the x_3-axis, in the absence of body forces. The sphere is shown in Figure 3.8. Also appearing in Figure 3.8 is the spherical coordinate system, (z_1, z_2, z_3) to which the solution is referenced. This solution will allow the evaluation of a number of important types of interactions between neighboring spheres and the mixture phase. The types of interactions to be considered are

1. A uniform pressure applied to the surface of the sphere by the mixture phase.

2. The contact between neighboring spheres.

3. The mixture phase acting as a binder between neighboring spheres.

These types of interactions will result in known surface tractions on a sphere. The relationship between these surface tractions and the effective stress tensor or the effective strain tensor is yet to be determined. For the present, it will be assumed that these relationships are known.

The solution for a weightless, homogeneous, linear elastic sphere subject to torsion free symmetric surface tractions about the x_3-axis will be presented in a form convenient for use. The solution for the stress tensor, σ'_{ij}, and the strain tensor, ε'_{ij}, referred to the spherical coordinates, (z_1, z_2, z_3), is given by

$$\sigma'_{ij} = K^\sigma \left[\sum_{n=1}^{\infty} \mu^{2n-2} a_{-2n-1} [A^\sigma_{-2n-1}]_{ij} + \sum_{n=1}^{\infty} \mu^{2n} b_{-2n-2} \right.$$

$$\left. [B^\sigma_{-2n-2}]_{ij} \right] \tag{3.97}$$

$$\epsilon'_{ij} = \frac{K^\sigma}{G} \left[\sum_{n=1}^{\infty} \mu^{2n-2} a_{-2n-1} [A^\epsilon_{-2n-1}]_{ij} + \sum_{n=0}^{\infty} \mu^{2n} b_{-2n-2} \right.$$

$$\left. [B^\epsilon_{-2n-2}]_{ij} \right] \tag{3.98}$$

where

$$\mu = \frac{z_1}{R} \tag{3.99}$$

and

$$[A^\sigma_m]_{ij}, [B^\sigma_m]_{ij} = \text{component stress solutions,}$$

$$[A^\epsilon_m]_{ij}, [B^\epsilon_m]ij = \text{component strain solutions,}$$

$$a_m, b_m = \text{coefficients of superposition,}$$

$$G = \text{the shear modulus,}$$

$$K^\sigma = \text{a constant determined from the surface}$$

$$\text{tractions, and}$$

$$R = \text{the radius of the sphere.}$$

The component stress solutions are given by

$$[A^\sigma_{-2n-1}]_{11} = 2n(2n-1)\ P_{2n} \tag{3.100a}$$

$$[A^\sigma_{-2n-1}]_{22} = P'_{2n-1} - 2n(2n-1)\ P_{2n} \tag{3.100b}$$

$$[A^\sigma_{-2n-1}]_{33} = -P'_{2n-1} \tag{3.100c}$$

$$[A^{\sigma}_{-2n-1}]_{12} = -(2n-1)\sin(z_2)P'_{2n} \qquad (3.100d)$$

$$[A^{\sigma}_{-2n-1}]_{23} = 0 \qquad (3.100e)$$

$$[A^{\sigma}_{-2n-1}]_{31} = 0 \qquad (3.100f)$$

$$[B^{\sigma}_{-2n-2}]_{11} = -(2n-1)[(2n+1)(2n-2)-2\nu]P_{2n} \qquad (3.100g)$$

$$[B^{\sigma}_{-2n-2}]_{22} = (2n+1)(4n^2+10n-7+2\nu)P_{2n}-(2n+5-4\nu)P'_{2n+1} \qquad (3.100h)$$

$$[B^{\sigma}_{-2n-2}]_{33} = (2n+5-4\nu)P'_{2n+1} -(4n+3)(2n+1)(1-2\nu)P_{2n} \qquad (3.100i)$$

$$[B^{\sigma}_{-2n-2}]_{12} = (4n^2+4n-1+2\nu)\sin(z_2)P'_{2n} \qquad (3.100j)$$

$$[B^{\sigma}_{-2n-2}]_{23} = 0 \qquad (3.100k)$$

$$P'_m = \frac{dP_m}{d(\cos(z_2))} \tag{3.1001}$$

where

ν = Poisson's ratio, and

P_m = Legendre polynominals of order m.

In Equations 3.100, the argument of P_m is $\cos(z_2)$ and P'_m is given by

$$[B^{\sigma}_{-2n-2}]_{31} = 0 \tag{3.101}$$

The component stress solutions, $[A^{\sigma}_m]_{ij}$ and $[B^{\sigma}_m]_{ij}$, are symmetric giving the condition

$$[A^{\sigma}_m]_{ij} = [A^{\sigma}_m]_{ji} \tag{3.102a}$$

$$[B^{\sigma}_m]_{ij} = [B^{\sigma}_m]_{ji} \tag{3.102b}$$

The component strain solutions are

$$[A^{\epsilon}_{-2n-1}]_{11} = n(2n-1)P_{2n} \tag{3.103a}$$

$$[A^{\epsilon}_{-2n-1}]_{22} = 1/2[P'_{2n-1} - 2n(2n-1)P_{2n}) \tag{3.103b}$$

$$[A^{\epsilon}_{-2n-1}]_{33} = -1/2\, P'_{2n-1} \tag{3.103c}$$

$$[A^{\epsilon}_{-2n-1}]_{12} = -1/2(2n-1)\sin(z_2)P'_{2n} \tag{3.103d}$$

$$[A^{\epsilon}_{-2n-1}]_{23} = 0 \tag{3.103e}$$

$$[A^{\epsilon}_{-2n-1}]_{31} = 0 \tag{3.103f}$$

$$[B^{\epsilon}_{-2n-2}]_{11} = -1/2(2n+1)^2(2n-2+4\nu)P_{2n} \tag{3.103g}$$

$$[B^{\epsilon}_{-2n-2}]_{22} = -1/2\{(2n+5-4\nu)P'_{2n+1} -$$

$$(2n+1)[(2n+1)^2 + 2(n+1)(3-4\nu)]P_{2n}\} \tag{3.103h}$$

$$[B^{\epsilon}_{-2n-2}]_{33} = -1/2[(4n+3)(2n+1)P_{2n} -$$

$$(2n+5-4\nu)P'_{2n+1}] \tag{3.103i}$$

$$[B^{\epsilon}_{-2n-2}]_{12} = 1/2[4n(n+1)-1+2\nu]\sin(z_2)P'_{2n} \tag{3.103j}$$

$$[B^{\epsilon}_{-2n-2}]_{23} = 0 \tag{3.103k}$$

$$[B^{\varepsilon}_{-2n-2}]_{31} = 0 \tag{3.1031}$$

The component strain solutions, $[A^{\varepsilon}_m]_{ij}$ and $[B^{\varepsilon}_m]_{ij}$, are symmetric giving the conditions

$$[A^{\varepsilon}_m]_{ij} = [A^{\varepsilon}_m]_{ji} \tag{3.104a}$$

$$[B^{\varepsilon}_m]_{ij} = [B^{\varepsilon}_m]_{ji} \tag{3.104b}$$

The coefficients of superposition, a_m and b_m, are

$$a_{-2n-1} = \frac{(4n^2+4n-1+2\nu)\xi_{2n}+2(2n+1)(2n^2-n-1-\nu)\eta_{2n}}{2(2n-1)[4n^2+2n+1+(4n+1)\nu]} \tag{3.105a}$$

$$b_{-2n-2} = \frac{\xi_{2n}+2n\eta_{2n}}{2[4n^2+2n+1+(4n+1)\nu]} \tag{3.105b}$$

where ξ_{2n} and η_{2n} are constants determined from the specified surface tractions. The specified surface tractions for torsion-free rotational symmetry about the z_3-axis are

$$\sigma'_{11} \, [R, \cos(\bar{z}_2)] = f_{11}[\cos(\bar{z}_2)],$$

$$-1 \leq \cos(\bar{z}_2) \leq \cos(\pi - \bar{z}_2), \; \cos(\overline{\bar{z}_2}) \leq \cos(\bar{z}_2) \leq 1 \qquad (3.106a)$$

$$\sigma'_{12} \, [R, \cos(\bar{z}_2)] = f_{12}[\cos(\bar{z}_2)],$$

$$-1 \leq \cos(\bar{z}_2) \leq \cos(\pi - \bar{z}_2), \; \cos(\overline{\bar{z}_2}) \leq \cos(\bar{z}_2) \leq 1 \qquad (3.106b)$$

The constants, ξ_{2n} and η_{2n}, which result from the specified surface tractions are

$$\xi_{2n} = \frac{(4n+1)}{K^{\sigma}} \int_{\cos(\bar{z}_2)}^{1} f_{11}(u) P_{2n}(u) du,$$

$$(n = 0, 1, 2, \ldots) \qquad (3.107a)$$

$$\eta_{2n} = \frac{(4n+1)}{4n(2n+1)K} \int_{\cos(\bar{z}_2)}^{1} f_{12}(u) \, \sqrt{1-u^2} \, P'_{2n}(u) du,$$

$$(n = 0, 1, 2, \ldots) \qquad (3.107b)$$

Equations 3.97 through 3.107 provide an elastic solution for a weightless sphere subjected to surface tractions of the form given by Equations 3.106.

The solution thus far given is for a sphere with a single set of prescribed surface tractions, symmetric about a particular axis. The

spheres in the system under consideration will be subject to multiple sets of surface tractions of the form given by Equations 3.106. This is due to interactions with neighboring spheres and the mixture phase. The spheres in the system are linear elastic, and the principle of superposition may be used to determine the stress and strain fields due to multiple interactions. To apply the principle of superposition, all stress and strain fields resulting from a single interaction must be referenced to a single coordinate system. Toward this end a global coordinate system $(\theta_1, \theta_2, \theta_3)$ will be established. The solution for the set of surface tractions m, will be referenced to the spherical coordinate system $(\bar{z}_1^m, \bar{z}_2^m, \bar{z}_3^m)$. The surface tractions will have rotational symmetry about the x_3-axis of the coordinate system (x_1^m, x_2^m, x_3^m). For a particular set of surface tractions m, the $(\bar{z}_1, \bar{z}_2, \bar{z}_3)$ coordinates are related to the (x_1^m, x_2^m, x_3^m) coordinates as indicated in Figure 3.8. The angles β_m and ψ_m will define the (x_1, x_2, x_3) coordinate system in relation to the global coordinate system as shown in Figure 3.9. The stress and strain fields for the set of surface tractions m, referenced to the global coordinate system, $(\theta_1, \theta_2, \theta_3)$, are given by

$$(\sigma_{ij})_m = a_{ki}^m \, a_{1j}^m \, (\sigma_{k1}')_m \tag{3.108a}$$

$$(\varepsilon_{ij})_m = a_{ki}^m \, a_{1j}^m \, (\varepsilon_{k1}')_m \tag{3.108b}$$

where
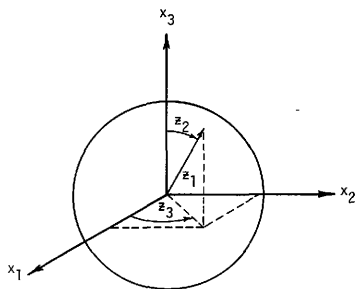
Figure 3.8 -- Spherical Coordinate System, (z_1, z_2, z_3)
in Relation to Cartesian Coordinate System,
(x_1, x_2, x_3).
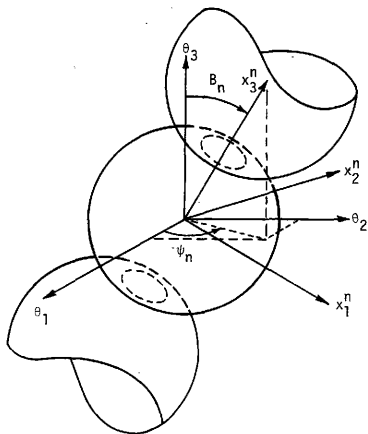
Figure 3.9 -- Cartesian Coordinate System, (x_1^n, x_2^n, x_3^n), in Relation to Cartesian Coordinate System $(\theta_1, \theta_2, \theta_3)$.

$(\sigma_{ij})_m$ = the stress tensor due to the set of surface

tractions m, referred to the global coordinate

system, and

$(\varepsilon_{ij})_m$ = the strain tensor due to the set of surface

tractions m, referred to the global coordinate

system.

The quantities a_{ij} are determined by

$$a_{ij}^m = b_{ik}^m \ c_{kj}^m \qquad\qquad (3.109)$$

where

$$[b_{ij}^m] = \begin{bmatrix} \sin(z_2^m)\cos(z_3^m) & \sin(z_2^m)\sin(z_3^m) & \cos(z_2^m) \\ \cos(z_2^m)\cos(z_3^m) & \cos(z_2^m)\sin(z_3^m) & -\sin(z_2^m) \\ -\sin(z_3^m) & \cos(z_3^m) & 0 \end{bmatrix} \quad (3.110)$$

$$[c_{ij}^m] = \begin{bmatrix} \cos\beta_m\cos\psi_m & -\sin\psi_m & \sin\beta_m\cos\psi_m \\ \cos\beta_m\sin\psi_m & \cos\psi_m & \sin\beta_m\sin\psi_m \\ -\sin\beta_m & 0 & \cos\beta_m \end{bmatrix} \qquad (3.111)$$

Details of the transformations given by Equations 3.108 through 3.111

are given in Appendix B. With the global stress and strain tensors

for the set of surface tractions m, the total stress and strain

tensors may be determined as

$$\sigma_{ij} = \sum_{m=1}^{M} (\sigma_{ij})_m \qquad\qquad (3.112a)$$

$$\epsilon_{ij} = \sum_{m=1}^{M} (\epsilon_{ij})_m$$

(3.112b)

where

σ_{ij} = the total stress tensor,

ϵ_{ij} = the total strain tensor, and

M = the total number of sets of surface tractions.

The strain energy density of a single sphere, subject to M sets of

surface tractions of the form given by Equations 3.106, will not be

determined from Equations 3.93 and 3.95. As previously stated, the

system is initially at rest and undergoes only isothermal processes.

The strain energy density is equal to the Helmholtz Complementary free

energies per unit initial volume. Therefore, according to Equations

3.93, 3.95 and 3.112a, the strain energy density for a sphere in the

system is

$$\overline{\pi}_p = \frac{1}{2} \, \overline{(\sigma_{ij} \epsilon_{ij})}_p = \frac{1}{2V_p} \int_{V_p} \sum_{n=1}^{M} (\sigma_{ij})_n \sum_{m=1}^{M} (\epsilon_{ij})_m \, dV$$

(3.113)

where

$\overline{\pi}_p$ = the strain energy density of a single sphere,

V_p = the initial volume of a single sphere, and

M = the total number of sets of surface tractions.

In Equations (3.113), $\overline{\pi}_p$ is used to denote the strain energy density. It is equal to the Helmholtz free energy per unit initial volume for the conditions cited. Equation 3.113 may be rewritten in the following form

$$\overline{\pi}_p = \overline{\pi}_p^{\circ} + \overline{\pi}_p^{\ i} \tag{3.114a}$$

where

$$\overline{\pi}_p^{\circ} = \frac{1}{2V_p} \int_{V_p} \sum_{m=1}^{M} (\sigma_{ij})_m (\varepsilon_{ij})_m dV \tag{3.114b}$$

and

$$\overline{\pi}_p^{\ i} = \frac{1}{2V_p} \int_{V_p} \sum_{\substack{m=1 \\ m=n}}^{M} \sum_{n=1}^{M} (\sigma_{ij})_m (\varepsilon_{ij})_n dV \tag{3.114c}$$

The term $\overline{\pi}_p^{\circ}$ appearing in Equations 3.114 is the sum of the strain energies per unit initial volume, resulting from each set of surface tractions. The term $\overline{\pi}_p^{\ i}$ appearing in Equations 3.114 is the sum of the interaction strain energies per unit initial volume. The interaction strain energies being the strain energy determined for

the stress field from one set of surface tractions acting on the
strain field from another set of surface tractions.

The strain energy density of the particulate phase contained in
the representative volume, has been determined when the surface
tractions are of the form given by Equations 3.106. It will be
required that certain derivatives of $\bar{\pi}_p$ be known in order to
determine effective quantities such as the effective stress,
strain, compliance and stiffness tensors. The derivatives which
will be of interest when the effective strain tensor is known are

$$\frac{\partial \bar{\pi}_p}{\partial \bar{\epsilon}_{ij}} = \frac{\partial \bar{\pi}_p{}^o}{\partial \bar{\epsilon}_{ij}} + \frac{\partial \bar{\pi}_p{}^i}{\partial \bar{\epsilon}_{ij}} \qquad (3.115a)$$

$$\frac{\partial^2 \bar{\pi}_p}{\partial \bar{\epsilon}_{ij} \partial \bar{\epsilon}_{kl}} = \frac{\partial^2 \bar{\pi}_p{}^o}{\partial \bar{\epsilon}_{ij} \partial \bar{\epsilon}_{kl}} + \frac{\partial^2 \bar{\pi}_p{}^i}{\partial \bar{\epsilon}_{ij} \partial \bar{\epsilon}_{kl}} \qquad (3.115b)$$

For this case it is assumed that the relationship between the
specified surface tractions and the effective strain tensor are
known. Equations 3.114 are used to determine the derivatives
appearing in Equations 3.115. These derivatives are

$$\frac{\partial \bar{\pi}_p{}^o}{\partial \bar{\epsilon}_{pq}} = \frac{1}{2V_p} \int_{V_p} \left\{ \sum_{m=1}^{M} \frac{\partial (\sigma_{ij})_m}{\partial \bar{\epsilon}_{pq}} (\epsilon_{ij})_m \right.$$

$$\left. + (\sigma_{ij})_m \frac{\partial (\epsilon_{ij})}{\partial \bar{\epsilon}_{pq}} m \right\} \, dV \qquad (3.116a)$$

$$\frac{\partial \overline{\pi}_p^i}{\partial \overline{\epsilon}_{pq}} = \frac{1}{2V_p} \int\limits_{V_p} \sum_{\substack{m=1 \\ m=n}}^{M} \sum_{n=1}^{M} \left\{ \frac{\partial (\sigma_{ij})_m}{\partial \overline{\epsilon}_{pq}} (\epsilon_{ij})_m \right.$$

$$\left. + (\sigma_{ij})_m \frac{\partial (\epsilon_{ij})_n}{\partial \overline{\epsilon}_{pq}} \right\} dV \tag{3.116b}$$

$$\frac{\partial^2 \overline{\pi}_p^o}{\partial \overline{\epsilon}_{pq} \partial \overline{\epsilon}_{pq}} = \frac{1}{2V_p} \int\limits_{V_p} \sum_{m=1}^{M} \left\{ \frac{\partial^2 (\sigma_{ij})_m}{\partial \overline{\epsilon}_{pq} \partial \overline{\epsilon}_{pq}} (\epsilon_{ij})_m + 2 \frac{\partial (\sigma_{ij})_m}{\partial \overline{\epsilon}_{pq}} \frac{\partial (\epsilon_{ij})_m}{\partial \overline{\epsilon}_{rs}} \right.$$

$$\left. + (\sigma_{ij})_m \frac{\partial^2 (\epsilon_{ij})_m}{\partial \overline{\epsilon}_{pq} \partial \overline{\epsilon}_{rs}} \right\} dV \tag{3.116c}$$

$$\frac{\partial^2 \overline{\pi}_p^i}{\partial \overline{\epsilon}_{pq} \partial \overline{\epsilon}_{rs}} = \frac{1}{2V_p} \int\limits_{V_p} \sum_{m=1}^{M} \sum_{n=1}^{M} \left\{ \frac{\partial^2 (\sigma_{ij})_m}{\partial \overline{\epsilon}_{pq} \partial \overline{\epsilon}_{rs}} (\epsilon_{ij})_n \right.$$

$$+ \frac{\partial (\sigma_{ij})_m}{\partial \overline{\epsilon}_{pq}} \frac{\partial (\epsilon_{ij})_n}{\partial \overline{\epsilon}_{rs}} + \frac{\partial (\sigma_{ij})_m}{\partial \overline{\epsilon}_{rs}} \frac{\partial (\epsilon_{ij})_n}{\partial \overline{\epsilon}_{pq}}$$

$$\left. + (\sigma_{ij})_m \frac{\partial^2 (\epsilon_{ij})_n}{\partial \overline{\epsilon}_{pq} \partial \overline{\epsilon}_{rs}} \right\} dV \tag{3.116d}$$

In evaluating the derivatives of the global stress and strain tensors for surface tractions m, it is recognized that the only terms appearing the series solutions for these quantities which are dependent on the effective strain tensor, $\overline{\varepsilon}_{ij}$, are the constants, ξ_{2n} and η_{2n}. These constants are determined by the surface tractions and will change with respect to the effective strain tensor, $\overline{\varepsilon}_{ij}$. Using the chain rule of differentation and Equations 3.97 through 3.112 yields the following expressions for the derivatives of (σ_{ij})m and (ε_{ij})m, which appear in Equations 3.116.

$$\frac{\partial(\sigma_{ij})_m}{\partial\overline{\varepsilon}_{pq}} = \sum_{k=0}^{\infty} \left\{ \frac{\partial(\sigma_{ij})_m}{\partial(\xi_{2k})_m} \frac{\partial(\xi_{2k})_m}{\partial\overline{\varepsilon}_{pq}} + \frac{\partial(\sigma_{ij})_m}{\partial(\eta_{2k})_m} \frac{\partial(\eta_{2n})_m}{\partial\overline{\varepsilon}_{pq}} \right\} \quad (3.117a)$$

$$\frac{\partial(\varepsilon_{ij})_m}{\partial\overline{\varepsilon}_{pq}} = \sum_{k=0}^{\infty} \left\{ \frac{\partial(\varepsilon_{ij})_m}{\partial(\xi_{2k})_m} \frac{\partial(\xi_{2k})_m}{\partial\overline{\varepsilon}_{pq}} + \frac{\partial(\varepsilon_{ij})_m}{\partial(\eta_{2k})_m} \frac{\partial(\eta_{2k})_m}{\partial\overline{\varepsilon}_{pq}} \right\} \quad (3.117b)$$

$$\frac{\partial^2(\sigma_{ij})_m}{\partial\overline{\varepsilon}_{pq}\partial\overline{\varepsilon}_{rs}} = \sum_{k=0}^{\infty} \left\{ \frac{\partial(\sigma_{ij})_m}{\partial(\xi_{2k})_m} \frac{\partial^2(\xi_{2k})_m}{\partial\overline{\varepsilon}_{pq}\partial\overline{\varepsilon}_{rs}} \right.$$

$$\left. + \frac{\partial(\sigma_{ij})_m}{\partial(\eta_{2k})_m} \frac{\partial^2(\eta_{2k})_m}{\partial\overline{\varepsilon}_{pq}\partial\overline{\varepsilon}_{rs}} \right\} \quad (3.117c)$$

$$\frac{\partial^2 (\varepsilon_{ij})_m}{\partial \varepsilon_{pq} \partial \varepsilon_{rs}} = \sum_{k=0}^{\infty} \left\{ \frac{\partial (\varepsilon_{ij})_m}{\partial (\xi_{2k})_m} \frac{\partial^2 (n_{2k})_m}{\partial \varepsilon_{pq} \partial \varepsilon_{rs}} \right.$$

$$\left. + \frac{\partial (\varepsilon_{ij})_m}{\partial (n_{2k})_m} \frac{\partial^2 (n_{2k})_m}{\partial \varepsilon_{pq} \partial \varepsilon_{rs}} \right\} \qquad (3.117d)$$

where

$(\xi_{2k})_m$, $(n_{2k})_m$ = the constants determined from the specified

surface tractions for contact number m.

The expressions given by Equations 3.117 are evaluated by replacing

the constants $(\xi_{2k})_m$ and $(n_{2k})_m$, appearing in the series solutions for

$(\sigma_{ij})_m$ and $(\varepsilon_{ij})_m$, by the proper derivatives of these quantities. The

substitutions in the series solutions to $(\sigma_{ij})_m$ and $(\varepsilon_{ij})_m$, necessary

to evaluate Equations (3.117) are summarized in Table 3.1.

The other case which will arise is that when the effective stress

tensor, $\bar{\sigma}_{ij}$, is known. For this case the derivatives of the strain

energy density of the particulate phase, $\bar{\pi}_p$, which will be required

are

$$\frac{\partial \bar{\pi}_p}{\partial \bar{\sigma}_{ij}} = \frac{\partial \bar{\pi}_p^0}{\partial \bar{\sigma}_{ij}} + \frac{\partial \bar{\pi}_p^i}{\partial \bar{\sigma}_{ij}} \qquad (3.118a)$$

$$\frac{\partial^2 \bar{\pi}_p}{\partial \bar{\sigma}_{ij} \partial \bar{\sigma}_{kl}} = \frac{\partial^2 \bar{\pi}_p^0}{\partial \bar{\sigma}_{ij} \partial \bar{\sigma}_{kl}} + \frac{\partial^2 \bar{\pi}_p^i}{\partial \bar{\sigma}_{ij} \partial \bar{\sigma}_{kl}} \qquad (3.118b)$$

Table 3.1. Evaluation of Derivatives of the Global Stress and Strain Tensors with Respect to the Effective Strain Tensor, for a Single Set of Surface Tractions.

	Substitutions into series solutions for $(\sigma_{ij})_m$ and $(\varepsilon_{ij})_m$	
Derivative	Replace $(\varepsilon_{2k})_m$ by	Replace $(\eta_{2k})_m$ by
$\dfrac{\partial(\sigma_{ij})_m}{\partial\bar{\varepsilon}_{pq}}$	$\dfrac{\partial(\varepsilon_{2k})_m}{\partial\bar{\varepsilon}_{pq}}$	$\dfrac{\partial(\eta_{2k})_m}{\partial\bar{\varepsilon}_{pq}}$
$\dfrac{\partial(\varepsilon_{ij})_m}{\partial\bar{\varepsilon}_{pq}}$	$\dfrac{\partial(\varepsilon_{2k})_m}{\partial\bar{\varepsilon}_{pq}}$	$\dfrac{\partial(\eta_{2k})_m}{\partial\bar{\varepsilon}_{pq}}$
$\dfrac{\partial^2(\sigma_{ij})_m}{\partial\bar{\varepsilon}_{pq}\partial\bar{\varepsilon}_{rs}}$	$\dfrac{\partial^2(\varepsilon_{2k})_m}{\partial\bar{\varepsilon}_{pq}\partial\bar{\varepsilon}_{rs}}$	$\dfrac{\partial^2(\eta_{2k})_m}{\partial\bar{\varepsilon}_{pq}\partial\bar{\varepsilon}_{rs}}$
$\dfrac{\partial^2(\varepsilon_{ij})_m}{\partial\bar{\varepsilon}_{pq}\partial\bar{\varepsilon}_{rs}}$	$\dfrac{\partial^2(\varepsilon_{2k})_m}{\partial\bar{\varepsilon}_{pq}\partial\bar{\varepsilon}_{rs}}$	$\dfrac{\partial^2(\eta_{2k})_m}{\partial\bar{\varepsilon}_{pq}\partial\bar{\varepsilon}_{rs}}$

To evaluate the derivatives appearing in Equations 3.118, it is
assumed that the relationship between the specified surface
tractions and the effective stress tensor are known. Use of
Equations 3.114 result in the following expressions for the
derivatives appearing in Equations 3.118.

$$\frac{\partial \bar{\pi}_p{}^0}{\partial \overline{\sigma}_{pq}} = \frac{1}{2V_p} \int_{V_p} \sum_{m=1}^{M} \left\{ \frac{\partial (\sigma_{ij})_m}{\partial \overline{\sigma}_{pq}} (\sigma_{ij})_m + \right.$$

$$\left. \partial(\varepsilon_{ij})_m \frac{\partial (\varepsilon_{ij})_m}{\partial \overline{\sigma}_{pq}} \right\} dV \qquad (3.119a)$$

$$\frac{\partial \bar{\pi}_p{}^i}{\partial \overline{\sigma}_{pq}} = \frac{1}{2V_p} \int_{V_p} \sum_{\substack{m=1 \\ m \neq n}}^{M} \sum_{n=1}^{M} \left\{ \frac{\partial (\sigma_{ij})}{\partial \overline{\sigma}_{pq}} (\varepsilon_{ij})_n + \right.$$

$$\left. (\sigma_{ij})_m \frac{\partial (\varepsilon_{ij})_n}{\partial \overline{\sigma}_{pq}} \right\} dV \qquad (3.119b)$$

$$\frac{\partial^2 \bar{\pi}_p{}^0}{\partial \overline{\sigma}_{pq} \partial \overline{\sigma}_{rs}} = \frac{1}{2V_p} \int_{V_p} \left\{ \sum_{m=1}^{M} \frac{\partial^2 (\sigma_{ij})}{\partial \overline{\sigma}_{pq} \partial \overline{\sigma}_{rs}} (\varepsilon_{ij})_m + \right.$$

$$\left. 2 \frac{\partial (\sigma_{ij})_m}{\partial \overline{\sigma}_{pq}} \frac{\partial (\varepsilon_{ij})_m}{\partial \overline{\sigma}_{rs}} + (\sigma_{ij}) \frac{\partial^2 (\varepsilon_{ij})_m}{\partial \overline{\sigma}_{pq} \partial \overline{\sigma}_{rs}} \right\} dV \qquad (3.119c)$$

$$\frac{\partial^2 \overline{\pi}_p i}{\partial \overline{\sigma}_{pq} \partial \overline{\sigma}_{rs}} = \frac{1}{2 V_p} \int\limits_{V_p} \sum_{m=1}^{M} \sum_{n=1}^{M} \left\{ \frac{\partial^2 (\sigma_{ij})_m}{\partial \overline{\sigma}_{pq} \partial \overline{\sigma}_{rs}} \ (\varepsilon_{ij})_n + \right.$$

$$\frac{\partial (\sigma_{ij})_m}{\partial \overline{\sigma}_{pq}} \cdot \frac{\partial (\varepsilon_{ij})_n}{\partial \overline{\sigma}_{rs}} + \frac{\partial (\sigma_{ij})_m}{\partial \overline{\sigma}_{rs}} \ \frac{\partial (\varepsilon_{ij})_n}{\partial \overline{\sigma}_{pq}} +$$

$$\left. (\sigma_{ij})_m \ \frac{\partial^2 (\varepsilon_{ij})_n}{\partial \overline{\sigma}_{pq} \partial \overline{\sigma}_{rs}} \right\} \ dV \tag{3.119d}$$

In evaluating the derivatives of the global stress and strain tensors for surface tractions m, it is recognized that the only terms appearing in the series solutions for these quantities which will depend on the effective stress tensor, $\overline{\sigma}_{ij}$, are the constants ξ_{2n} and η_{2n}. These constants are determined by the surface tractions and will change with respect to the effective stress tensor, $\overline{\sigma}_{ij}$. Using the chain rule of differentiation and Equations 3.97 through 3.112 yields the following expressions for the derivatives of $(\sigma_{ij})_m$ and $(\varepsilon_{ij})_m$, which appear in Equation 3.119.

$$\frac{\partial (\sigma_{ij})_m}{\partial \overline{\sigma}_{pq}} = \sum_{k=0}^{\infty} \left\{ \frac{\partial (\sigma_{ij})_m}{\partial (\xi_{2k})_m} \ \frac{\partial (\xi_{2k})_m}{\partial \overline{\sigma}_{pq}} + \frac{\partial (\sigma_{ij})_m}{\partial (\eta_{2k})_m} \ \frac{\partial (\eta_{2k})_m}{\partial \overline{\sigma}_{pq}} \right\} \tag{3.120a}$$

$$\frac{\partial (\varepsilon_{ij})_m}{\partial \overline{\sigma}_{pq}} = \sum_{k=0}^{\infty} \left\{ \frac{\partial (\varepsilon_{ij})_m}{\partial (\xi_{2k})_m} \ \frac{\partial (\xi_{2k})_m}{\partial \overline{\sigma}_{pq}} + \frac{\partial (\varepsilon_{ij})_m}{\partial (\eta_{2k})_m} \ \frac{\partial (\eta_{2k})_m}{\partial \overline{\sigma}_{pq}} \right\} \tag{3.120b}$$

$$\frac{\partial^2(\sigma_{ij})_m}{\partial\overline{\sigma}_{pq}\partial\overline{\sigma}_{rs}} = \sum_{k=0}^{\infty}\left\{\frac{\partial(\sigma_{ij})_m}{\partial(\xi_{2k})_m}\frac{\partial^2(\xi_{2k})_m}{\partial\overline{\sigma}_{pq}\partial\overline{\sigma}_{rs}} + \frac{\partial(\sigma_{ij})_m}{\partial(\eta_{2k})_m}\frac{\partial^2(\eta_{2k})_m}{\partial\overline{\sigma}_{pq}\partial\overline{\sigma}_{rs}}\right\} \quad (3.120c)$$

$$\frac{\partial^2(\epsilon_{ij})_m}{\partial\overline{\sigma}_{pq}\partial\overline{\sigma}_{rs}} = \sum_{k=0}^{\infty}\left\{\frac{\partial^2(\epsilon_{ij})_m}{\partial(\xi_{2k})_m}\frac{\partial^2(\xi_{2k})_m}{\partial\overline{\sigma}_{pq}\partial\overline{\sigma}_{rs}} + \frac{\partial(\epsilon_{ij})_m}{\partial(\xi_{2k})_m}\frac{\partial^2(\xi_{2k})_m}{\partial\overline{\sigma}_{pq}\partial\overline{\sigma}_{rs}}\right\} \quad (3.120d)$$

The expressions given in Equations 3.120 are evaluated by replacing the constants, $(\xi_{2k})_m$ and $(\eta_{2k})_m$, appearing in the series solutions for $(\sigma_{ij})_m$ and $(\epsilon_{ij})_m$, by the proper derivatives of these quantities. The substitutions in the series solutions to $(\sigma_{ij})_m$ and $(\epsilon_{ij})_m$, necessary to evaluate Equations 3.120 are summarized in Table 3.2. The constants, ξ_{2k} and η_{2k}, and their derivatives will be determined for the surface tractions under consideration.

Surface Tractions Resulting From an Uniform Pressure Acting on the Surface of the Sphere

The constants, ξ_{2n} and η_{2n}, which are determined from the specified surface tractions will be determined for the case of a uniform pressure, $\overline{P}_m$, acting on the surface of a sphere. This situation is shown in Figure 3.10. For this case the specified surface tractions of the form given by Equations 3.106 are

$$\sigma_{11}'(R,\cos(z_2)) = -\overline{P}_m, \quad 0 \leq z_2 \leq \pi \quad (3.121a)$$

$$\sigma_{12}'(R,\cos(z_2)) = 0, \quad 0 \leq z_2 \leq \pi \quad (3.121b)$$

The constants, ξ_{2n} and η_{2n}, which result from these surface tractions are determined by Equations 3.107. For the surface

Table 3.2. Evaluation of Derivatives of the Global Stress and Strain Tensors with Respect to the Effective Stress Tensor, for a Single Set of Surface Tractions.

Derivative	Substitutions into series solutions for $(\sigma_{ij})_m$ and $(\varepsilon_{ij})_m$	
	Replace $(\varepsilon_{2k})_m$ by	Replace $(\eta_{2k})_m$ by
$\dfrac{\partial(\sigma_{ij})_m}{\partial\overline{\sigma}_{pq}}$	$\dfrac{\partial(\varepsilon_{2k})_m}{\partial\overline{\sigma}_{pq}}$	$\dfrac{\partial(\eta_{2k})_m}{\partial\overline{\sigma}_{pq}}$
$\dfrac{\partial(\varepsilon_{ij})_m}{\partial\overline{\sigma}_{pq}}$	$\dfrac{\partial(\varepsilon_{2k})_m}{\partial\overline{\sigma}_{pq}}$	$\dfrac{\partial(\eta_{2k})_m}{\partial\overline{\sigma}_{pq}}$
$\dfrac{\partial^2(\sigma_{ij})_m}{\partial\overline{\sigma}_{pq}\partial\overline{\sigma}_{rs}}$	$\dfrac{\partial^2(\varepsilon_{2k})_m}{\partial\overline{\sigma}_{pq}\partial\overline{\sigma}_{rs}}$	$\dfrac{\partial^2(\varepsilon_{2k})_m}{\partial\overline{\sigma}_{pq}\partial\overline{\sigma}_{rs}}$
$\dfrac{\partial^2(\varepsilon_{ij})_m}{\partial\overline{\sigma}_{pq}\partial\overline{\sigma}_{rs}}$	$\dfrac{\partial^2(\varepsilon_{2k})_m}{\partial\overline{\sigma}_{pq}\partial\overline{\sigma}_{rs}}$	$\dfrac{\partial^2(\eta_{2k})_m}{\partial\overline{\sigma}_{pq}\partial\overline{\sigma}_{rs}}$

Figure 3.10 -- Uniform Pressure $\bar{P}_m$ Acting on Surface of Sphere.

tractions appearing in Equations 3.121, the constants, ξ_{2n} and η_{2n}, are given by

$$\xi_{2n} = -\frac{(4n+1)}{2}\overline{P}_m \int_{-1}^{1} P_{2n}(s)\,ds, \quad n=0,1,2,\ldots \quad (3.122a)$$

$$\eta_{2n} = 0, \quad n=1,2,3,\ldots \quad (3.122b)$$

In Equations 3.122, the constants K^σ and $\overline{\varepsilon_2}$, which appear in Equations 3.107, have been taken as 1 and $\pi/2$, respectively. The integral appearing in Equation 3.122a was extended to $-\pi \leq \overline{\varepsilon_2} \leq 0$ so that the following orthogonality relationship for Legrendre polynominals could be employed.

$$\int_{1}^{1} P_m(s)\, P_n(s)\, ds = \begin{cases} 0, & m \neq n \\ \frac{2}{2n+1}, & m=n \end{cases} \quad (3.123)$$

Evaluating Equation 3.122a in accordance with Equation 3.123 yields

$$\xi_0 = -\overline{P}_m \quad (3.124a)$$

$$\xi_{2n} = 0, \quad n=1,2,3,\ldots \quad (3.124b)$$

The derivatives of ξ_{2n} and η_{2n}, required to evaluate the terms appearing in Table 3.1 are

$$\frac{\partial \xi_0}{\partial \overline{\varepsilon}_{pq}} = \frac{\partial \overline{P}_m}{\partial \overline{\varepsilon}_{pq}} \quad (3.125a)$$

$$\frac{\partial \xi_{2n}}{\partial \overline{\varepsilon}_{pq}} = 0, \quad n=1,2,3,\ldots \quad (3.125b)$$

$$\frac{\partial \eta_{2n}}{\partial \overline{\epsilon}_{pq}} = 0, \ n=1,2,3,\ldots \tag{3.125c}$$

$$\frac{\partial^2 \xi_0}{\partial \overline{\epsilon}_{pq} \partial \overline{\epsilon}_{rs}} = \frac{\partial^2 \overline{P}_m}{\partial \overline{\epsilon}_{pq} \partial \overline{\epsilon}_{rs}} \tag{3.125d}$$

$$\frac{\partial^2 \xi_{2n}}{\partial \overline{\epsilon}_{pq} \partial \overline{\epsilon}_{rs}} = 0, \ n=1,2,3,\ldots \tag{3.125e}$$

$$\frac{\partial^2 \eta_{2n}}{\partial \overline{\epsilon}_{pq} \partial \overline{\epsilon}_{rs}} = 0, \ n=1,2,3,\ldots \tag{3.125f}$$

The derivatives of ξ_{2n} and η_{2n}, required to evaluate the terms appearing in Table 3.2 are

$$\frac{\partial \xi_0}{\partial \overline{\sigma}_{pq}} = -\frac{\partial \overline{P}_m}{\partial \overline{\sigma}_{pq}} \tag{3.126a}$$

$$\frac{\partial \xi_{2n}}{\partial \overline{\sigma}_{pq}} = 0, \ n=1,2,3,\ldots \tag{3.126b}$$

$$\frac{\partial \eta_{2n}}{\partial \overline{\sigma}_{pq}} = 0, \ n=1,2,3,\ldots \tag{3.126c}$$

$$\frac{\partial^2 \epsilon_0}{\partial \bar{\sigma}_{pq} \partial \bar{\sigma}_{rs}} = \frac{\partial^2 \bar{P}_m}{\partial \bar{\sigma}_{pq} \partial \bar{\sigma}_{rs}} \tag{3.126d}$$

$$\frac{\partial^2 \epsilon_{2n}}{\partial \bar{\sigma}_{pq} \partial \bar{\sigma}_{rs}} = 0, \quad n=1,2,3,\ldots \tag{3.126e}$$

$$\frac{\partial^2 \eta_{2n}}{\partial \bar{\sigma}_{pq} \partial \bar{\sigma}_{rs}} = 0, \quad n=1,2,3,\ldots \tag{3.126f}$$

To evaluate the derivatives appearing in Equations 3.125 and 3.126, the relationship between the pressure, $\bar{P}_m$, and the effective strain or stress tensors must be known. This relationship will be developed in a later section.

Surface Tractions Resulting From the Contact Between Adjacent Spheres

The constants, ξ_{2n} and η_{2n}, which result from the specified surface tractions will be determined for the case of contact of a single sphere with two adjacent spheres. The spheres make contact along an axis of symmetry as shown in Figure 3.11. The constants ξ_{2n} and η_{2n} will be determined for the center sphere shown in Figure 3.11. Surface tractions of the form given by Equations 3.106 which result from the contact with two neighboring spheres are
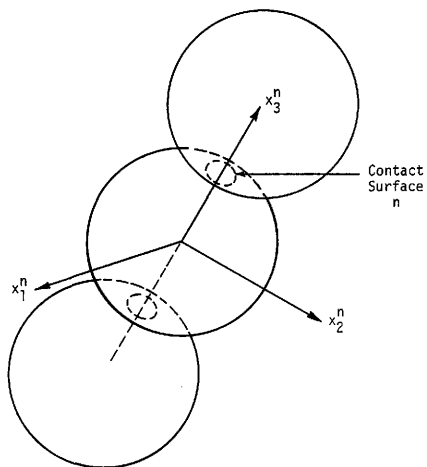
Figure 3.11 -- Three Spheres in Contact Along an Axis
of Symmetry.

$$\sigma_{11}{}' = \begin{cases} -K^{\sigma}[\cos^2(\bar{z}_2) - \cos^2(\bar{\bar{z}}_2)]^{1/2}\cos^2(\bar{z}_2), & 0 \le \bar{z}_2 \le \bar{\bar{z}}_2, \ \pi - \bar{\bar{z}}_2 \le \bar{z}_2 \le \pi \\ \\ 0 & \bar{\bar{z}}_2 < \bar{z}_2 < \pi - \bar{\bar{z}}_2 \end{cases}$$

$$(3.127a)$$

$$\sigma_{12} = \begin{cases} K^{\sigma}[\cos^2(\bar{z}_2) - \cos^2(\bar{\bar{z}}_2)]^{1/2}\sin(\bar{z}_2)\cos(\bar{z}_2), & 0 \le \bar{z}_2 \le \bar{\bar{z}}_2, \le \pi - \bar{\bar{z}}_2 \le \bar{z}_2 \le \pi \\ \\ 0, & \bar{\bar{z}}_2 \le \bar{z}_2 \le \pi - \bar{\bar{z}}_2 \end{cases}$$

$$(3.127b)$$

where

$$K^{\sigma} = \frac{2E}{\pi(1-\nu^2)}$$

$$(3.127c)$$

and

$\bar{\bar{z}}_2$ = the angle defining the contact surface as shown in Figure 3.11.

Details of the determination of the surface tractions given in Equations 3.127 appear in Appendix C. The surface tractions given by Equations 3.127 exist only when the spheres appearing in Figure 3.11 are being pressed together by a compressive force. The angle, $\bar{\bar{z}}_2$, defining the contact surface is dependent on the total compressive force transmitted through the contact. This dependence is given by

$$\bar{\bar{z}}_2 = \sin^{-1}\left[\left(\frac{3(1-\nu^2)F_c}{4R^2E}\right)^{1/3}\right]$$

$$(3.128)$$

where F_c = the total compressive force transmitted through the contact,

ν = Poisson's ratio,

E = Young's modulus, and

R = the radius of the sphere.

For the surface tractions given by Equations 3.127, the constants ξ_{2n} and η_{2n} are given by

$$\xi_{2n} = -(4n+1) \int_{\cos(\overline{z}_2)}^{1} \sqrt{s^2 - \cos^2(\overline{z}_2)} \; s^2 P_{2n}(s)ds, \qquad (3.129a)$$

$n = 0,1,2,\ldots$

$$N_{2n} = \frac{(4n+1)}{4n(2n+1)} \int_{\cos(\overline{z}_2)}^{1} \sqrt{s^2 - \cos^2(\overline{z}_2)} \; (1-s^2)s \; P'_{2n}(s)ds, \qquad (3.129b)$$

$n = 1,2,3,\ldots$

where

s = a dummy variable of integration.

In determining the required derivatives of the constants ξ_{2n} and η_{2n} as given by Equations 3.129, it is recognized that the angle, $\overline{z}_2$, which defines the contact surface varies with the compressive force F_c. The angle $\overline{z}_2$ is the only term appearing in Equations 3.129 which will vary with the effective strain and effective stress tensors. Using the chain rule of differentiation the derivatives required to evaluate the terms appearing in Table 3.1 are

$$\frac{\partial \xi_{2k}}{\partial \overline{\epsilon}_{pq}} = \frac{\partial \xi_{2k}}{\partial (\cos(\overline{z}_2))} \; \frac{\partial(\cos(\overline{z}_2))}{\partial \overline{\epsilon}_{pq}} \qquad (3.130a)$$

$$\frac{\partial n_{2k}}{\partial \overline{\epsilon_{pq}}} = \frac{\partial n_{2k}}{\partial(\cos(\overline{z}_2))} \; \frac{\partial(\cos(\overline{z}_2))}{\partial \overline{\epsilon_{pq}}} \tag{3.130b}$$

$$\frac{\partial^2 \xi_{2k}}{\partial \overline{\epsilon_{pq}} \partial \overline{\epsilon_{rs}}} = \frac{\partial^2 \xi_{2k}}{\partial^2(\cos(\overline{z}_2))} \; \frac{\partial(\cos(\overline{z}_2))}{\partial \overline{\epsilon_{pq}}} \; \frac{\partial(\cos(\overline{z}_2))}{\partial \overline{\epsilon_{rs}}}$$

$$+ \frac{\partial \xi_{2k}}{\partial(\cos(\overline{z}_2))} \; \frac{\partial^2(\cos(\overline{z}_2))}{\partial \overline{\epsilon_{pq}} \partial \overline{\epsilon_{rs}}} \tag{3.130c}$$

$$\frac{\partial^2 n_{2k}}{\partial \overline{\epsilon_{pq}} \partial \overline{\epsilon_{rs}}} = \frac{\partial^2 n_{2k}}{\partial^2(\cos(\overline{z}_2))} \; \frac{\partial(\cos(\overline{z}_2))}{\partial \overline{\epsilon_{pq}}} \; \frac{\partial(\cos(\overline{z}_2))}{\partial \overline{\epsilon_{rs}}} \tag{3.130d}$$

$$+ \frac{\partial n_{2k}}{\partial(\cos(\overline{z}_2))} \; \frac{\partial^2(\cos(\overline{z}_2))}{\partial \overline{\epsilon_{pq}} \partial \overline{\epsilon_{rs}}}$$

The derivatives required to evaluate the terms appearing in Table 3.2 are

$$\frac{\partial \xi_{2k}}{\partial \overline{\sigma_{pq}}} = \frac{\partial \xi_{2k}}{\partial(\cos(\overline{z}_2))} \; \frac{\partial(\cos(\overline{z}_2))}{\partial \overline{\sigma_{pq}}} \tag{3.131a}$$

$$\frac{\partial n_{2k}}{\partial \overline{\sigma_{pq}}} = \frac{\partial n_{2k}}{\partial(\cos(\overline{z}_2))} \; \frac{\partial(\cos(\overline{z}_2))}{\partial \overline{\sigma_{pq}}} \tag{3.131b}$$

$$\frac{\partial^2 \xi_{2k}}{\partial \overline{\sigma_{pq}} \partial \overline{\sigma_{rs}}} = \frac{\partial^2 \xi_{2k}}{\partial^2(\cos(\overline{z}_2))} \; \frac{\partial(\cos(\overline{z}_2))}{\partial \overline{\sigma_{pq}}} \; \frac{\partial(\cos(\overline{z}_2))}{\partial \overline{\sigma_{rs}}} \tag{3.131c}$$

$$+ \frac{\partial \xi_{2k}}{\partial(\cos(\overline{z}_2))} \; \frac{\partial^2(\cos(\overline{z}_2))}{\partial \overline{\sigma_{pq}} \partial \overline{\sigma_{rs}}}$$

$$\frac{\partial^2 n_{2k}}{\partial \overline{\sigma}_{pq} \partial \overline{\sigma}_{rs}} = \frac{\partial^2 n_{2k}}{\partial^2(\cos(\overline{z}_2))} \quad \frac{\partial(\cos(\overline{z}_2))}{\partial \overline{\sigma}_{pq}} \quad \frac{\partial(\cos(\overline{z}_2))}{\partial \overline{\sigma}_{rs}} \tag{3.131d}$$

$$+ \frac{\partial n_{2k}}{\partial(\cos(\overline{z}_2))} \quad \frac{\partial^2(\cos(\overline{z}_2))}{\partial \overline{\sigma}_{pq} \partial \overline{\sigma}_{rs}}$$

The derivatives of ξ_{2k} and n_{2k} with respect to $\cos(\overline{z}_2)$, may be determined using Equations 3.129. Using Leibnitz's rule for differentiation of an integral gives

$$\frac{\partial \xi_{2k}}{\partial(\cos(\overline{z}_2))} = (4k+1)\cos(\overline{z}_2)\left\{ \sqrt{1-\cos^2(\overline{z}_2)} \right. \tag{3.132a}$$

$$\left. - \int_{\cos(\overline{z}_2)}^{1} \sqrt{s^2-\cos^2(\overline{z}_2)} \ [P_{2k}(s)+Ps_{2k}(s)] \ ds \right\}$$

$$\frac{\partial n_{2k}}{\partial(\cos(\overline{z}_2))} = \frac{(4k+1)\cos(\overline{z}_2)}{2} \int_{\cos(\overline{z}_2)}^{1} \sqrt{s^2-\cos^2(\overline{z}_2)} \ P_{2k}(s) \ ds \tag{3.132b}$$

$$\frac{\partial^2 \xi_{2k}}{\partial^2(\cos(\bar{z}_2))} = \frac{1}{\cos(\bar{z}_2)} \frac{\partial \xi_{2k}}{(\cos(\bar{z}_2))} + (4k+1) \cos^2(\bar{z}_2) \left\{ \right.$$

$$[1 + P'_{2k}(1)] \log_e \left[\frac{\sqrt{1-\cos^2(\bar{z}_2)} + 1}{\cos(\bar{z}_2)} \right] - \frac{1}{\sqrt{1-\cos^2(\bar{z}_2)}}$$

$$- \int_{\cos(\bar{z}_2)}^{1} \log_e \left[\frac{\sqrt{s^2-\cos^2(\bar{z}_2)} + s}{\cos(\bar{z}_2)} \right] \left[2 P'_{2k}(s) + s P''_{2k}(s) \right] ds \left. \right\} \quad (3.132c)$$

$$\frac{\partial^2 \xi_{2k}}{\partial^2(\cos(\bar{z}_2))} = \frac{1}{(\cos(\bar{z}_2))} \frac{\partial \eta_{2k}}{(\cos(\bar{z}_2))} + \frac{(4k+1) \cos^2(\bar{z}_2)}{2} \left\{ \right.$$

$$\log_e \left[\frac{\sqrt{1-\cos^2(\bar{z}_2)} + 1}{\cos(\bar{z}_2)} \right]$$

$$- \int_{\cos(\bar{z}_2)}^{1} \log_e \left[\frac{\sqrt{2-\cos^2(\bar{z}_2)} + s}{\cos(\bar{z}_2)} \right] P'_{2k}(s) \, ds \left. \right\} \quad (3.132d)$$

In order to evaluate Equations 3.130 and 3.131, the relationships between $\cos(\bar{z}_2)$ and the effective stress and strain tensors is required. An approximation for these relationships will be given in a later section.

Surface Tractions Resulting From the Mixture Phase Acting as a Binder Between Adjacent Spheres

The constants, ξ_{2n} and η_{2n}, which result from the specified surface traction will be determined for the case of the mixture phase acting as a binder between adjacent spheres. The mixture phase acts as a binder between three spheres as shown in Figure 3.12. The binder acts along an axis of symetry. Surface tractions of the form given by Equations 1.106 which result from the situation shown in Figure 3.12 are

$$
\sigma_{11}' = \begin{cases} \dfrac{K_b{}^\sigma F_b[\cos^2(z_2) - \cot^2(\phi_b)\,\sin^2(z_2)][(1 - K_\rho)\csc(\bar{z}_2)}{\sqrt{\cos^2(z_2) - \cos^2(\bar{z}_2)}} + K_\rho], & 0 \leq z_2 \leq \bar{z}_2,\ \pi - \bar{z}_2 \leq z_2 \leq \pi \\[2mm] 0, & \bar{z}_2 \leq z_2 \leq \pi - \bar{z}_2 \end{cases}
$$
(3.133a)

$$
\sigma_{12}' = \begin{cases} \dfrac{-K_b{}^\sigma F_b \csc^2(\phi_b)\,\sin(z_2)\cos(z_2)[(1 - K_\rho)\csc(\bar{z}_2)}{\sqrt{\cos^2(z_2) - \cos^2(\bar{z}_2)}} + K_\rho], & 0 \leq z_2 \leq \bar{z}_2,\ \pi - \bar{z}_2 \leq z_2 \leq \pi \\[2mm] 0, & \bar{z}_2 \leq z_2 \leq \pi - \bar{z}_2 \end{cases}
$$
(3.133b)
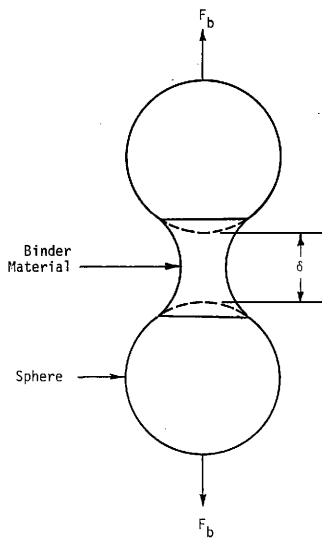
Figure 3.12 -- Mixture Phase Acting as a Binder
Between Neighboring Spheres.

$$K_b^{\sigma} = \frac{\csc^2(\bar{z}_2)}{\pi R^2 [2/3 + (\tfrac{1}{3}\pi - \bar{z}_2) \sec(\bar{z}_2)]} \tag{3.133c}$$

$$K = (\tfrac{1}{3}\pi - \bar{z}_2) \sec(\bar{z}_2) \tag{3.133d}$$

$$\emptyset_b = \pi/2 - (\pi/2 - \bar{z}_2)(z_2/\bar{z}_2)^2 \tag{3.133e}$$

and

   R = the radius of the spheres, and

   F_b = the total force transmitted through the mixture phase, and

   $\bar{z}_2$ = the angle defining the surface area of the sphere on which

      the mixture phase acts, and

   ϕ_b = an angle defining the approximate direction of the surface

      traction vector on the sphere.

The surface tractions given by Equations 3.133 are approximate.

Details of the determination of the surface tractions given by

Equations 3.133 appear in Appendix D. To evaluate the surface

tractions given by Equations 3.133, the total force, F_b, transmitted

by the mixture phase must be known. Cases may arise when the

displacement between the spheres, δ, is known rather than the force,

F_b. The force-displacement relationship for the mixture phase is

$$F_b = k_b \delta \tag{1.34}$$

where

k_b = the elastic spring constant for the mixture phase.

The spheres are assumed to be initially in contact under no load conditions. For this situation, the initial volume of the mixture phase for a single contact locations is given by

$$V_m = 2\pi R^3 \left\{ \left[1 - \cos(\bar{z}_2) \right] \left[\sin^2(\bar{z}_2) \; \frac{(1-\cos(\bar{z}_2))(2+\cos(\bar{z}_2))}{6} \right] \right.$$

$$- \left[\sec(\bar{z}_2) - 1 \right]^2 \left[\frac{\tan(\bar{z}_2)}{2} (\pi-2\bar{z}_2 - \sin(\pi-2\bar{z}_2) \right.$$

$$\left. + 2/3 \left[\sec(\bar{z}_2)-1 \right] \sin^3(\pi/2 - \bar{z}_2) \right\} \qquad (3.135)$$

The degree of saturation, D_s, is defined as the ratio of the volume of the mixture phase to the available volume for the mixture phase. In terms of the volume fractions of the two phases, the degree of saturation is

$$D_s = \frac{C_m}{(1-C_p)} \qquad (3.136)$$

where

C_m = the initial volume fraction of the mixture phase, and

C_p = the initial volume fraction of the particle phase.

The maximum values that the angle, $\bar{z}_2$, defining the surface area of the sphere covered by the binder material, are dependent on the sphere packing geometry. Maximum values of the angle, $\bar{z}_2$ for the different

packing configurations appear in Table 3.3. The surface tractions given by Equations 3.133 are valid for values of $\bar{z}_2$ less than or equal to those listed in Table 3.3. In the case that the volume of the mixture phase is greater than that given by Equation 3.135, only the volume of material as given by Equation 3.135, for the maximum values of the angle, $\bar{z}_2$, appearing in Table 3.3, will act as a binder between neighboring spheres. The remaining volume of the mixture phase will recognize changes in pressure only.

The constants ξ_{2n} and η_{2n}, which arise from the surface tractions given by Equations 3.133 are

$$\xi_{2n} = (4n+1)F_b \int_{\cos(\bar{z}_2)}^{1} [(1 + h(s)) s^2 - h(s)][(\pi/2 - \bar{z}_2) \sec(\bar{z}_2)$$

$$+ 1 - \sqrt{s^2 - \cos^2(\bar{z}_2)}] P_{2n}(s) \, dS \qquad (3.137a)$$

$$\eta_{2n} = \frac{-(4n+1)}{4n(2n+1)} F_b \int_{\cos(\bar{z}_2)}^{1} (1 + h(s))[(\pi/2 - \bar{z}_2) \sec (\bar{z}_2) + 1$$

$$- s^2 - \cos^2(\bar{z}_2) (1 - s^2)s \, P'_{2n}(s) \, ds \qquad (3.137b)$$

where

$$h(s) = \cot^2 [\pi/2 - (\pi/2 - \bar{z}_2)(\cos^{-1}(s)/\bar{z}_2)^2] \qquad (3.137c)$$

Table 3.3. Maximum Values of the Degree of Saturation, D_s, and the Angle, $\bar{z}_m^b$, for the Case of the Mixture Phase Acting as a Binder.

Configuration	Maximum Degree of Saturation D_s	Maximum Angle $\bar{z}_m^b$
Simple Cubic	8%	45°
Orthorhombic	11%	30°
Tetragonal-Spheroidal	20%	30°
Rhombohedral	32%	30°

and

    s = a dummy variable of integration.

For the surface tractions being considered, it is assumed that the

angle $\bar{\varepsilon}_2$ remains constant during deformation. Therefore, only the

force transmitted by the mixture phase, F_b, is dependent on the global

stress and strain tensors. In view of this, the derivatives of ξ_{2n}

and η_{2n} required to evaluate Table 3.1 are given by

$$\frac{\partial \xi_{2n}}{\partial \varepsilon_{pq}} = \frac{\xi_{2n}}{F_b} \frac{\partial F_b}{\partial \varepsilon_{pq}} \;,\; n=0,\, 1,\, 2,\, \ldots \ldots \tag{3.138a}$$

$$\frac{\partial \eta_{2n}}{\partial \varepsilon_{pq}} = \frac{\eta_{2n}}{F_b} \frac{\partial F_b}{\partial \varepsilon_{pq}} \;,\; n=1,\, 2,\, 3,\, \ldots \ldots \tag{3.138b}$$

$$\frac{\partial^2 \xi_{2n}}{\partial \varepsilon_{pq} \partial \varepsilon_{rs}} = \frac{\xi_{2n}}{F_b} \frac{\partial^2 F_b}{\partial \varepsilon_{pq} \partial \varepsilon_{rs}} \;,\; n=0,\, 1,\, 2,\, \ldots \ldots \tag{3.138c}$$

$$\frac{\partial^2 \eta_{2n}}{\partial \varepsilon_{pq} \partial \varepsilon_{rs}} = \frac{\eta_{2n}}{F_b} \frac{\partial F_b}{\partial \varepsilon_{pq} \partial \varepsilon_{rs}} \;,\; n=1,\, 2,\, 3,\, \ldots \ldots \tag{3.138d}$$

The derivatives of ξ_{2n} and η_{2n}, required to evaluate Table 3.2 are given by

$$\frac{\partial \xi_{2n}}{\partial \overline{\sigma}_{pq}} = \frac{\xi_{2n}}{\overline{F}_b} \frac{\partial \overline{F}_b}{\partial \overline{\sigma}_{pq}} \ , \ n=0, 1, 2, \ \ldots\ldots \tag{3.139a}$$

$$\frac{\partial \eta_{2n}}{\partial \overline{\sigma}_{pq}} = \frac{\eta_{2n}}{\overline{F}_b} \frac{\partial \overline{F}_b}{\partial \overline{\sigma}_{pq}} \ , \ n=1, 2, 3, \ \ldots\ldots \tag{3.139b}$$

$$\frac{\partial^2 \xi_{2n}}{\partial \overline{\sigma}_{pq} \partial \overline{\sigma}_{rs}} = \frac{\xi_{2n}}{\overline{F}_b} \frac{\partial^2 \overline{F}_b}{\partial \overline{\sigma}_{pq} \partial \overline{\sigma}_{rs}} \ , \ n=0, 1, 2, \ \ldots\ldots \tag{3.139c}$$

$$\frac{\partial \eta_{2n}}{\partial \overline{\sigma}_{pq} \partial \overline{\sigma}_{rs}} = \frac{\eta_{2n}}{\overline{F}_b} \frac{\partial^2 \overline{F}_b}{\partial \overline{\sigma}_{pq} \partial \overline{\sigma}_{rs}} \ , \ n=1, 2, 3, \ \ldots\ldots \tag{3.139d}$$

To evaluate Equations 3.138 and 3.139, the relationship between the force, F_b, and the effective stress or strain tensors must be known. This relationship will be developed in a later section.

Strain Energy Density of Mixture Phase

The strain energy density of the mixture phase will be determined. Two cases have to be considered in determining the strain energy density. Case one represents an air-water mixture which exerts a uniform pressure on the spheres contained in the system. Case two represents the mixture phase acting as a cohesive material, binding neighboring spheres together. Combined, these two cases will model the mixture phase in both compression and tension.

Mixture Phase in Compression. The strain energy density of an air-water mixture in compression will be determined. The situation to be considered is shown in Figure 3.13. The air-water mixture applies a uniform pressure on the surfaces of the spheres in the system. The air in the mixture is assumed to be occluded. The following four assumptions are made concerning the air-water mixture:

1. Boyle's Law may be used to represent the pressure volume behavior of the air contained in the air-water mixture.

2. Henry's Law may be used to determine the volume of dissolved air present in the liquid phase.
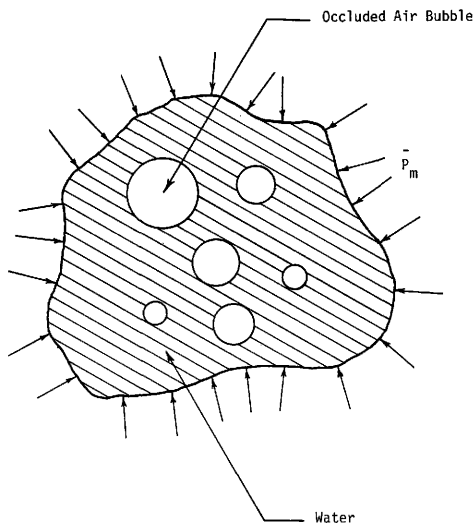
Figure 3.13 -- Air-Water Mixture

3. When considering the compressibility of the air-water
    mixture, the compressibility of the water is negligible.

4. The surface tension present in the water phase surrounding
    the occluded air is negligible.

Boyle's Law states that the product of the absolute pressure and
volume of an ideal gas is constant under constant temperature. The
form of Boyle's Law which will be employed is

$$\bar{P}_{oa} \bar{V}_{oa} = \bar{P}_a V_a \tag{3.140}$$

where P_{oa} = the absolute initial air pressure,

V_{oa} = the initial volume of the air,

P_a = the current absolute air pressure, and

V_a = the current volume of the air

The form of Henry's Law which will be used states that the
volume of dissolved air present in an air-water mixture is directly
proportional to the total volume of water. This relationship is given
by

$$V_d = k_h V_w \tag{3.141}$$

where V_d = the volume of dissolved air,

V_w = the total volume of water, and

k_h = the coefficient of solubility.

Present in the free air of the air-water mixture will be saturated water vapor. Dalton's division law shows that the saturated water vapor pressure does not obey Boyle's Law. However, the saturated water vapor pressure is usually very small and will be neglected.

In obtaining an expression for the strain energy density of the air-water mixture, only isothermal processes will be considered. Under these conditions the Helmholtz free energy and the Complementary free energy of the mixture are equal to the strain energy density. Equations 3.94 and 3.96 yield the following expression for the strain energy density of the air-water mixture.

$$\bar{\pi}_m = 1/2 \; (\overline{\sigma_{ij} \; \epsilon_{ij}}) = \frac{1}{V_m} \int_{V_m} \sigma_{ij} \; \epsilon_{ij} dV \tag{3.142}$$

where π_m = the strain energy density of the air-water mixture

V_m = the initial volume of the air-water mixture

As a result of the assumption that the surface tension of the water is negligible, the air and the water pressures present in the mixture are considered to be equal. This pressure is constant throughout the air-water mixture contained in the representative volume. The air-water mixture is subject to changes in the mean hydrostatic stress only. All principal stresses in the mixture are equal. It is assumed that the air-water mixture is unstrained at

atmospheric pressure. For these conditions, Equation 3.142 is evaluated as

$$\bar{\pi}_m = -\ 1/2\ P_w\ \epsilon^m_{kk} \tag{3.143a}$$

where $-P_w = {}^1/3\ \sigma^m_{kk}$

$$\tag{3.143b}$$

and P_w = the gage pressure of the water phase,

$\ ^1/3\sigma^m_{kk}$ = the mean hydrostatic stress of the mixture, and

σ^m_{kk} = the volumetric strain of the mixture.

Under the assumption that the compressibility of the water is negligible in comparison to that of the air, the volumetric strain of the air-water mixture may be determined in terms of the initial and final volumes of air. The total initial volume of the air in the mixture is

$$V_{ao} = V_{ab} + V_{ad} \tag{3.144}$$

where V_{ao} = the total initial volume of air,

V_{ab} = the initial volume of free air in the form of occluded bubbles, and

V_{ad} = the initial volume of dissolved air.

Using Henry's Law as given by Equation 3.141, Equation 3.144 is rewritten as

$$V_{ao} = V_{ab} + k_h V_w \qquad (3.145)$$

where V_w = the volume of water present in the mixture.

Combining Boyle's Law given by Equation 3.140 with Equation 3.146, gives the following expression for the volume of air resulting from a change in the water pressure P_w.

$$V_a = [V_{ab} + k_n V_w](\frac{P_{atm}}{P_w + P_{atm}}) \qquad (3.146)$$

where V_a = the current total volume of air, and

P_{atm} = atmospheric pressure.

In Equation 3.146, it is implied that the air-water mixture is unstrained at atmospheric pressure. The change in volume of the

mixture is determined as that for the air contained in the mixture. The volumetric strain, σ_{kk}^m, is given by

$$\varepsilon^m_{kk} = \frac{V_a - V_{ao}}{V_m} = -\frac{(V_{ab} + k_h V_w)}{V_m} \frac{P_w}{(P_w + P_{atm})} \qquad (3.147)$$

where V_m = the initial volume of the mixture.

Substitution of Equation 3.147 into Equation 3.143a gives the following expression for the strain energy density of the air-water mixture.

$$\bar{\pi}_m = 1/2 \frac{(V_{ab} + k_n V_w)}{V_w} \frac{P_w^2}{(P_w + P_{atm})} \qquad (3.148)$$

Equation 3.148 may be rewritten in terms of the degree of saturation as defined by Equation 3.136. In determining the degree of saturation the volume of dissolved air is included in the total volume of water. Expressing Equation 3.148 in terms of the initial degree of saturation, D_{so}, yields

$$\bar{\pi}_m = 1/2 \left(1 + D_{so} + k_h D_{so} \right) \frac{P_w^2}{(P_a + P_{atm})} \qquad . \qquad (3.149)$$

For the thermodynamic conditions imposed on the system, the strain energy density given by Equation 3.149, is equal to the Helmholtz and Complementary free energies of the mixture phase. Equation 3.149 may be used to evaluate the derivatives of these

quantities which appear in Equations 3.89 through 3.92. The derivatives of interest are

$$\frac{\partial \overline{F}_m}{\partial \overline{\epsilon}_{ij}} = \frac{\partial \overline{\pi}_m}{\partial \overline{\epsilon}_{ij}} = + 1/2 \left[1 + D_{so} + k_h D_{so}\right] \left[\frac{2 P_w}{\overline{P}_w} - \frac{P_w^2}{\overline{P}_w^2}\right] \frac{\partial P_w}{\partial \overline{\epsilon}_{ij}} \qquad (3.150a)$$

$$\frac{\partial \overline{F}_{cm}}{\partial \overline{\sigma}_{ij}} = \frac{\partial \overline{\pi}_m}{\partial \overline{\sigma}_{ij}} = 1/2 \left[1 + D_{so} + k_h D_{so}\right] \left[\frac{2 P_w}{\overline{P}_w} - \frac{P_w^2}{\overline{P}_w^2}\right] \frac{\partial P_w}{\partial \overline{\sigma}_{ij}} \qquad (3.150b)$$

$$\frac{\partial^2 \overline{F}_m}{\partial \overline{\epsilon}_{ij} \, \partial \overline{\epsilon}_{kl}} = \frac{\partial^2 \overline{\pi}_m}{\partial \overline{\epsilon}_{ij} \, \partial \overline{\epsilon}_{kl}} = 1/2 \left[1 + D_{so} + k_n D_{so}\right] \quad \left[\frac{2 P_w}{\overline{P}_w} - \frac{P_w^2}{\overline{P}_w^2}\right] \times$$

$$\frac{\partial^2 P_w}{\partial \overline{\epsilon}_{ij} \, \partial \overline{\epsilon}_{kl}} + \left[1 + D_{so} + k_n \cdot D_{so}\right] \left[\frac{1}{\overline{P}_w} - \frac{2 P_w}{\overline{P}_w^2} + \frac{P_w^2}{\overline{P}_w^3}\right] \frac{\partial P_w}{\partial \overline{\epsilon}_{ij}} \frac{\partial P_w}{\partial \overline{\epsilon}_{kl}} \quad (3.150c)$$

$$\frac{\partial^2 \overline{F}_{cm}}{\partial \overline{\sigma}_{ij} \, \partial \overline{\sigma}_{kl}} = \frac{\partial^2 \overline{\pi}_m}{\partial \overline{\sigma}_{ij} \, \partial \overline{\sigma}_{kl}} = 1/2 \left[1 + D_{so} + k_h D_{so}\right] \left[\frac{2 \overline{P}_w}{\overline{P}_w} - \frac{P_w^2}{\overline{P}_w^2}\right] \frac{\partial^2 P_w}{\partial \overline{\sigma}_{ij} \, \partial \overline{\sigma}_{kl}}$$

$$+ [1 + D_{so} + k_h D_{so}] \left[\frac{1}{\bar{P}_w} - \frac{2 P_w}{\bar{P}_w^2} + \frac{P_w^2}{\bar{P}_w^3} \right] \frac{\partial P_w}{\partial \bar{\sigma}_{ij}} \frac{\partial P_w}{\partial \bar{\sigma}_{kl}} \qquad (3.150d)$$

where $\bar{P}_w = P_w + P_{atm}$ \qquad (3.150e)

To evaluate the derivatives of the water pressure P_w, which appear in Equations 3.150, the dependence of this quantity on either the effective strain tensor, σ_{ij}, or the effective stress tensor, ε_{ij}, must be known. One case which is simple to evaluate is when the increase in water and air pressures in the system have dissipated and the air and water pressures have returned to their initial states. For these conditions, all the derivatives of the water pressure, P_w, appearing in Equations 3.150 are equal to zero. For this case, the air-water mixture contributes nothing to the determination of the effective quantities.

Mixture Phase Acting As a Binder

The strain energy density of the mixture phase when it acts as a binder between neighboring spheres will be determined. For the thermodynamic conditions under consideration, the strain energy density will be equal to the work done per unit initial volume. The binder material is assumed to have the following force-displacement relationship:

$$F_b = k_b \delta \tag{3.151}$$

where F_b = the force transmitted by the binder material,

k_b = the elastic spring constant for the binder material, and

δ = the displacement between the sphere on which the binder material acts.

The work per unit initial volume done on the binder material is

$$W_b = \frac{1}{V_m} \int_0^\delta F_b \, \partial \bar{\delta} = \frac{k_b \delta^2}{2 V_m} \tag{3.152}$$

where V_m = the intial volume of the binder material

The strain energy density of the binder material is equal to the work W_b. The strain energy density of the binder material is given by.

$$\bar{\pi}_m = \frac{k_b \delta^2}{2 V_m} = \frac{F_b^2}{2 k_b V_m} \tag{3.153}$$

The derivatives of the strain energy density as given by Equation 3.153, which are required to evaluate Equations 3.89 through 3.92 are

$$\frac{\partial \bar{F}_m}{\partial \bar{\varepsilon}_{ij}} = \frac{\partial \bar{\pi}_m}{\partial \bar{\varepsilon}_{ij}} = \frac{F_b}{k_b V_m} \frac{\partial F_b}{\partial \bar{\varepsilon}_{ij}} \qquad (3.154a)$$

$$\frac{\partial \bar{F}_{cm}}{\partial \bar{\sigma}_{ij}} = \frac{\partial \pi_m}{\partial \bar{\sigma}_{ij}} = \frac{F_b}{k_b V_m} \frac{\partial F_b}{\partial \bar{\sigma}_{ij}} \qquad (3.154b)$$

$$\frac{\partial^2 \bar{F}_m}{\partial \bar{\varepsilon}_{ij} \partial \bar{\varepsilon}_{kl}} = \frac{\partial^2 \bar{\pi}_m}{\partial \bar{\varepsilon}_{ij} \partial \bar{\varepsilon}_{kl}} = \frac{1}{k_b V_m} \frac{\partial F_b}{\partial \bar{\varepsilon}_{ij}} \frac{\partial F_b}{\partial \bar{\varepsilon}_{kl}} + \frac{F_b}{k_b V_m} \frac{\partial^2 F_b}{\partial \bar{\varepsilon}_{ij} \partial \bar{\varepsilon}_{kl}} \qquad (3.154c)$$

$$\frac{\partial^2 \bar{F}_{cm}}{\partial \bar{\sigma}_{ij} \partial \bar{\sigma}_{kl}} = \frac{\partial^2 \bar{\pi}_m}{\partial \bar{\sigma}_{ij} \partial \bar{\sigma}_{kl}} = \frac{1}{k_b V_m} \frac{\partial F_b}{\partial \bar{\sigma}_{ij}} \frac{\partial F_b}{\partial \sigma_{kl}} + \frac{F_b}{k_b V_m} \frac{\partial^2 F_b}{\partial \bar{\sigma}_{ij} \partial \bar{\sigma}_{kl}} \qquad (3.154d)$$

Equations 3.154 are in terms of the force F_b, Equation 3.151 may be used to evaluate Equations 3.154. The relationship between the force F_b or the displacement δ, and the effective stress and strain tensors must be known in order to evaluate Equations 3.154. An approximate relationship will be given in a later section.

EVALUATION OF EFFECTIVE QUANTITIES

In this section the evaluation of the effective quantities is discussed. The equations required to determine the effective quantities will be presented in a manageable form. Estimations for determining the loads transmitted through particle contacts or the mixture material acting as a binder, will be given.

To summarize the results of the previous sections, the equations which will be used to evaluate the effective quantities of interest are

$$\bar{\sigma}_{ij} = C_p \frac{\partial \bar{\pi}_p}{\partial \bar{\epsilon}_{ij}} + C_m \frac{\partial \bar{\pi}_m}{\partial \bar{\epsilon}_{ij}} \tag{3.155a}$$

$$\bar{\epsilon}_{ij} = C_p \frac{\partial \bar{\pi}_p}{\partial \bar{\sigma}_{ij}} + C_m \frac{\partial \bar{\pi}_m}{\partial \bar{\sigma}_{ij}} \tag{3.155b}$$

$$\overline{C_{ijkl}} = C_p \frac{\partial^2 \bar{\pi}_p}{\partial \bar{\epsilon}_{ij} \, \partial \bar{\epsilon}_{kl}} + C_m \frac{\partial^2 \bar{\pi}_m}{\partial \bar{\epsilon}_{ij} \, \partial \bar{\epsilon}_{kl}} \tag{3.155c}$$

$$\overline{S_{ijkl}} = C_p \frac{\partial^2 \pi_m}{\partial \bar{\sigma}_{ij} \, \partial \bar{\sigma}_{kl}} + C_m \frac{\partial^2 \pi_m}{\partial \bar{\sigma}_{ij} \, \partial \bar{\sigma}_{kl}} \tag{3.155d}$$

where $\bar{\sigma}_{ij}$ = the effective stress tensor,

$\bar{\epsilon}_{ij}$ = the effective strain tensor,

$\bar{C}_{ijkl}$ = the effective compliance tensor,

$\bar{S}_{ijkl}$ = the effective stiffness tensor,

$\bar{\pi}_p$ = the strain energy density of the particulate phase,

$\bar{\pi}_m$ = the strain energy density of the mixture phase,

C_p = the initial volume fraction of the particulate phase,

and

C_m = the initial volume fraction of the mixture phase.

Only the effective compliance and stiffness tensors will be considered in the remainder of this section. Knowledge of these quantities will allow the determination of the effective stress and strain tensors. The relationship between these quantities is determined by integration of Equations 3.155c and 3.155d. These integrations yield the following relationships.

$$\Delta\bar{\sigma}_{ij} = \int_{\bar{\epsilon}_{kl}^{\circ}}^{\bar{\epsilon}_{kl}} \overline{C_{ijkl}} \; d\tilde{\epsilon}_{kl} \tag{3.156a}$$

$$\Delta\bar{\epsilon}_{ij} = \int_{\bar{\sigma}_{kl}^{\circ}}^{\bar{\sigma}_{kl}} \overline{S_{ijkl}} \; d\tilde{\sigma}_{kl} \tag{3.156b}$$

where $\Delta\bar{\sigma}_{ij}$ = the change in a component of the effective stress tensor,

$\Delta\bar{\epsilon}_{ij}$ = the change in a component of the effective strain tensor,

$\bar{\sigma}^{o}_{ij}$ = the initial value of a component of the effective stress tensor, and

$\bar{\epsilon}^{o}_{ij}$ = the initial value of a component of the effective strain tensor.

The integrals appearing in Equations 3.156 are necessary because the effective compliance tensor and effective stiffness tensor will be functions of the effective strain tensor and effective stress tensor, respectively. The reason for this is the non-linear force-displacement relationship for the surfaces of the spheres in contact. A suitable numerical technique must be used to evaluate the change in the effective stress and strain tensors, given by Equations 3.156. The initial volume fractions of the particulate and mixture phases for the different packing configurations appear in Table 3.4. These initial volume fractions are needed to evaluate the effective compliance and effective stiffness.

The effective compliance and stiffness tensors will be referenced to the cartesion coordinates, $(\theta_1, \theta_2, \theta_3)$ as defined previously. The location of pairs of contacts on a particular sphere in the system, are defined by the angles β_m and ψ_m, measured relative to the coordinates $(\theta_1, \theta_2, \theta_3)$. The values of these angles for the different packing configurations are given in Table 3.5. The

Table 3.4. Initial Volume Fractions and Maximum Tensile Stressed
Volume of the Mixture Phase for the Different Packing
Configurations.

Packing Configuration	Initial Volume Fraction of Particle Phase C_p	Initial Volume Fraction of Mixture Phase C_m	Maximum Tensile Stressed Volume Fraction of Mixture Phase $(Ds)_{max} C_m{}^*$
Cubic	0.52	0.48	0.038
Orthorhombic	0.61	0.39	0.043
Tetragonal-Spheroidal	0.69	0.31	0.062
Rhombohedral	0.75	0.25	0.08

* Ds_{max} taken from Table 3.3.

Table 3.5. Angles Defining Location of Contact Pairs with Respect to Cartesian Coordinates $(\theta_1, \theta_2, \theta_3)$.

Packing Configuration	Angles Defining Locations of Contact Pairs											
	Contact Pair 1		Contact Pair 2		Contact Pair 3		Contact Pair 4		Contact Pair 5		Contact Pair 6	
	β_1	ψ_1	β_2	ψ_2	β_3	ψ_3	β_4	ψ_4	β_5	ψ_5	β_6	ψ_6
Cubic	0°	0°	90°	0°	90°	90°	-	-	-	-	-	-
Orthorhombic	45°	0°	45°	90°	45°	180°	45°	270°	-	-	-	-
Tetragonal-Spheroidal	35.3°	30°	35.3°	210°	90°	0°	90°	60°	90°	120°	-	-
Rhombohedral	35.3°	30°	35.3°	150°	35.3°	270°	90°	0°	90°	60°	90°	120°

effective compliance and stiffness tensors will be determined using
the values of the angles, β_m and ψ_m, listed in Table 3.5. This in
effect fixes the cartesian coordinates $(\theta_1, \theta_2, \theta_3)$, with respect to a
particular packing configuration. To determine the effective
quantities with respect to a coordinate system other than $(\theta_1, \theta_2, \theta_3)$, tensor transformation laws may be employed.

To evaluate the effective compliance and stiffness tensors,
Equations 3.155c and 3.155d are rewritten as

$$\overline{C}_{ijkl} = C_p \, \overline{C^p}_{ijkl} + C_m \, \overline{C^m}_{ijkl} \tag{3.157a}$$

$$\overline{S}_{ijkl} = C_p \, \overline{S^p_{ijkl}} + C_m \, \overline{S^m_{ijkl}} \tag{3.157b}$$

$$\overline{C^p}_{ijkl} = \frac{\partial^2 \overline{\pi}_p}{\partial \overline{\varepsilon}_{ij} \, \partial \overline{\varepsilon}_{kl}} \tag{3.157c}$$

$$\overline{C^m}_{ijkl} = \frac{\partial^2 \overline{\pi}_m}{\partial \overline{\varepsilon}_{ij} \, \partial \overline{\varepsilon}_{kl}} \tag{3.157d}$$

$$\overline{S^p_{ijkl}} = \frac{\partial^2 \overline{\pi}_m}{\partial \overline{\sigma}_{ij} \, \partial \overline{\sigma}_{kl}} \tag{3.157e}$$

$$\overline{S^m_{ijkl}} = \frac{\partial^2 \overline{\pi}_m}{\partial \overline{\sigma}_{ij} \, \partial \overline{\sigma}_{kl}} \tag{3.157f}$$

The quantities, $\overline{C^p_{ijkl}}$ and $\overline{C^m_{ijkl}}$, are the effective compliances of the particulate and mixture phases, respectively. The quantities, $\overline{S^p_{ijkl}}$ and $\overline{S^m_{ijkl}}$, are the effective stiffnesses of the particulate and mixture phases, respectively. Simple expressions for these quantities will be given.

Effective Compliance and Stiffness Tensors of Particulate Phase

The effective compliance and stiffness tensors of the particulate phase are determined as

$$\overline{C^p_{ijkl}} = (\overline{C^p_{ijkl}})^o + (\overline{C^p_{ijkl}})^i \tag{3.158a}$$

$$\overline{S^p_{ijkl}} = (\overline{S^p_{ijkl}})^o + (\overline{S^p_{ijkl}})^i \tag{3.158b}$$

where $(\overline{C^p_{ijkl}})^o$ = the contribution to the effective compliance of the particulate phase by all sets of surface tractions,

$(\overline{C^p_{ijkl}})^i$ = the contribution to the effective compliance of the particulate phase by all interactions between sets of surface tractions,

$(\overline{S^p_{ijkl}})^0$ = the contribution to the effective stiffness of the particulate phase by all sets of surface tractions, and

$(\overline{S^p_{ijkl}})^i$ = the contribution to the effective stiffness of the particulate phase by all interactions between sets of surface tractions.

The effective quantities, $(\overline{C^p_{ijkl}})^0$ and $(\overline{S^p_{ijkl}})^0$, are given by

$$(C^p_{ijkl})_0 = \frac{(K^\sigma_p)^2}{G} \left[\overline{P}_m \frac{\partial^2 \overline{P}_m}{\partial \overline{\varepsilon}_{ij} \partial \overline{\varepsilon}_{kl}} + \frac{\partial \overline{P}_m}{\partial \overline{\varepsilon}_{ij}} \frac{\partial \overline{P}_m}{\partial \overline{\varepsilon}_{kl}} \right] +$$

$$\frac{(K^\sigma_c)^2}{G} \sum_{n=1}^{N_c} \left[\left((A_c)_n + (B_c)_n \right) \frac{\partial C_n}{\partial \overline{\varepsilon}_{kl}} \frac{\partial C_n}{\partial \overline{\varepsilon}_{kl}} + \right.$$

$$(C_c)_n \frac{\partial^2 C_n}{\partial \overline{\varepsilon}_{ij} \partial \overline{\varepsilon}_{kl}} + \frac{(K^\sigma_b)^2}{G} \sum_{n=1}^{N_b}$$

$$\left. (D_b)_n \left(\frac{\partial F_{bn}}{\partial \overline{\varepsilon}_{ij}} \frac{\partial F_{bn}}{\partial \overline{\varepsilon}_{kl}} + F_{bn} \frac{\partial^2 F_{bm}}{\partial \overline{\varepsilon}_{ij} \partial \overline{\varepsilon}_{kl}} \right) \right] \tag{3.159a}$$

$$(\overline{S}^{p}_{ijkl})^{0} = K^{\sigma}_{p} \left[\overline{P}_{m} \frac{\partial^{2}\overline{P}_{m}}{\partial\overline{\sigma}_{ij}\,\partial\overline{\sigma}_{kl}} + \frac{\partial\overline{P}_{m}}{\partial\overline{\sigma}_{ij}} \frac{\partial\overline{P}_{m}}{\partial\overline{\sigma}_{kl}} \right] +$$

$$\frac{(K^{\sigma}_{c})^{2}}{G} \sum_{n=1}^{N_{c}} \left[\left((A_{c})_{n} + (B_{c})_{n} \right) \frac{\partial C_{n}}{\partial\overline{\sigma}_{ij}} \frac{\partial C_{n}}{\partial\overline{\sigma}_{kl}} + (C_{c})_{n} \frac{\partial^{2}C_{n}}{\partial\overline{\sigma}_{ij}\,\partial\overline{\sigma}_{kl}} \right] +$$

$$\frac{(K_{b}\sigma)^{2}}{G} \sum_{n=1}^{N_{b}} (D_{b})_{n} \left[\frac{\partial F_{bn}}{\partial\overline{\sigma}_{ij}} \frac{\partial F_{bn}}{\partial\overline{\sigma}_{kl}} + \frac{\partial^{2}F_{bn}}{\partial\overline{\sigma}_{ij}\,\partial\overline{\sigma}_{kl}} F_{bn} \right] \qquad (3.159b)$$

where

$$K^{\sigma}_{p} = \frac{(1-2\nu)}{2(1+\nu)} \qquad (3.159c)$$

$$K^{\sigma}_{c} = \frac{2E}{\pi(1-\nu^{2})} \qquad (3.159d)$$

$$K^{\sigma}_{b} = \frac{1}{\pi R^{2}} \qquad (3.159e)$$

and P_{m} = the pressure of the mixture phase

C_{n} = the cosine of the angle $\overline{z}_{2}$. Defining contact surface n,

F_{bn} = the total force which is transmitted by the mixture phase

acting as a binder at location n,

N_{c} = the number contact type surface tractions,

N_{b} = the number of binder type surface tractions,

G = the shear modulus of the particulate phase,

E = Young's modulus of the particulate phase,

ν = Poisson's ratio for the particulate phase, and

R = the radius of the spheres representing the particulate phase.

The sum of the quantities N_c and N_b, which appear in Equations 3.159, must be less than or equal to the total number of contact pairs. The case where this sum may be less than the total number of contact pairs would occur when a tensile load is present at a contact location where there is no mixture material acting as a binder. The terms $(A_c)_n$, $(B_c)_n$, $(C_c)_n$ and $(D_b)_n$ which appear in Equations 3.159 are dimensionless quantities for surface traction set n. They are determined from the series solution presented in the previous section. The quantities $(A_c)_n$, $(B_c)_n$, and $(C_c)_n$ arise from contact type surface tractions for contact n. These quantities are determined as

$$(A_c)_n = \frac{G}{(K^\sigma)^2 V_p} \int_{V_p} \frac{\partial (\sigma_{pq}{}^c)_n}{\partial c_n^2} \ (\varepsilon_{pq}^c)_n \ dV \qquad (3.160a)$$

$$(B_c)_n = \frac{G}{(K^\sigma)^2 V_p} \int_{V_p} \frac{\partial(\sigma_{pq}{}^c)_n}{\partial C_n} \frac{\partial(\varepsilon_{pq})_n}{\partial C_n} \, dV \tag{3.160b}$$

$$(C_c)_n = \frac{G}{(K^\sigma)^2 V_p} \int_{V_p} \frac{\partial(\sigma_{pq}^c)_n}{\partial C_n} (\varepsilon_{pq}^c)_n \, dV \tag{3.160c}$$

where $(\sigma_{pq}^c)_n$ = the stress tensor resulting from contact type surface

traction n, and

$(\varepsilon_{pq}^c)_n$ = the strain tensor resulting from contact type surface

traction n.

The quantity $(D_b)_n$ arises from surface tractions where the mixture phase acts as a binder between neighboring spheres. This quantity is determined as

$$(D_b)_n = \frac{G}{F_b{}^2 (K_b{}^\sigma)^2 V_p} \int_{V_p} (\sigma_{pq}{}^b)_n (\varepsilon_{pq}{}^b)_n \, dV \tag{3.161}$$

where $(\sigma_{pq}{}^b)_n$ = the stress tensor resulting from binder type surface

tractions n, and

$(\varepsilon_{pq}{}^b)_n$ = the strain tensor resulting from binder type surface

tractions n.

The dimensionless quantities given by Equations 3.160 and 3.161 are independent of the effective stress or strain tensors. The dimensionless quantities appearing in Equations 3.160 and 3.161 require evaluation by use of a computer. The computer evaluation of these quantities is discussed in the next chapter.

The effective quantities, $(\overline{C_{ijkl}^p})^i$ and $(\overline{S_{ijkl}^p})^i$, are given by

$$(\overline{C_{ijkl}^p})^i = \frac{K_b^\sigma K_p^\sigma}{G} \sum_{n=1}^{N_b} \left[(D_{bp})_n \left(\frac{\partial^2 F_{bn}}{\partial \bar{\varepsilon}_{ij} \, \partial \bar{\varepsilon}_{kl}} \quad \overline{P_m} + \frac{\partial F_{bn}}{\partial \bar{\varepsilon}_{ij}} \right. \right.$$

$$\left. \left. \frac{\partial \overline{P_m}}{\partial \bar{\varepsilon}_{kl}} + \frac{\partial \overline{P_m}}{\partial \bar{\varepsilon}_{ij}} + F_{bn} \frac{\partial^2 \overline{P_m}}{\partial \bar{\varepsilon}_{ij} \, \partial \bar{\varepsilon}_{kl}} \right) \right] \quad \frac{\partial F_{bn}}{\partial \bar{\varepsilon}_{kl}} +$$

$$\frac{K_b^\sigma K_p^\sigma}{G} \sum_{n=1}^{N_c} \left[(A_{cp})_n \frac{\partial C_n}{\partial \bar{\varepsilon}_{ij}} \quad \frac{\partial C_n}{\partial \bar{\varepsilon}_{kl}} \quad \overline{P_m} + \right.$$

$$(C_{cp})_n \left(\frac{\partial^2 C_n}{\partial \varepsilon_{ij} \, \partial \varepsilon_{kl}} \quad \overline{P_m} + \frac{\partial C_n}{\partial \bar{\varepsilon}_{ij}} \frac{\partial \overline{P_m}}{\partial \bar{\varepsilon}_{kl}} + \frac{\partial C_n}{\partial \bar{\varepsilon}_{kl}} \frac{\partial \overline{P_m}}{\partial \bar{\varepsilon}_{ij}} \right)$$

$$+ (D_{cp})_n \; \frac{\partial^2 \overline{p_m}}{\partial \overline{\epsilon}_{ij} \, \partial \overline{\epsilon}_{kl}} \Bigg] \quad + \frac{K_b^\sigma K_c^\sigma}{G} \sum_{\substack{m=1 \\ m \neq n}}^{N_b} \sum_{n=1}^{N_b}$$

$$\Bigg[(D_{bb})_{mn} \left(\frac{\partial^2 F_{bm}}{\partial \overline{\epsilon}_{ij} \, \partial \overline{\epsilon}_{kl}} \; F_{bn} + \frac{\partial F_{bm}}{\partial \overline{\epsilon}_{ij}} \; \frac{\partial F_{bn}}{\partial \overline{\epsilon}_{kl}} + \frac{\partial F_{bm}}{\partial \overline{\epsilon}_{kl}} \; \frac{\partial F_{bn}}{\partial \overline{\epsilon}_{ij}} + \right.$$

$$\left. F_{bm} \; \frac{\partial^2 F_{bn}}{\partial \overline{\epsilon}_{ij} \, \partial \overline{\epsilon}_{kl}} \right) \Bigg] + \frac{(K_c^\sigma)^2}{G} \sum_{\substack{m=1 \\ m \neq n}}^{N_c} \sum_{n=1}^{N_c} \Bigg[(A_{cc})_{mn}$$

$$\frac{\partial C_m}{\partial \overline{\epsilon}_{ij}} \; \frac{\partial C_m}{\partial \overline{\epsilon}_{kl}} + (B_{cc})_{mn} \left(\frac{\partial C_m}{\partial \overline{\epsilon}_{ij}} \; \frac{\partial C_n}{\partial \overline{\epsilon}_{kl}} + \frac{\partial C_m}{\partial \overline{\epsilon}_{kl}} \; \frac{\partial C_n}{\partial \overline{\epsilon}_{ij}} \right) +$$

$$(C_{cc})_{mn} \; \frac{\partial^2 C_m}{\partial \overline{\epsilon}_{ij} \, \partial \overline{\epsilon}_{kl}} \; + \; (C_{cc})_{nm} \; \frac{\partial^2 C_n}{\partial \overline{\epsilon}_{ij} \, \partial \overline{\epsilon}_{kl}} \; +$$

$$(A_{cc})_{nm} \; \frac{\partial C_n}{\partial \overline{\epsilon}_{ij}} \; \frac{\partial C_n}{\partial \overline{\epsilon}_{kl}} \Bigg] \tag{3.162a}$$

$$(S^p_{ijkl})^i = \frac{K_b{}^\sigma K_p{}^\sigma}{G} \sum_{n=1}^{N_b} \left[(D_{bp})_n \left(\frac{\partial F_{bn}}{\partial \overline{\sigma}_{ij} \, \partial \overline{\sigma}_{kl}} \, \overline{P_m} + \right. \right.$$

$$\left. \left. \frac{\partial F_{bn}}{\partial \overline{\sigma}_{ij}} \, \frac{\partial \overline{P_m}}{\partial \overline{\sigma}_{kl}} + \frac{\partial F_{bn}}{\partial \overline{\sigma}_{kl}} \, \frac{\partial \overline{P_m}}{\partial \overline{\sigma}_{ij}} + F_{bn} \, \frac{\partial^2 \overline{P_m}}{\partial \overline{\sigma}_{ij} \, \partial \overline{\sigma}_{kl}} \right) \right] +$$

$$\frac{K_c{}^\sigma K_p{}^\sigma}{G} \sum_{n=1}^{N_c} \left[(A_{cp})_n \, \frac{\partial C_n}{\partial \overline{\sigma}_{ij}} \, \frac{\partial C_n}{\partial \overline{\sigma}_{kl}} + (C_{cp})_n \right.$$

$$\left(\frac{\partial^2 C_n}{\partial \overline{\sigma}_{ij} \, \partial \overline{\sigma}_{kl}} \, \overline{P_m} + \frac{\partial C_n}{\partial \overline{\sigma}_{ij}} \, \frac{\partial \overline{P_m}}{\partial \overline{\sigma}_{kl}} + \frac{\partial C_n}{\partial \overline{\sigma}_{kl}} \, \frac{\partial \overline{P_m}}{\partial \overline{\sigma}_{ij}} \right) +$$

$$\left. (D_{cp})_n \, \frac{\partial^2 \overline{P_m}}{\partial \overline{\sigma}_{ij} \, \partial \overline{\sigma}_{kl}} \right] + \frac{2K_b{}^\sigma K_c{}^\sigma}{G} \sum_{m=1}^{N_b} \sum_{n=1}^{N_c}$$

$$(A_{bc})_{mn} \, F_{bm} \, \frac{\partial C_n}{\partial \overline{\sigma}_{ij}} \, \frac{\partial C_n}{\partial \overline{\sigma}_{kl}} + (C_{bc})_{mn}$$

$$\left(F_{bm} \, \frac{\partial^2 C_n}{\partial \overline{\sigma}_{ij} \, \partial \overline{\sigma}_{kl}} + \frac{\partial F_{bm}}{\partial \overline{\sigma}_{ij}} \, \frac{\partial C_n}{\partial \overline{\sigma}_{kl}} + \frac{\partial F_{bm}}{\partial \overline{\sigma}_{kl}} \, \frac{\partial C_n}{\partial \overline{\sigma}_{ij}} \right) +$$

$$(D_{bc})_{mn} \; \frac{\partial^2 F_{bm}}{\partial \overline{\sigma}_{ij} \, \partial \overline{\sigma}_{kl}} \Bigg] \quad + \quad \frac{(K_b^{\sigma})^2}{G} \sum_{m=1}^{N_b} \sum_{\substack{n=1 \\ m \neq n}}^{N_b}$$

$$\Bigg[(D_{bb})_{mn} \; \left(\frac{\partial F_{bm}}{\partial \overline{\sigma}_{ij} \, \partial \overline{\sigma}_{kl}} \; F_{bn} \; + \; \frac{\partial F_{bm}}{\partial \overline{\sigma}_{ij}} \frac{\partial F_{bn}}{\partial \overline{\sigma}_{kl}} \; + \; \frac{\partial F_{bm}}{\partial \overline{\sigma}_{kl}} \frac{\partial F_{bn}}{\partial \overline{\sigma}_{ij}} \; + \right.$$

$$\left. F_{bm} \; \frac{\partial^2 F_{bn}}{\partial \overline{\sigma}_{ij} \, \partial \overline{\sigma}_{kl}} \right) \Bigg] \quad + \quad \frac{(K_c^{\sigma})^2}{G} \sum_{m=1}^{N_c} \sum_{\substack{n=1 \\ m=n}}^{N_c}$$

$$\Bigg[(A_{cc})_{mn} \; \frac{\partial C_m}{\partial \overline{\sigma}_{ij}} \frac{\partial C_m}{\partial \overline{\sigma}_{kl}} \; + \; (B_{cc})_{mn} \; x$$

$$\left(\frac{\partial C_m}{\partial \overline{\sigma}_{ij}} \frac{\partial C_n}{\partial \overline{\sigma}_{kl}} \; + \; \frac{\partial C_m}{\partial \overline{\sigma}_{kl}} \frac{\partial C_n}{\partial \overline{\sigma}_{ij}} \right) \quad + \quad (C_{cc})_{mn} \; x$$

$$\frac{\partial^2 C_m}{\partial \overline{\sigma}_{ij} \, \partial \overline{\sigma}_{kl}} \; + \; (C_{cc})_{nm} \; \frac{\partial^2 C_n}{\partial \overline{\sigma}_{ij} \, \partial \overline{\sigma}_{kl}} \; + \; (A_{cc})_{nm} \; \frac{\partial C_n}{\partial \overline{\sigma}_{ij}} \frac{\partial C_n}{\partial \overline{\sigma}_{kl}} \Bigg] \qquad (3.162b)$$

The terms appearing in Equations 3.162 have all been previously
defined except dimensionless quantities. The dimensionless quantity,
$(D_{bp})_n$, arises from the interaction between uniform pressure type
surface tractions and binder type surface tractions for contact n.
This quantity is given by

$$(D_{bp})_n = \frac{G}{2F_{bn}\ \overline{P_m}\ K_b^{\sigma}\ K_p^{\sigma}\ V_p} \int_{V_p} (\sigma_{pq}^{\ b})_n\ \epsilon_{pq}^{\ p}\ dV \tag{3.163}$$

where $\overline{\epsilon}_{ij}^{\ p}$ = the strain tensor due to the uniform pressure, P_m, acting
on the surface of a sphere.

The dimensionless quantities, $(A_{cp})_n$, $(C_{cp})_n$ and $(D_{cp})_n$ arise from the
interaction between uniform pressure type surface tractions and
contact type surface tractions for location n. These quantities are
given by

$$(A_{cp})_n = \frac{G}{2\overline{P_m}\ K_c^{\sigma}\ K_p^{\sigma}\ V_p} \int_{V_p} \frac{\partial^2(\sigma_{pq}^{\ c})_n}{\partial C_n^{\ 2}}\ \epsilon_{pq}^{\ p}\ dV \tag{3.164a}$$

$$(C_{cp})_n = \frac{G}{2\overline{P_m}\ K_c^{\sigma}\ K_p^{\sigma}\ V_p} \int_{V_p} \frac{\partial(\sigma_{pq}^{\ c})_n}{\partial C_n}\ \epsilon_{pq}^{\ p}\ dV \tag{3.164b}$$

$$(D_{cp})_n = \frac{G}{2\overline{P_m}\, K_c^{\sigma}\, K_p^{\sigma} v_p} \int_{V_p} (\sigma_{pq}{}^c)_n\; \varepsilon_{pq}^p \;\; dV$$

$$(3.164c)$$

The dimensionless quantities $(A_{bc})_{mn}$, $(C_{bc})_{mn}$ and $(D_{bc})_{mn}$ arise from the interaction of binder type surface tractions for location m, with contact type surface tractions for contact n. These quantities are given by

$$(A_{bc})_{mn} = \frac{G}{2F_{bm}\, K_b^{\sigma}\, K_c^{\sigma} v_p} \int_{V_p} (\varepsilon_{pq}^b)_m \;\; \frac{\partial^2 (\sigma_{pq}{}^c)_n}{\partial C_n^2} \;\; dV$$

$$(3.165a)$$

$$(C_{bc})_n = \frac{G}{2F_{bm}\, K_b^{\sigma}\, K_c^{\sigma} v_p} \int_{V_p} (\varepsilon_{pq}^b)_m \;\; \frac{(\sigma_{pq}{}^c)_n}{\partial C_n} \;\; dV$$

$$(3.165b)$$

$$(C_{bc})_{mn} = \frac{G}{2F_{bm} \, K_b^{\sigma} \, K_c^{\sigma} \, V_p} \int_{V_p} (\epsilon_{ij}^b)_m \, (\sigma_{ij}{}^c)_n \, dV$$

$$(3.165c)$$

The dimensionless quantity $(D_{bn})_{mn}$ arises from the interaction of binder type surface tractions for location m, with binder type surface tractions for location n. This quantity is given by

$$(D_{bn})_{mn} = \frac{G}{2F_{bm} \, F_{bn} \, (K_b^{\sigma})^2 \, V_p} \int_{V_p} (\sigma_{pq}{}^b)_m \, (\epsilon_{pq}^b)_n \, dV$$

$$(3.166)$$

The dimensionless quantities $(A_{cc})_{mn}$, $(B_{cc})_{mn}$ and $(C_{cc})_{mn}$ arise from the interaction of contact type surface tractions at location m with contact type surface tractions at location n. These quantities are given by

$$(A_{cc})_{mn} = \frac{G}{2(K_c^{\sigma})^2 V_p} \int_{V_p} \frac{\partial^2 (\sigma_{pq}{}^c)_m}{\partial^2 C_m} \, (\epsilon_{pq}^c)_m \, dV$$

$$(3.167a)$$

$$(B_{cc})_{mn} = \frac{G}{2(K_c^{\sigma})^2 V_p} \cdot \int_{V_p} \frac{\partial (\sigma_{pq}{}^c)_m}{\partial C_m} \, \frac{(\epsilon_{pq}^c)_n}{\partial C_n} \, dV$$

$$(3.167b)$$

$$(C_{cc})_{mn} = \frac{G}{2(K_c^{\sigma})^2 V_p} \int\limits_{V_p} \frac{\partial (\sigma_{pq}^C)_m}{\partial C_m} \; (c_{pq}^C)_n \; dV$$

(3.167c)

Values of the dimensionless quantities appearing in Equations 3.163 through 3.167, require evaluation by a computer. Evaluation of these quantities is discussed in Chapter IV. The dimensionless quantities determined from the interactions between contact type and binder type surface tractions are dependent on the angle, θ_{mn}, which defines the location of the surface tractions of location m, with respect to the surface traction at location n, or vice versa. Figure 3.14 shows the angle θ_{mn} in relation to the axes x_3^m and x_3^n, which are axes of symmetry for the surface tractions at locations m and n, respectively. The possible locations for contact and binder type surface tractions with respect to the global coordinate system, $(\theta_1, \theta_2, \theta_3)$, are determined by the angles, β_m and ψ_m, which appear in Table 3.5. Tables 3.6 through 3.9 give values of θ_{mn} for the different surface traction locations for each of the packing configurations.

The effective compliance and effective stiffness of the particulate phase may be determined using Equations 3.158, 3.159 and 3.162. To evaluate these quantities, the dependence of the pressure in the mixture phase, P_m, the cosines of the contact angles, C_n, and the binder force, F_{bn}, on the effective stress and strain tensors must be known. Approximate relations of this type will be given in a later section.
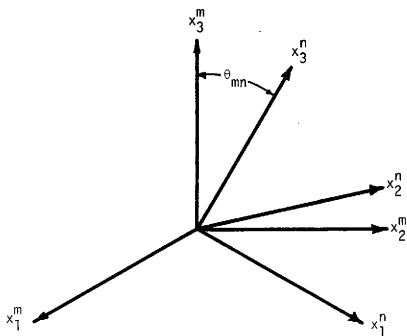
Figure 3.14. -- Angle θ_{mn} Relative to x_3^m and x_3^n Coordinate Axes.

Table 3.6. Values of the Angle θ_{mn} for Simple Cubic Packing Configuration.

<table>
<tr><td colspan="2"></td><td colspan="6" align="center">Surface Traction
Location n</td></tr>
<tr><td colspan="2"></td><td>β_1
0°</td><td>ψ_1
0°</td><td>β_2
90°</td><td>ψ_2
0°</td><td>β_3
90°</td><td>ψ_3
90°</td></tr>
<tr><td rowspan="6">Surface Traction
Location m</td><td>β_1 0°</td><td colspan="2" align="center" rowspan="2">0°</td><td colspan="2" align="center" rowspan="2">90°</td><td colspan="2" align="center" rowspan="2">90°</td></tr>
<tr><td>ψ_1 0°</td></tr>
<tr><td>β_2 90°</td><td colspan="2" align="center" rowspan="2">90°</td><td colspan="2" align="center" rowspan="2">0°</td><td colspan="2" align="center" rowspan="2">90°</td></tr>
<tr><td>ψ_2 0°</td></tr>
<tr><td>β_3 90°</td><td colspan="2" align="center" rowspan="2">90°</td><td colspan="2" align="center" rowspan="2">90°</td><td colspan="2" align="center" rowspan="2">0°</td></tr>
<tr><td>ψ_3 90°</td></tr>
</table>

Table 3.7. Values of the Angle θ_{mn} for Orthorhombic Packing Configuration.

		Surface Traction Location n							
		β_1	ψ_1	β_2	ψ_2	β_3	ψ_3	β_4	ψ_4
		45°	0°	45°	90°	45°	180°	45°	270°
β_1	45°								
ψ_1	0°	0°		60°		90°		60°	
β_2	45°								
ψ_2	90°	60°		0°		60°		90°	
β_3	45°								
ψ_3	180°	90°		60°		0°		60°	
β_4	45°								
ψ_4	270°	60°		90°		60°		0°	

Surface Traction Location m

Table 3.8. Values of the Angle θ_{mn} for Spheroidal-Tetragonal Packing Configuration.

		Surface Traction Location n								
		β_1	ψ_1	β_2	ψ_2	β_3	ψ_3	β_4	ψ_4	β_5	ψ_5
		35.3°	30°	35.3°	210°	90°	0°	90°	60°	90°	120°
β_1	35.3°	0°		70.5°		60°		60°		90°	
ψ_1	30°										
β_2	35.3°	70.5°		0°		90°		60°		60°	
ψ_2	210°										
β_3	90°	60°		90°		0°		60°		60°	
ψ_3	0°										
β_4	90°	60°		60°		60°		60°		60°	
ψ_4	60°										
β_5	90°	90°		60°		60°		60°		60°	
ψ_5	120°										

Table 3.9. Values of the Angle θ_{mn} for Rhombohedral Packing Configuration.

		Surface Traction Location n											
		β_1	ψ_1	β_2	ψ_2	β_3	ψ_3	β_4	ψ_4	β_5	ψ_5	β_6	ψ_6
		35.3°	30°	35.3°	150°	35.3°	270°	90°	0°	90°	60°	90°	120°
β_1	35.3°	0°		60°		60°		60°		60°		90°	
ψ_1	30°												
β_2	35.3°	60°		0°		60°		60°		90°		60°	
ψ_2	150°												
β_3	35.3°	60°		60°		0°		90°		60°		60°	
ψ_3	270°												
β_4	90°	60°		60°		90°		0°		60°		60°	
ψ_4	0°												
β_5	90°	60°		90°		60°		60°		0°		60°	
ψ_5	60°												
β_6	90°	90°		60°		60°		60°		60°		0°	
ψ_6	120°												

Surface Traction Location m

Effective Compliance and Stiffness of Mixture Phase

The effective compliance and stiffness of the mixture phase must be determined for two types of conditions. One condition is when the mixture phase exists in the void space around the spheres in the system at a pressure P_m. The other condition is when it acts as a binder between neighboring spheres. For the case when the mixture phase fills the void space and is subject to a pressure P_m, Equations 3.150 give expressions for the effective compliance and stiffness of the mixture. These equations yield

$$\overline{C}^m_{ijkl} = 1/2 \quad \left[1 + D_{so} + k_h D_{so} \right] \quad \left[\frac{2 \overline{P}_m}{(\overline{P}_m + P_{atm})} - \frac{\overline{P}_m^2}{(\overline{P}_m + P_{atm})^2} \right]$$

$$\frac{\partial^2 \overline{P}_m}{\partial \overline{\sigma}_{ij} \, \partial \overline{\sigma}_{ij}} \quad + \quad \left[1 + D_{so} + k_h D_{so} \right] \quad \left[\frac{1}{(\overline{P}_m + P_{atm})} - \frac{2\overline{P}_m}{(\overline{P}_m + P_{atm})^2} \right.$$

$$\left. + \frac{\overline{P}_m^2}{(\overline{P}_m + P_{atm})^3} \right] \quad \frac{\partial \overline{P}_m}{\partial \overline{\epsilon}_{ij}} \frac{\partial \overline{P}_m}{\partial \overline{\epsilon}_{kl}} \qquad\qquad (3.168a)$$

$$\overline{S_{ijkl}^m} = 1/2 \left[1 + D_{so} + k_h \, D_{so} \right] \left[\frac{2\overline{P_m}}{(\overline{P_m} + P_{atm})} - \frac{\overline{P_m}^2}{(\overline{P_m} + P_{atm})^2} \right] \times$$

$$\frac{\partial^2 \overline{P_m}}{\partial \overline{\sigma}_{ij} \, \partial \overline{\sigma}_{kl}} + \left[1 + D_{so} + k_h \, D_{so} \right] \left[\frac{1}{(\overline{P_m} + P_{atm})} - \frac{2\overline{P_m}}{(\overline{P_m} + P_{atm})^2} + \right.$$

$$\left. \frac{\overline{P_m}^2}{(\overline{P_m} + P_{atm})^3} \right] \frac{\partial \overline{P_m}}{\partial \overline{\sigma}_{ij}} \frac{\partial \overline{P_m}}{\partial \overline{\sigma}_{kl}} \qquad (3.168b)$$

where D_{so} = the initial degree of saturation,

$\quad k_h$ = solubility coefficient, and

$\quad P_{atm}$ = atmospheric pressure.

Equations 3.168 differ in appearance from Equations 3.150 in that the water pressure, P_w, has been replaced by the mixture pressure P_m. These two are equal since surface tension has been neglected.

When the mixture phase acts as a binder Equations 3.154 gives expressions for the effective compliance and stiffness of the mixture phase. Equations 3.154 apply to one surface traction location where the mixture material acts as a binder. Using these expressions the effective compliance and stiffness of the mixture phase for these conditions are

$$\overline{C_{ijkl}^m} = \frac{1}{V_m \, k_b} \sum_{n=1}^{N_b} \left[\frac{\partial F_{bn}}{\partial \epsilon_{ij}} \frac{\partial F_{bn}}{\partial \epsilon_{kl}} + F_{bn} \frac{\partial^2 F_{bn}}{\partial \epsilon_{ij} \, \partial \epsilon_{kl}} \right]$$

$$(3.169a)$$

$$\overline{s^m_{ijkl}} = \frac{1}{V_m \, k_b} \sum_{n=1}^{N_b} \left[\frac{\partial F_{bn}}{\partial \overline{\sigma}_{ij}} \frac{\partial F_{bn}}{\partial \overline{\sigma}_{kl}} + F_{bn} \frac{\partial^2 F_{bn}}{\partial \overline{\sigma}_{ij} \, \partial \overline{\sigma}_{kl}} \right]$$

(3.169b)

where V_m = the total volume of the mixture phase,

k_n = the elastic spring constant for the mixture phase,

N_b = the total number of binder type surface tractions, and

F_{bn} = the total force transmitted by the mixture material at location n.

If the displacement between spheres is known, Equations 3.151 may be used to evaluate Equations 3.169.

To evaluate Equations 3.168, the dependence of the mixture pressure, P_m, on the effective stress tensor or the effective strain tensor must be known. To evaluate Equations 3.169, the dependence of the force transmitted by the binder, F_b, on the effective stress or strain tensor must be known. These relationships will be approximated in the subsequent section.

RELATIONSHIP OF SURFACE TRACTIONS TO GLOBAL QUANTITIES

In this section, parameters needed to evaluate the surface tractions present on a single sphere will be related to the effective stress and effective strain tensors. To evaluate the effective quantities of the system as a whole, it is assumed that either the effective stress tensor or effective strain tensor is known. When one of these effective quantities is known, the results of the previous section may be used to determine the effective compliance tensor when the effective strain tensor is known, or the effective stiffness tensor when the effective stress tensor is known. The effective quantity which is known will be that which is observable on the macroscale. These being the macroscopically observable stress or strain fields.

Contact and Binder Type Surface Tractions When the Effective Strain Tensor is Known

In this section the parameters needed to evaluate contact and binder type surface tractions will be related to the effective strain tensor. The relationships to be developed would be used when the macroscopically observable strain field, ε_{ij}, is known.

To determine the relationships between the surface tractions present in the system on a sphere and the effective strain tensor, a single sphere which surface tractions at location n is considered. The location n is defined relative to the Cartesian coordinates,

$(\theta_1, \theta_2, \theta_3)$ by the angles, β_n and ψ_n, as shown in Figure 3.15. The Cartesian coordinates, (x_1^n, x_2^n, x_3^n), are local Cartesian coordinates for location n. The x_3^n axis is an axis of symmetry for the surface tractions at location n. The transformation laws given in Appendix B may be used to determine the effective strain tensor relative to the Cartesian coordinates (x_1^n, x_2^n, x_3^n). In particular, the component of the effective strain tensor along the x_3^n axis is desired. This strain component is given by

$$(\hat{\varepsilon}_{33})_n = \sin^2 \beta_n \cos^2 \psi_n \bar{\varepsilon}_{11} + \sin^2 \beta_n \sin^2 \psi_n \bar{\varepsilon}_{22} + \cos^2 \beta_n \bar{\varepsilon}_{33} +$$

$$2 \sin^2 \beta_n \sin \psi_n \cos \psi_n \bar{\varepsilon}_{12} + 2 \sin \beta_n \cos \beta_n \cos \psi_n \bar{\varepsilon}_{13} +$$

$$2 \sin \beta_n \cos \beta_n \sin \psi_n \bar{\varepsilon}_{23}$$

$$(3.170)$$

where $(\hat{\varepsilon}_{33})_n$ = the component of the strain tensor along the x_3 coordinate axis, and

$\bar{\varepsilon}_{ij}$ = the components of the effective strain tensor.

To determine the displacement across the sphere along the x_3 axis, Equation 3.170 may be integrated with respect to the coordinate x_3. Performing the integration gives

$$(\Delta \hat{u}_3)_n = \int_{-R}^{R} (\hat{\epsilon}_{33})_n \, dx_3^n = 2R \, (\hat{\epsilon}_{33})_n$$

(3.171a)

where $(\Delta \hat{u}_3)_n = (\hat{u}_3)_n (R) - (\hat{u}_3)_n (-R)$

(3.171b)

and $(\hat{u}_3)_n$ = the displacement in the x_3 coordinate direction, and

R = the radius of the sphere.

Equation 3.171a assumes that the effective strain tensor is spacewise constant throughout the representative volume. The quantity $(\hat{u}_3)_n$ is the displacement along the x_3^n axis, across the sphere. The displacement at each surface of the sphere, $(x_3^n = \pm R)$ will be half of $(\hat{u}_3)_n$. Therefore, the displacement at $x_3^n = R$ is

$$(\hat{u}_3)_n \Big|_{x_3^n = R} = R \, (\hat{\epsilon}_{33})_n$$

(3.172)

Equation 3.172 will be used to determine parameters for contact and binder type surface tractions for the case when the effective strain tensor, $\overline{\epsilon}_{ij}$, is known.

For contact type surface tractions, the solution to the contact problem given in Appendix C are used to determine the relationship between the angle, $(\bar{z}_2)_n$, defining the contact surface for contact n, and the displacement given by Equation 3.172. The displacement given by Equation 3.172 will be that at the center of the contact region. The angle $(\bar{z}_2)_n$ is related to this displacement by

$$(\bar{z}_2)_n = \sin^{-1} \left[\sqrt{\frac{|\hat{u}_3|}{R}} \right] \qquad (3.173)$$

In Equation 3.173, the absolute value of $(\hat{u}_3)_n$ is necessary since this quantity is negative. This displacement must be negative for a contact type surface traction to exist. The derivatives of Equation 3.173 which are required to evaluate the effective compliance tensor are

$$\frac{\partial C_n}{\partial \bar{\epsilon}_{ij}} = \frac{1}{2R} \left(\frac{R}{|(\hat{u}_3)_n|} \right)^{1/2} \tan (\bar{z}_2)_n \frac{(U_3)_n}{\partial \bar{\epsilon}_{ij}} \qquad (3.174a)$$

$$\frac{\partial^2 C_n}{\partial \bar{\epsilon}_{ij} \partial \bar{\epsilon}_{kl}} = -\frac{1}{4R^2} \frac{R}{(\hat{u}_3)_n} \left[\left(\frac{R}{|(\hat{u}_3)_n|} \right)^{1/2} \tan (\bar{z}_2)_n \right.$$

$$\left. - \sec^3 (\bar{z}_2)_n \right] \frac{\partial (\hat{u}_3)_n}{\partial \bar{\epsilon}_{ij}} \frac{\partial (\hat{u}_3)_n}{\partial \bar{\epsilon}_{kl}} \qquad (3.174b)$$

where C_n = the cosine of the angle $(\bar{z}_2)_n$.

The derivatives of $(\hat{u}_3)_n$ appearing in Equations 3.174 are given in Table 3.10.

For binder type surface tractions, the solution given in Appendix D is used to determine the relationship between the force, F_{bn}, transmitted by the binder at location n, and the displacement, δ_n, between adjacent spheres. This relationship is given as

$$F_{bm} = k_b \, \delta_n \tag{3.175}$$

where k_b = the elastic spring constant for the material acting as a binder.

The displacement, δ_n, between neighboring spheres will be equal to twice the displacement $(\hat{u}_3)_n$, given by Equation 3.172. Equation 3.175 may be rewritten as

$$F_{bn} = 2 \, k_b \, (\hat{u}_3)_n \tag{3.176}$$

The derivatives of Equation 3.176 which are required to evaluate the effective compliance are

$$\frac{F_{bn}}{\partial \bar{\epsilon}_{ij}} = 2 \, k_b \, \frac{\partial(\hat{u}_3)_n}{\partial \bar{\epsilon}_{ij}} \tag{3.177a}$$

$$\frac{\partial^2 F_{bn}}{\partial \bar{\epsilon}_{ij} \, \partial \bar{\epsilon}_{kl}} = 0 \tag{3.177b}$$

Table 3.10 may be used to evaluate Equations 3.177.

Table 3.10. Derivatives of $(\hat{u}_3)_n$ with Respect to Effective Strain Tensor.

$\bar{\varepsilon}_{ij}$	$\dfrac{\partial(\hat{u}_3)_n}{\partial\bar{\varepsilon}_{ij}}$
$\bar{\varepsilon}_{11}$	$R \sin^2 \beta_n \cos^2 \psi_n$
$\bar{\varepsilon}_{12}$	$R \sin^2 \beta_n \sin \psi_n \cos \psi_n$
$\bar{\varepsilon}_{13}$	$R \sin^2 \beta_n \cos \beta_n \cos \psi_n$
$\bar{\varepsilon}_{21}$	$R \sin^2 \beta_n \sin \psi_n \cos \psi_n$
$\bar{\varepsilon}_{22}$	$R \sin^2 \beta_n \sin^2 \psi_n$
$\bar{\varepsilon}_{23}$	$R \sin \beta_n \cos \beta_n \sin \psi_n$
$\bar{\varepsilon}_{31}$	$R \sin \beta_n \cos \beta_n \cos \psi_n$
$\bar{\varepsilon}_{32}$	$R \sin \beta_n \cos \beta_n \sin \psi_n$
$\bar{\varepsilon}_{33}$	$R \cos^2 \beta_n$

Contact and Binder Type Surface Tractions When the Effective Stress
Tensor is Known

In this section the parameters needed to evaluate contact and
binder type surface tractions will be related to the effective stress
tensor. These relationships would be used when the macroscopically
observable stress field, $\overline{\sigma}_{ij}$, is known.

The surface tractions at location n, as defined in Figure 3.15,
will be related to the effective stress tensor $\overline{\sigma}_{ij}$. The effective
stress tensor, $\overline{\sigma}_{ij}$, is known relative to the Cartesian coordinates
(θ_1, θ_2, θ_3), as shown in Figure 3.15. The solutions given for the
contact and binder type surface tractions are in terms of the total
force transmitted between adjacent spheres. In both cases, the total
force is directed along the x_3^n coordinate axis shown in Figure 3.15.
The force transmitted between spheres will be approximated as

$$(F_{\hat{3}})_n = (K_a)_n R^2 (\sigma_{\hat{33}})_n \tag{3.178}$$

where $(F_3)_n$ = the total force directed along the x_3^n coordinate axis,

R^2 = the radius of the sphere, and

$(\sigma_{\hat{33}})_n$ = the component of the effective stress tensor directed
along the x_3^n coordinate axis.

The term, $(K_a)_n$, appearing in Equation 3.178 is a factor which depends
on the packing geometry of the system. These constants depend on the

area transmitting the stress, $(\hat{\sigma}_{33})_n$, between adjacent spheres at location n. Values of (K_n) for the different packing configurations are given in Table 3.11. The stress, $(\sigma_{\hat{3}3})_n$, may be determined using the transformation laws given in Appendix B. The stress $(\sigma_{\hat{3}3})_n$ is given by

$$(\sigma_{\hat{3}3})_n = \sin^2 \beta_n \cos^2 \psi_n \, \overline{\sigma_{11}} + \sin^2 \beta_n \sin^2 \psi_n \, \overline{\sigma_{22}} +$$

$$+ \cos^2 \beta_n \, \overline{\sigma_{33}} + 2 \sin^2 \beta_n \sin \psi_n \cos \psi_n \cdot \overline{\sigma_{12}} +$$

$$+ 2 \sin \beta_n \cos \beta_n \cos \psi_n \, \overline{\sigma_{13}} + 2 \sin \beta_n \cos \beta_n \sin \psi_n \, \overline{\sigma_{23}}$$

$$(3.179)$$

where the angles, β_n and ψ_n, are shown in Figure 3.15.

For contact type surface tractions, Equation 3.128 gives the relationship between the angle, $(\overline{z}_2)_n$, defining the contact surface at location n, and the force, F_c, transmitted by the contact. In terms of the force $(\hat{F}_3)_n$, given by Equation 3.178, this relationship is

$$(\overline{z}_2)_n = \sin^{-1} \left[\frac{3(1-\nu^2)|(\hat{F}_3)_n|}{4R^2 \, E} \right]^{1/3} \qquad (3.180)$$

where E = Young's Modulus for the sphere, and

ν = Poisson's ratio for the sphere.

Table 3.11. Factors for the Different Packing Configurations.

Packing Configuration	$(K_a)_n$ Factor
Simple Cubic	4
Orthorhombic	2.83
Tetragonal Spheroidal	2.33
Rhombohedral	2.0

Equation 3.180 may be used to determine the derivatives required to evaluate the expressions for the effective stiffness. These derivatives are

$$\frac{\partial C_n}{\partial \overline{\sigma}_{ij}} = \frac{1}{2\pi R^2 K_c^\sigma} \left[\frac{2 R^2 K_c^\sigma}{3|(\hat{F}_3)_n|} \right]^{2/3} \tan (\overline{z}_2)_n \frac{\partial(\hat{F}_3)_n}{\partial \overline{\sigma}_{ij}}$$

$$(3.181a)$$

$$\frac{\partial^2 C_n}{\partial \sigma_{ij} \, \partial \sigma_{kl}} = \frac{-1}{2\pi R^2 K_c^\sigma} \left[\frac{2\pi R^2 K_c^\sigma}{3|(\hat{F}_3)_n|} \right]^{2/3} \left\{ \tan (\overline{z}_2)_n \frac{\partial^2(\hat{F}_3)_n}{\partial \overline{\sigma}_{ij} \, \partial \overline{\sigma}_{kl}} \right. +$$

$$\frac{1}{2\pi R^2 K_c^\sigma} \left[\frac{2\pi R^2 K_c^\sigma}{3|(\hat{F}_3)_n|} \right] \left[\right.^{2/3} \sec^3(\overline{z}_2)_n$$

$$- 2 \left[\frac{2\pi R^2 K_c^\sigma}{3|(F_3)_n|} \right]^{1/3} \tan (\overline{z}_2)_n \frac{(\hat{F}_3)_n}{\partial \overline{\sigma}_{ij}} \frac{(\hat{F}_3)_n}{\partial \overline{\sigma}_{kl}} \right\}$$

$$(3.181b)$$

$$K_c^\sigma = \frac{2 E}{\pi(1-\nu^2)}$$

$$(3.181c)$$

The derivatives of $(\hat{F}_3)_n$ with respect to the effective stress tensor, $\overline{\sigma}_{ij}$, are determined using Equations 3.178 and 3.179. These derivatives are given in Table 3.12.

For binder type surface tractions, the force transmitted by the mixture phase is that given by Equation 3.178. Rewriting Equation

Table 3.12. Derivatives of $(\hat{F}_3)_n$ with Respect
to Effective Stress Tensor.

$\overline{\sigma}_{ij}$	$\dfrac{\partial (\hat{F}_3)_n}{\partial \sigma_{ij}}$
$\overline{\sigma}_{11}$	$(K_a)_n \, R^2 \, \sin^2 \beta_n \, \cos^2 \psi_n$
$\overline{\sigma}_{12}$	$(K_a)_n \, R^2 \, \sin^2 \beta_n \, \sin \psi_n \, \cos \psi_n$
$\overline{\sigma}_{13}$	$(K_a)_n \, R^2 \, \sin \beta_n \, \cos \beta_n \, \cos \psi_n$
$\overline{\sigma}_{21}$	$(K_a)_n \, R^2 \, \sin^2 \beta_n \, \sin \psi_n \, \cos \psi_n$
$\overline{\sigma}_{22}$	$(K_a) \, R^2 \, \sin^2 \beta_n \, \sin^2 \psi_n$
$\overline{\sigma}_{23}$	$(K_a)_n \, R^2 \, \sin \beta_n \, \cos \beta_n \, \sin \psi_n$
$\overline{\sigma}_{31}$	$(K_a)_n \, R^2 \, \sin \beta_n \, \cos \beta_n \, \cos \psi_n$
$\overline{\sigma}_{32}$	$(K_a)_n \, R^2 \, \sin \beta_n \, \cos \beta_n \, \sin \psi_n$
$\overline{\sigma}_{33}$	$(K_a)_n \, R^2 \, \cos^2 \beta_n$

3.178 in terms of the force, F_{bn}, transmitted by the binder at location n, gives

$$F_{bn} = (\hat{F}_3)_n = (K_a)_n \, R^2 \, (\hat{\sigma}_{33})_n \qquad (3.182)$$

The derivatives required for evaluation of the effective stiffness are

$$\frac{\partial F_{bn}}{\partial \bar{\sigma}_{ij}} = \frac{\partial (\hat{F}_3)_n}{\partial \bar{\sigma}_{ij}} \qquad (3.183a)$$

$$\frac{\partial^2 F_{bn}}{\partial \bar{\sigma}_{ij} \, \partial \bar{\sigma}_{kl}} = \frac{\partial^2 (\hat{F}_3)_n}{\partial \bar{\sigma}_{ij} \, \partial \bar{\sigma}_{kl}} = 0 \qquad (3.183b)$$

The derivatives appearing in Equation 3.183a are evaluated from Table 3.12.

CHAPTER IV

RESULTS

In this chapter the numerical determination of the dimensionless quantities, required to evaluate the expressions for the effective compliance and stiffness tensors contained in Chapter III, will be reviewed. Results for some of the dimensionless quantities will be presented and their validity discussed.

The dimensionless constants which appear in Chapter III were evaluated using numerical integration techniques. The numerical integrations were performed on a computer. The integrals which involve the prescribed surface tractions present on the spheres in the system were evaluated using an eighty point, Gauss type integration formula. This integration method approximates these one-dimensional integrals by

$$\int_a^b f(s) \, ds = \sum_{n=1}^{N_p} W_n \, f(s_n)$$

$$a < s_n < b, \ n = 1, \, 2, \, \ldots, \, N_p \qquad (4.1)$$

where s_n = integration point n;

W_n = weight factor n; and

N_p = the number of integration points.

For the problem under consideration, the integral appearing in Equation 4.1 is that involving the prescribed surface tractions.

The volume integrals which are required to evaluate the dimensionless quantities appearing in Chapter III, were evaluated using a spherical product formula. The spherical product formula used was for the three-dimensional sphere and is given by Stroud (28). The spherical product formula transforms three dimensional volume integrals into the products of three one dimensional integrals. Gauss type integration formulae are used to approximate the one-dimensional integrals. The final result is an integration formula of the type

$$\iiint_{V_s} f(\theta_1, \theta_2, \theta_3) \; d\theta_1 \; d\theta_2 \; d\theta_3 =$$

$$\sum_{n=1}^{N_p} W_n f(\theta_{1n}, \theta_{2n}, \theta_{3n})$$

$$0 < \theta_{1n}^2 + \theta_{2n}^2 + \theta_{3n}^2 < R^2, \quad n=1, 2, \ldots, N_p \qquad (4.2)$$

where V_s = the volume of the sphere; and

$(\theta_{1n}, \theta_{2n}, \theta_{3n})$ = the global coordinates for integration point n.

The other terms appearing in Equation 4.2 have the same meanings as those in Equation 4.1. Spherical product formulae for the three dimensional sphere are available in (28) using m^3 integration points

where $m = 2, 3, \ldots$. These formulae provide exact solutions to the integral appearing in Equation 4.2 when $f(\theta_1, \theta_2, \theta_3)$ is a polynominal of order $2m-1$ or less.

Equations 4.1 and 4.2 were used in a computer program to evaluate the dimensionless quantities appearing in Chapter III.

In evaluating the dimensionless quantities, two factors were recognized as having a significant effect on the calculated results. These two factors are

1. The number of terms taken in the series solution for the axisymmetric sphere.

2. The number of integration points used to evaluate the volume integrals by Equation 4.2.

Addressing the first of these factors, inspection of the series solution in Chapter III shows that when evaluated at the center of the sphere, only one non-zero term remains in the series. Therefore, at the center of the sphere the solution as obtained using a single term in the series. The number of terms in the series which is required for convergence to the correct result increases as the series is evaluated at points farther away from the origin. The maximum number of terms required in the series to converge to the correct result will occur on the surface of the sphere. The series solution was checked to determine the number of terms required to yield a calculated result within five percent of a known result, when evaluated on the surface of the sphere. The surface tractions used in this check were that of a uniform pressure acting over a portion of the sphere as shown in Figure 4.1. Analysis
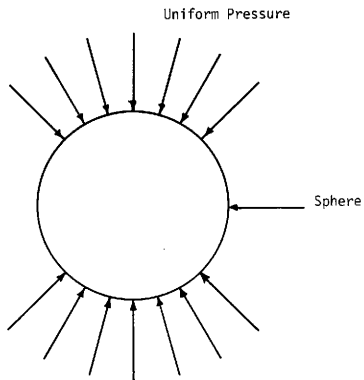
Figure 4.1. -- Uniform Pressure Acting Over a
Portion of a Sphere.

showed that approximately thirty terms in the series were required for calculated results within five percent of the actual. The computer program employed to evaluate the dimensionless quantities used fifty terms in the series solution.

The other factor that affected the results of the computer program was the number of integration points used to evaluate the volume integrals in Equation 4.2. To study the dependence of the computer results on the number of integration points, the contact problem appearing in Figure 3.9 was used. A non-dimensionalized measure of the volume averaged strain energy density was determined for the center sphere of this configuration, using the computer program. This quantity was determined as

$$\pi_d = \frac{G}{2(\kappa_c^\sigma)^2 V_p} \int_{V_p} \sigma_{ij}^c \, \epsilon_{ij}^c \, dV \qquad (4.3a)$$

$$\kappa_c^\sigma = \frac{2E}{\pi(1-\nu^2)} \qquad (4.3b)$$

and E = Young's modulus;

G = the shear modulus;

V_p = the sphere volume;

σ_{ij}^c = the stress tensor due to contact type surface tractions;

ϵ_{ij}^c = the strain tensor due to contact type surface tractions; and

ν = Poisson's ratio.

The quantity, π_d, given by Equation 4.3a was determined using 512, 1000, and 1728 integration points in Equation 4.2. The computer results for different contact surfaces and a Poisson's ratio of 0.3, appear in Figure 4.2. Figure 4.2 shows that the quantity π_d increases as the number of integration points increases. The rate of increase of π_d with respect to the number of integrations points, N_p, is greatest for small contact surfaces. This suggests that the computer results for the larger values of the contact surfaces are closer to the true values, for a given number of integration points.

In summary, the accuracy of the computer results depend on the two factors previously mentioned. The number of integration points used to evaluate Equation 4.2 appears to have the largest effect on the computer results. Since for m^3 integration points, Equation 4.2 gives exact results for polynominals of order 2m-1 or less, it stands to reason that increasing the number of integration points would provide more accurate results. This is because term m of the series solution involves polynominals of order 2m. Unfortunately, as the number of integrations points is increased, computer costs are also greatly increased. At the time of this writing, funds were unavailable to study the problem of obtaining accurate computer results. As a result the evaluation of the dimensionless quantities appearing in Chapter III was not performed.

The dimensionless quantities which result in a single pair of either contact or binder type surface tractions were determined using 1728 integration points in Equation 4.2. The dimensionless quantities resulting from a single set of contact type surface tractions are given
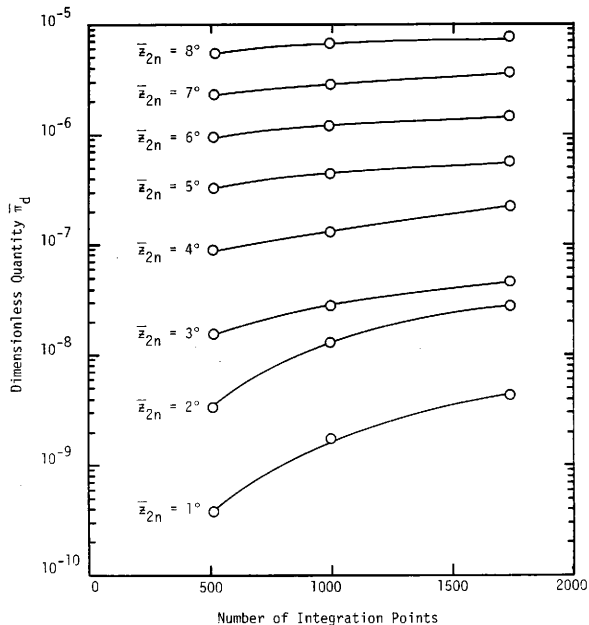
Figure 4.2. -- Dependence of Non-Dimensionalized Measure of Strain
Energy Density on the Number of Integration Points
Used in the Numerical Volume Integration Technique.

by Equations 3.160. Graphs of these quantities appear in Figures 4.3, 4.4 and 4.5. The dimensionless quantity resulting from a single set of binder type surface tractions is given by Equation 3.161. A graph of this quantity appears in Figure 4.6. As previously stated, the accuracy of the results appearing in Figures 4.3 through 4.6 are questionable. The computer program used to obtain the results shown in Figures 4.2 to 4.6 is contained in Appendix E.

200
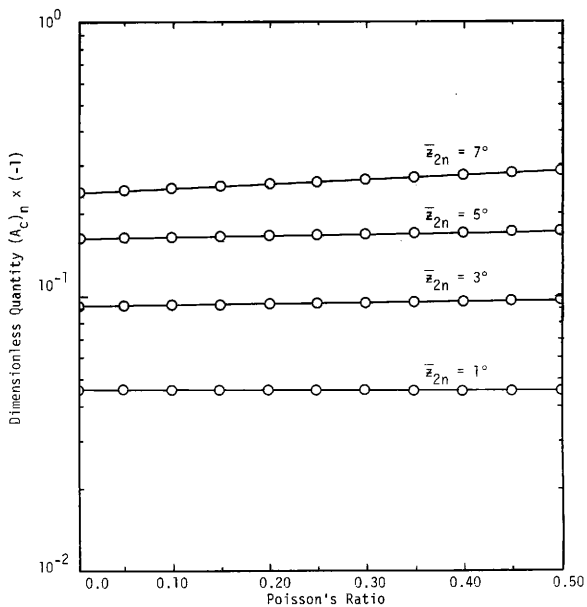
Figure 4.3. -- Dimensionless Quantity $(A_c)_n$ Versus Poisson's Ratio for Various Values of $\bar{z}_{2n}$.
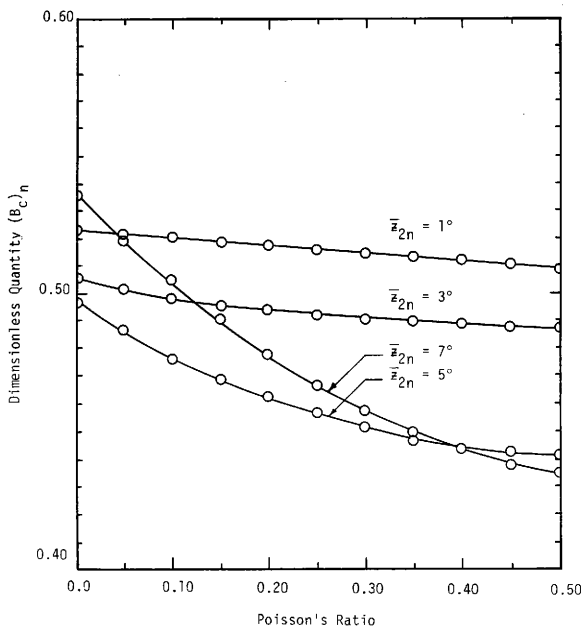
Figure 4.4. -- Dimensionless Quantity $(B_c)_n$ Versus Poisson's Ratio for Various Values of $\bar{z}_{2n}$.
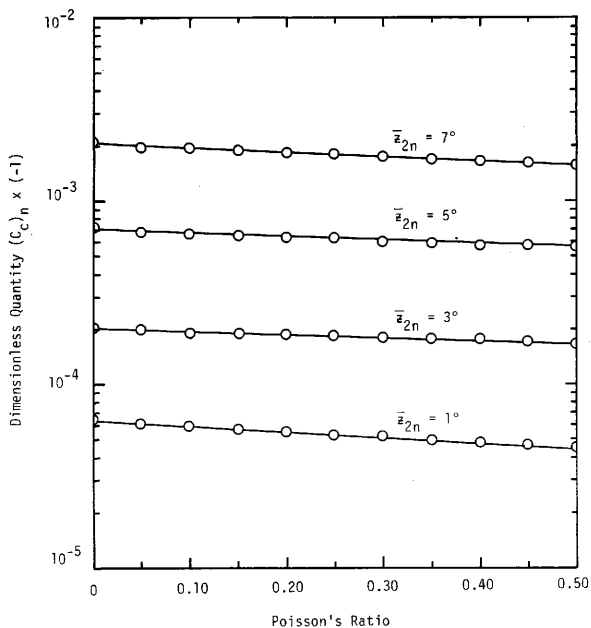
Figure 4.5. -- Dimensionless Quantity $(C_c)_n$ Versus Poisson's Ratio for Various Values of $\bar{z}_{2n}$.
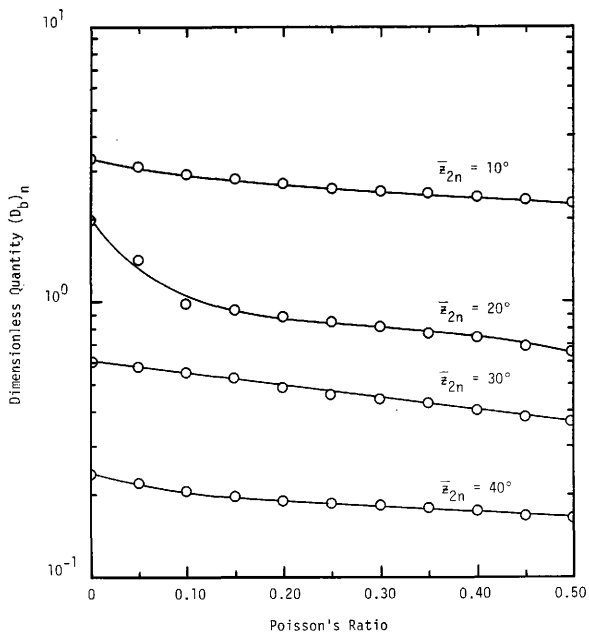
Figure 4.6. -- Dimensionless Quantity $(D_b)_n$ Versus Poisson's Ratio for Various Values of $\bar{z}_{2n}$.

CHAPTER V

CONCLUSIONS AND RECOMMENDATIONS

Expressions for the effective compliance and effective stiffness have been developed for an idealized two phase system. The idealized system consists of equal spheres in contact, surrounded by an air-water mixture. The effective compliance and stiffness tensor are expressed in terms of the initial volume fractions of the two phases, the material properties of the two phases, dimensionless quantities dependent on the surface tractions present on the spheres in the system, and functions describing the loads transmitted between spheres in the system. When the effective strain input to the system is known the effective compliance tensor may be determined, allowing calculation of the effective stress response. When the effective stress input to the system is known the effective stiffness tensor may be determined, allowing the calculation of the effective strain response. The constitutive equations were developed by treating the two phase system as a homogeneous, non-linear elastic body.

The constitutive equations were developed using micromechanics. They seek to recognize actual deformation mechanisms which act on the microscale. Since the constitutive equations were developed using micromechanics, they should find applicability to two phase systems other than soils. The approximations made in the development of the constitutive equations dealt with the geometry, the phase materials, and the stress distributions present in the idealized two phase system. If a particular system may be represented by the idealized two phase system, then the constitutive equations given in this paper should apply.

Highway materials are systems for which the constitutive equations developed here may apply.

In the development of the constitutive equations, non-symmetric shear stresses, with respect to the centers of the contact areas between adjacent spheres, were neglected. Neglect of these stresses represents a correction to the expressions obtained for the effective compliance and stiffness tensors. Solutions for the stresses and displacements due to shear loading of this type on the contact surfaces are available. They may be used to determine a partial correction to the expressions obtained for the effective compliance and stiffness tensors. To obtain the full correction, the effect of the interaction of a surface traction of this type with all other surface tractions must be evaluated. This would require an elastic solution for a sphere subject to non-symmetric shear loadings on a surface of contact. This problem was not considered.

A recommendation for future work would first be to investigate the accurate determination of the dimensionless quantities required for the evaluation of the effective properties. These dimensionless quantities must be determined so that the behavior of the constitutive equations may be observed. The computer program contained in Appendix E may be used for this purpose. The correction to the effective compliance and stiffness tensors, due to non-symmetric shear stresses on contact surfaces needs investigation. A finite element computer code may provide a relatively inexpensive means of determining the significance of this correction. The expressions for the effective compliance and stiffness are dependent on functions which approximate the loads transmitted between adjacent spheres in the system. The quality of these

approximations needs investigation. Better approximations may be possible. These approximate functions will allow that the expressions for the effective compliance and stiffness tensors be fitted or calibrated to data.

Further recommendations for future work would be to apply a Correspondence Principle to the model so that viscoelastic material could be modeled. This would entail representing the particulate phase of the soil system by a viscoelastic material. Because of the non-linear force-displacement relationship present on surfaces in contact, a non-linear Correspondence Principle would have to be employed. Correspondence principles of this type are given by Schapery (28). Application of such a Correspondence Principle is worthy of investigation.

REFERENCES

1. Barden, L., Ismail, H., and Tong, P., "Plane Deformation of Granular
   Material at Low and High Pressures", Geotechnique, Vol. 19, 1969, pp.
   441-452.

2. Bhatt, J. J., Carroll, M. M., and Schatz, J. F., "A Spherical Model
   Calculation for the Volumetric Response of Porous Rocks", Journal of
   Applied Mechanics, Vol. 42, 1975, pp. 363-368.

3. Butkovitch, T. R., "A Technique for Generating Pressure-Volume
   Relationships and Failure Envelopes for Rocks", Lawrence Livermore
   Laboratory Report UCRL-51441, Livermore, California, 1973.

4. Caroll, M. M., and Holt, A. C., "Suggested Modification of the P-2
   Relation for Porous Materials", Journal of Applied Physics, Vol. 43,
   1972, pp. 759-761.

5. Carroll, M. M., and Holt, A. C., "Static and Dynamic Pore-Collapse
   Relations for Ductile Porous Materials", Journal of Applied Physics,
   Vol. 43, 1972, pp. 1626-1636.

6. Chadwick, P., "Compression of a Spherical Shell of Work Hardening
   Material", International Journal of Mechanical Science, Vol. 5, 1963,
   pp. 165-182.

7. Chu, T. Y., and Hashin, Z., "Plastic Behavior of Composites and
   Porous Media Under Isotropic Stress", International Journal of
   Engineering Science, Vol. 9, 1971, pp. 971-994.

8. Duncan, J. M., and Chang, C. Y., "Non-Linear Analysis of Stress and
    Strain in Soils", Journal of the Soil Mechanics and Foundations
    Division, ASCE, Vol. 96, No. SM5, 1970, pp. 1629-1653.

9. Frydman, S., Zeitlen, J. G., and Alpan, I., "The Yielding Behavior of
    Particulate Media", Canadian Geotechnical Journal, Vol. 10, 1973, pp.
    341-362.

√ 10. Hashin, Z., "The Elastic Moduli of an Elastic Solid Containing
    Spherical Particles of Another Elastic Solid", Non-Homogeneity in
    Elasticity and Plasticity, Pergamon Press, New York, New York, 1959,
    pp. 463-479.

. 11. Hashin, Z., "The Elastic Moduli of Heterogeneous Materials", Journal
    of Applied Mechanics, Vol. 29, 1962, pp. 143-150.

12. Herrmann, W., "Constitutive Equations for Compaction of Porous
    Materials", Applied Mechanics Aspects of Nuclear Effects in
    Materials, Ed. by C. C. Wan, ASME, New York, New York, 1971.

13. Kakar, A. K., and Chaklader, A. C. D., "Plastic Flow During
    Hot-Pressing", Journal of the American Ceramic Society, Vol. 55,
    1972, pp. 596-601.

14. Ko, H. Y., and Scott, R. F., "Deformation of Sand in Hydrostatic
    Compression", Journal of the Soil Mechanics and Foundations Division,
    ASCE, Vol. 93, 1967, pp. 137-156.

15. Kreher, W., and Schopt, H. G., "Effective Elastic-Plastic Compressibility of Porous Bodies", _International Journal of Solids and Structures_, Vol. 9, 1973, pp. 1331-1348.

16. Mackenzie, J. K., "The Elastic Constants of a Material Containing Spherical Holes", _Proc. Phys. Soc._, Vol. B63, 1950, pp. 2-11.

17. Mandl, A., and Luque, R. F., "Fully Developed Plastic Shear Flow of Granular Materials", _Geotechnique_, Vol. 20, 1970, pp. 277-302.

18. Nemat-Nasser, S., "On Behavior of Granular Materials in Simple Shear", _Soils and Foundations_, Vol. 20, No. 3, 1980, pp. 59-73.

19. O'Connel, R. J., and Budiansky, B., "Sesmic Velocities in Dry and Saturated Cracked Solids", _Journal of Geophysical Research_, Vol. 79, 1974, pp. 5412-5426.

20. Rowe, P. N., "The Stress-Dilatancy Relation of Static Equilibrium of an Assembly of Particles in Contact", _Proc. Roy. Soc. A._, Vol. 269, 1962, pp. 500-527.

21. Sandler, I. S., and Baron, M. L., "Recent Developments in the Constitutive Modeling of Geologic Materials", Third International Conference on Numerical Methods in Geomechanics, ASCE, Athens, 1984, pp. 363-376.

22. Schapery, R. A., "On Viscoelastic Deformation and Failure Behavior of Composite Materials with Destributed Flaws", Eds. S. S. Wang and

W. J. Renton, Advances in Aerospace Structures and Materials - AD - 01, ASME, New York, New York, 1981, pp. 5-20.

23. Schapery, R. A., and Riggins, M., "Development of Cyclic Non-Linear Viscoelastic Constitutive Equations for Marine Sediment", Mechanics of Materials Center Report No. MM 3168-82-4, Texas A&M University, College Station, Texas, 1982.

24. Schapery, R. A., "Correspondence Principles and a Generalized J Integral for Large Deformation and Fracture Analysis of Viscoelastic Media", International Journal of Fracture, Vol. 25, 1984, pp. 195-223.

25. Schatz, J. F., Carroll, M. M., and Chung, D. H., "A Model for the Inelastic Volume Deformation of Dry Porous Rocks", Trans. Amer. Geophys. U., Vol 56, 1974, pp. 1195-1203.

26. Schofield, A., and Wroth, P., Critical State Soil Mechanics, McGraw-Hill, London, 1968.

27. Sternberg, E., and Rosenthal, F., "The Elastic Sphere Under Concentrated Loads", Journal of Applied Mechanics, Vol. 19, 1952, pp. 413-421.

28. Stroud, A. H., Approximate Calculation of Multiple Integrals, Prentice-Hall, Englewood Cliffs, New Jersey, 1971.

29. Torre, C., "Theorie und Verhalten Zusammengepre Bteer Pulver", Berg-u., Huttenmannische Monatshefie, 93, 1948, pg. 62.

30. Truesdell, C., ed., _Continuum Mechanics III Foundations of Elasticity Theory_, Gordon and Breach, New York, New York, 1965, pp. 31-100.

31. Warren, N., and Anderson, O. L., "Elastic Properties of Granular Materials Under Uniaxial Compaction Cycles", _Jour. Geophys. Res._, Vol. 78, 1973, pp. 6911-6925.

32. Wilkins, J. K., "A Theory for the Shear Strength of Rock Fill", _Rock Mechanics_, Vol. 2, 1970, pp. 205-277.

APPENDIX A

The following notations were used:

$(A_{bc})_{mn}$ = dimensionless quantity resulting from the interaction between binder type surface tractions at location m and contact type surface tractions at location n;

$(A_c)_n$ = dimensionless quantity resulting from contact type surface tractions at location n;

$(A_{cc})_{mn}$ = dimensionless quantity resulting from the interaction between contact type surface tractions at locations m and n;

$(A_{cp})_n$ = dimensionless quantity resulting from the interaction between uniform pressure type surface tractions and contact type surface tractions at location n;

$[A_m^\varepsilon]_{ij}$ = component strain solution;

$[A_m^\sigma]_{ij}$ = component stress solution;

A_1, A_2 = constants in "Cam Clay" model;

a = crack length;

$\mathring{a}$ = rate of damage growth;

a_m = coefficient of superposition;

a_{ij}^m = transformation matrix;

$(B_c)_n$ = dimensionless quantity resulting from contact type surface tractions at location n;

$(B_{cc})_{mn}$ = dimensionless quantity resulting from the interaction between contact type surface tractions at locations m and n;

$[B_m^\varepsilon]_{ij}$ = component strain solution;

$[B_m^\sigma]_{ij}$ = component stress solution;

B_i (i=1,2,...,6) = constants in cap model;

b_m = coefficient of superposition;

b_{ij}^m = transformation matrix;

$(C_{bc})_{mn}$ = dimensionless quantity resulting from the interaction between binder type surface tractions at location m and contact type surface tractions at location n;

$(C_c)_n$ = dimensionless quantity resulting from contact type surface tractions at location n;

$(C_{cc})_{mn}$ = dimensionless quantity resulting from the interaction of contact type surface tractions at locations m and n;

$(C_{cp})_n$ = dimensionless quantity resulting from the interaction between pressure type surface tractions and contact type surface tractions at location n;

C_{ijkl} = compliance tensor;

$\overline{C_{ijkl}}$ = effective compliance tensor;

$\overline{C^m_{ijkl}}$ = effective compliance tensor of mixture phase;

$\overline{C^p_{ijkl}}$ = effective compliance tensor of particulate phase;

$(\overline{C^p_{ijkl}})^i$ = contribution to the effective compliance of the particulate phase by interactions between surface tractions at different locations;

$(\overline{C^p_{ijkl}})^o$ = contribution to the effective compliance of the particulate phase by all surface tractions;

C_m = initial volume fraction of mixture phase;

C_n = cosine of the angle z_{2n};

C_p = initial volume fraction of particulate phase;

C_1, C_2 = constants;

C_α = constant;

c = positive constant;

c_{ij}^m = transformation matrix;

c_p = a constant;

D = a constant;

$(D_b)_n$ = dimensionless quantity resulting from binder type
surface tractions at location n;

$(D_{bb})_{mn}$ = dimensionless quantity resulting from the
interaction between binder type surface tractions
at locations m and n;

$(D_{bc})_{mn}$ = dimensionless quantity resulting from the
interaction between binder type surface tractions
at location m and contact type surface tractions at
location n;

$(D_{bp})_n$ = dimensionless quantity resulting from the
interaction between pressure type surface tractions
and binder type surface tractions at location n;

$(D_{cp})_n$ = dimensionless quantity resulting from the
interaction between pressure type surface tractions
and contact type surface tractions at location n;

D_s = degree of saturation;

d = crack density;

E = Young's modulus;

E_i = initial tangent modulus;

F = Helmholtz free energy per unit initial volume;

$\bar{F}$ = frictional force on macroscopic shear plane;

$F*$ = frictional force on microscopic shear plane;

F_{bn} = force transmitted by binder material at location n;

F_c = Complementary free energy per unit initial volume;

$\bar{F}_{cm}$ = volume averaged Complementary free energy per unit initial volume for mixture phase;

$\bar{F}_{cp}$ = volume averaged Complementary free energy per unit initial volume for particulate phase;

$\bar{F}_m$ = volume averaged Helmholtz free energy per unit initial volume for mixture phase;

$\bar{F}_p$ = volume averaged Helmholtz free energy per unit initial volume for particulate phase;

F_α = a constant;

f_i = coefficient;

G = shear modulus;

G_f = instantaneous modulus for cap model;

G_r = spring modulus for cap model;

G_v = long term modulus for cap model;

H = heat addition to system per unit initial volume;

H_t = total heat addition to system;

I_i = first invariant of stress tensor;

J = linear viscoelastic creep compliance;

J_2' = second invariant of the deviatoric stress tensor;

K = bulk modulus;

K_b^σ = constant for binder type surface tractions;

K_c^σ = constant for contact type surface tractions;

K_p^σ = constant for pressure type surface tractions;

K_ρ = constant for binder type surface tractions;

k_f = friction parameter;

k_h = coefficient of solubility;

N_b = number of binder type surface tractions on a single sphere;

N_c = number of contact type surface tractions on a single sphere;

N_g = number of grains in a typical cross section;

N_y = parameter in cap model;

P = pressure;

P_a, P_b = pressures used as parameters in cap model;

$\overline{P}_a$ = current absolute air pressure;

$\overline{P}_{ao}$ = initial absolute air pressure;

P_{atm} = atmospheric pressure;

P_c = pressure required for complete pore closure;

P_e = pressure required for the onset of pore closure;

P_m = pressure present in mixture phase;

P_o = reference pressure;

P_w = water pressure;

P_i = volume fraction of particles having dilatancy angle $\hat{\phi}_i$;

q = positive constant;

R = sphere radius;

R_c = radius of contact surface;

S = entropy per unit initial volume;

S' = entropy production per unit initial volume;

$\overline{S}$ = effective entropy per unit initial volume;

$\overline{S}'$ = effective entropy production per unit initial volume;

S_d = damage parameter;

S_{ijkl} = stiffness tensor;

$\overline{S_{ijkl}}$ = effective stiffness tensor;

$\overline{S_{ijkl}^m}$ = effective stiffness tensor for mixture phase;

$\overline{S_{ijkl}^p}$ = effective stiffness tensor for particulate phase;

$(\overline{S_{ijkl}^p})^i$ = contribution to the effective stiffness tensor of the particulate phase by all the interactions between surface tractions;

$(\overline{S_{ijkl}^p})^o$ = contribution to the effective stiffness tensor of the particulate phase by all surface tractions;

$\overline{S_m}$ = volume averaged entropy per unit initial volume for mixture phase;

$\overline{S_p}$ = volume averaged entropy per unit initial volume for particulate phase;

S_t = total entropy;

S'_t = total entropy production;

s_{ij} = deviatoric stress tensor;

T = absolute temperature;

T_g = Gruneisen ratio;

t = time;

t_r = relaxation time;

U = internal energy per unit initial volume;

U_t = total internal energy;

u = specific internal energy;

u_i = components of displacement vector;

u_0 = reference value of specific internal energy;

$(\hat{u}_3)_n$ = displacement along x_3^n coordinate axis;

V = total volume;

V_a = current volume of air in mixture phase;

V_{ao} = initial volume of air in mixture phase;

V_d = initial volume of dissolved air in mixture phase;

V_{do} = initial volume of dissolved air in mixture phase;

V_m = total volume of mixture phase;

V_p = total volume of particulate phase;

V_s = total volume of single sphere;

V_w = volume of water in mixture phase;

v = specific volume;

W = work per unit initial volume;

W_t = total work;

W_b = work done on binder material;

(x_1^n, x_2^n, x_3^n) = Cartesian coordinate system for contact n;

Y = yield parameter;

(z_1^n, z_2^n, z_3^n) = spherical coordinate system for contact n;

α = porosity;

α_0 = initial porosity;

β_n = angle defining the location of contact pair n with respect to the global coordinates $(\theta_1, \theta_2, \theta_3)$;

$\overline{\sigma}$ = measure of shear strain;

$\overset{\circ}{\overline{\gamma}}$ = time rate of shear deformation;

δ = displacement between adjacent spheres;

δ_{ij} = Kronecker delta;

ε_{ij} = components of the strain tensor;

$\overline{\varepsilon_{ij}}$ = components of the effective strain tensor;

ε'_{ij} = components of the strain tensor referenced to the spherical coordinate system (z_1, z_2, z_3);

ε^m_{ij} = components of the strain tensor due to uniform pressure type surface tractions;

ε^p_{ij} = components of the plastic strain tensor;

$(\varepsilon^b_{ij})_n$ = components of the strain tensor due to binder type surface tractions at location n;

$(\varepsilon^c_{ij})_n$ = components of the strain tensor due to contact type surface tractions at location n;

$\overline{\varepsilon}^p_y$ = parameter in cap model;

ε_1 = maximum principle strain;

$(\epsilon_{33}^{\hat{}})_n$ = the components of the strain tensor directed along

the x_3^η coordinate axis;

η_m = constant determined from the type of surface

tractions;

θ_{mn} = angle defining the location of the x_3^m coordinate

axes with respect to the x_3^η coordinate axes;

$(\theta_1, \theta_2, \theta_3)$ = global Cartesian coordinate system;

μ_d = damping coefficient;

ν = Poisson's ratio;

ξ_m = constant determined from the type of surface

tractions;

$\widetilde{\pi}_m$ = volume averaged strain energy density of mixture

phase;

$\widetilde{\pi}_p$ = volume averaged strain energy density of particulate

phase;

$\widetilde{\pi}_p^i$ = the contributation to the volume averaged strain

energy density of the particulate phase due to the

interaction between surface tractions at different

locations;

$\overline{\pi}_p^0$ = the contributation to the volume averaged strain energy density of the particulate phase due to all sets of surface tractions;

ρ = radial coordinate for contact and binder type surface tractions;

$\overline{\sigma}$ = normal stress acting on macroscopic shear plane;

σ^* = normal stress acting on microscopic shear plane;

σ_{ij} = components of the stress tensor;

$\overline{\sigma_{ij}}$ = components of the effective stress tensor;

σ_{ij}' = components of the stress tensor referenced to the spherical coordinate system (z_1, z_2, z_3);

σ_{ij}^m = components of the stress tensor due to uniform pressure type surface tractions;

$(\sigma_{ij}^b)_n$ = components of the stress tensor due to binder type surface tractions at location n;

$(\sigma_{ij}^c)_n$ = components of the stress tensor due to contact type surface tractions at location n;

σ_1 = maximum principle stress;

σ_3 = least principle stress;

$(\hat{\sigma}_{33})_n$ = normal stress to the plane, x_3^n = constant;

$\bar{\tau}$ = shear stress on macroscopic shear plane;

τ^* = shear stress on microscopic shear plane;

$\bar{\phi}$ = angle of shearing resistance for macroscopic shear plane;

$\hat{\phi}$ = dilatancy angle;

ϕ^* = angle of shearing resistance for microscopic shear plane;

ϕ_u = undrained angle of shearing resistance;

ϕ_u' = effective undrained angle of shearing resistance;

X = work hardening parameter;

ψ_n = angle defining the location of contact pair n with respect to the global coordinates (θ_1, θ_2, θ_3).

APPENDIX B

Equations to transform second order tensors referred to a spherical coordinate system, into the same referred to a Cartesian coordinate system, will be developed. The second order tensor field is assumed to be known and referred to a spherical coordinate system (z_1, z_2, z_3). The Cartesian coordinate system (x_1, x_2, x_3) is related to the spherical coordinate system, (z_1, z_2, z_3) by the mapping

$$x_1 = z_1 \sin(z_2)\cos(z_3) \tag{B.1a}$$

$$x_2 = z_1 \sin(z_2)\sin(z_3) \tag{B.1b}$$

$$x_3 = z_1\cos(z_2) \tag{B.1c}$$

The spherical coordinate system, (z_1, z_2, z_3), is shown relative to the Cartesian coordinate system, (x_1, x_2, x_3) in Figure 3.8. Another Cartesian coordinate system, (θ_1, θ_2, θ_3), will be defined relative to the Cartesian coordinate system, (x_1, x_2, x_3), as shown in Figure 3.9. The Cartesian coordinate system (θ_1, θ_2, θ_3), is related to the Cartesian coordinate system (x_1, x_2, x_3) by the mapping

$$\theta_1 = x_1 \cos\beta \cos\psi - x_2 \sin\psi + x_3 \sin\beta \cos\psi \tag{B.2a}$$

$$\theta_2 = x_1 \cos\beta \sin\psi + x_2 \cos\psi + x_3 \sin\beta \sin\psi \tag{B.2b}$$

$$\theta_3 = -x_1 \sin\beta + x_3 \cos\beta \tag{B.2c}$$

It is desired to determine the second order tensor referred to the Cartesian coordinates, $(\theta_1, \theta_2, \theta_3)$. In determining the transformation equations we will use A_{ij} to denote the physical components of a second order tensor and B_{ij} to denote the tensorial components of a second order tensor. Only the tensorial components transform according to tensor transform laws. The distinction between physical and tensorial components will only be necessary when dealing with a tensor referred to the spherical coordinates, (z_1, z_2, z_3). For tensors referred to a Cartesian coordinate system, the physical and tensorial components are the same. The following rules regarding tensor notation will be followed.

1. A superscript denotes a contravariant tensor.

2. A subscript denotes a covariant tensor.

3. A repeated index implies summation from 1 to 3 unless otherwise indicated.

In addition to these rules, when referring to the physical components of a tensor only subscripts will be used. This is because for coordinate systems other than Cartesian, the physical components of a tensor are not a tensor quantity. Therefore their notation is arbitrary. For a tensor referred to a Cartesian coordinate system, a covariant tensor is equal to its counterpart contravariant tensor, the components of which in turn are equal to the physical components of the tensor. When referring to second order tensors relative to the three coordinate systems, primes will denote tensors referred to the coordinates (z_1, z_2, z_3), overbars will

denote tensors referred to the coordinates (x_1, x_2, x_3), and the absence of either will denote tensors referred to the coordinates $(\theta_1, \theta_2, \theta_3)$. The second order tensor referred to the Cartesian coordinates (x_1, x_2, x_3) will be determined when the physical components of the tensor, referred to the spherical coordinates, (z_1, z_2, z_3) are known. The base vectors of the coordinate system, (x_1, x_2, x_3) with respect to the coordinate system, (z_1, z_2, z_3), are

$$\bar{a}_i = \frac{\partial x_j}{\partial z_i} \hat{e}_j \tag{B.3}$$

where $\bar{a}_i$ = the base vectors in coordinate direction z_i.

$\hat{e}_i$ = the unit vector in coordinate direction x_i.

Use of Equations B.1 and B.3 yield the following expressions for the base vectors a_i.

$$\bar{a}_1 = \sin(z_2)\cos(z_3)\hat{e}_1 + \sin(z_2)\sin(z_3)\hat{e}_2 +$$
$$\cos(z_2)\hat{e}_3 \tag{B.4a}$$

$$\bar{a}_2 = z_1\cos(z_2)\cos(z_3)\hat{e}_1 + z_1\cos(z_2)\sin(z_3)\hat{e}_2 -$$
$$z_1\sin(z_2)\hat{e}_3 \tag{B.4b}$$

$$\bar{a}_3 = -z_1\sin(z_2)\sin(z_3)\hat{e}_1 + z_1\sin(z_2)\cos(z_3)\hat{e}_2 \tag{B.4c}$$

The metric tensor, g_{ij}, of the coordinate system (z_1, z_2, z_3) is determined by

$$g'_{ij} = \bar{a}_i \cdot \bar{a}_j \tag{B.5}$$

Use of Equations B.4 and Equation B.5 yields the following for the metric tensor g'_{ij}.

$$g'_{ij} = \begin{bmatrix} 1 & & 0 \\ 0 & (z_1)^2 & 0 \\ 0 & & (z_1)^2 \sin^2(z_2) \end{bmatrix} \tag{B.6}$$

The tensorial components, B'^{ij}, are related to the physical components A'_{ij}, by

$$B'_{ij} = \frac{A'_{ij}}{\sqrt{g_{ii}} \sqrt{g_{jj}}} \quad \text{(no sum on i or j)} \tag{B.7}$$

To determine the tensor field, $\bar{B}^{ij}$, the transformation law for a contravariant tensor of order two is used. The transformation law is

$$\bar{B}^{ij} = B'^{kl} \frac{\partial x_i}{\partial z_k} \frac{\partial x_j}{\partial z_l} \tag{B.8}$$

Combining Equations B.1., B.6, and B.8 will yield the following expression for the tensor $\bar{B}^{ij}$ referred to the Cartesian coordinates (x_1, x_2, x_3).

$$\bar{B}^{ij} = b_{ki} b_{lj} A'_{kl} \tag{B.9}$$

where

$$[b_{ij}] = \begin{bmatrix} \sin(z_2)\cos(z_3) & \sin(z_2)\sin(z_3) & \cos(z_2) \\ \cos(z_2)\cos(z_3) & \cos(z_2)\sin(z_3) & -\sin(z_2) \\ -\sin(z_3) & \cos(z_3) & 0 \end{bmatrix} \quad (B.10)$$

The second order tensor, B^{ij} will now be determined relative to the coordinates $(\theta_1, \theta_2, \theta_3)$. The base vectors of the coordinate system $(\theta_1, \theta_2, \theta_3)$, with respect to the coordinate system (x_1, x_2, x_3) are determined by

$$\overline{b}_i = \frac{\partial \theta_j}{\partial x_i} \, \hat{e}_j \quad (B.11)$$

where $\overline{b}_i$ = the base vectors in coordinate directions x_i, and

$\overline{e}_i$ = the unit vector in coordinate direction θ_i.

Use of Equations B.2 and B.11 yield the following expressions for the base vectors b_i.

$$\overline{b}_1 = \cos\beta\cos\psi\hat{e}_1 + \cos\beta\sin\psi\hat{e}_2 - \sin\beta\hat{e}_3 \quad (B.12a)$$

$$\overline{b}_2 = -\sin\psi\hat{e}_1 + \cos\psi\hat{e}_2 \quad (B.12b)$$

$$\overline{b}_3 = \sin\beta\cos\psi\hat{e}_1 + \sin\beta\sin\psi\hat{e}_2 + \cos\beta\hat{e}_3 \quad (B.12c)$$

The metric tensor, $\overline{g}_{ij}$, of the coordinate system (x_1, x_2, x_3) is determined by

$$\overline{g}_{ij} = \overline{b}_i \cdot \overline{b}_j \quad (B.13)$$

Combining Equations B.12 and B.13 yields the following for the metric tensor $\overline{g}_{ij}$.

$$\bar{g}_{ij} = \begin{bmatrix} 1 & 0 & 0 \\ 0 & 1 & 0 \\ 0 & 0 & 1 \end{bmatrix} \qquad\qquad (B.14)$$

For the coordinate system $(\theta_1, \theta_2, \theta_3)$, the tensorial components, B^{ij}, related to the physical components, A_{ij}, by

$$B^{ij} = \frac{A_{ij}}{\sqrt{g_{ii}} \ \sqrt{g_{jj}}} \qquad (\text{no sum on } i \text{ or } j) \qquad (B.15)$$

From Equations B.14 and B.15 it is seen that for a Cartesian coordinate system, the tensorial and physical components of a tensor are equal. In view of this, the transformation law for a second order contravariant tensor may be used to determine A_{ij}, as follows

$$A_{ij} = B^{ij} = \bar{B}^{kl} \frac{\partial \theta_i}{\partial x_k} \frac{\partial \theta_j}{\partial x_l} \qquad\qquad (B.16)$$

Combining Equations B.2 and B.16 yields the following expression for the tensor A_{ij}.

$$A_{ij} = c_{ki} \ c_{lj} \ \bar{B}^{kl} \qquad\qquad (B.17)$$

where

$$[c_{ij}] = \begin{bmatrix} \cos\beta\cos\psi & -\sin\psi & \sin\beta\cos\psi \\ \cos\beta\sin\psi & \cos\psi & \sin\beta\sin\psi \\ -\sin\beta & 0 & \cos\beta \end{bmatrix} \qquad (B.18)$$

Equations B.9 and B.17 may be combined to obtain

$$A_{ij} = a_{ik} \, a_{j1} \, A'_{k1} \qquad \text{(B.19)}$$

where

$$a_{ij} = b_{ik} \, c_{kj} \qquad \text{(B.20)}$$

Equations B.19 and B.20 relate a second order tensor referred to the Cartesian coordinate system $(\theta_1, \theta_2, \theta_3)$ to the same referred to the spherical coordinate system (z_1, z_2, z_3). This transformation may be used provided the relationships given by Equations B.1 and B.2 are known.

APPENDIX C

The Hertz solution for the pressure occurring between two spherical bodies in contact will be given. The force-displacement relationship for the center of the contact area will be determined. The problem under consideration is shown in Figure C.1. The two spherical bodies shown in Figure C.1 are of equal radii and have the same material properties. Both materials are homogeneous, linear elastic. In Figure C.1, the coordinate directions y_1 and y_2 are considered positive when directed from the center of the contact surface toward the centers of spheres 1 and 2, respectively. When there is no pressure between the two spheres, the coordinates y_1 and y_2, for the surfaces of spheres 1 and 2 are given by

$$y_1 = y_2 = R - \sqrt{R^2 - \rho^2} \tag{C.1}$$

where

R = the radius of the spheres, and

ρ = the distance from the center of the contact surface to a
       point on the surface of either sphere.

When ρ is small in comparison to R, a Taylor series expansion about $\rho = 0$ may be used to approximate the distances y_1 and y_2, given by Equation C.1. Retaining the first two terms of the series gives
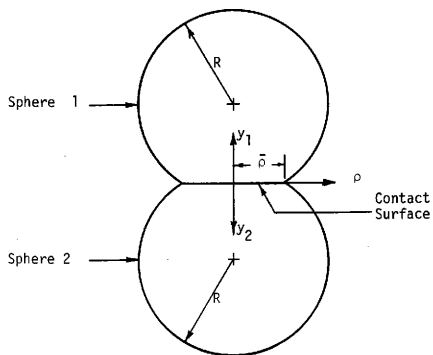
Figure C.1 -- Geometry for Hertz Contact Problem.

$$y_1 = y_2 = \frac{\rho^2}{2 R} \qquad\qquad\qquad (C.2)$$

When the spheres appearing in Figure C.1 are pressed together by a compressive force, contact will be made over a small circular surface. As the spheres are pressed together, the distance between two points lying on the surface of the spheres, at a distance from the center of the contact surface will diminish by

$$\zeta - (w_1 + w_2) \qquad\qquad\qquad (C.3)$$

where

$$\zeta = (w_1 + w_2) \Big|_{\rho = 0} \qquad\qquad\qquad (C.4)$$

and w_1 = the displacement of the surface of sphere 1 in the

direction y_1, due to local deformation, and

w_2 = the displacement of the surface of sphere 2 in the

direction y_2, due to local deformation.

For points lying within the surface of contact, the following relationship is obtained from Equations C.2 and C.3.

$$\zeta - (w_1 + w_2) = y_1 + y_2 = \frac{\rho^2}{R} \qquad\qquad\qquad (C.5)$$

When considering local deformation within the contact surface, the spheres may be considered to be represented by a half-space. The solution for the displacement occurring on the surface of a half space due to a distributed load may be employed to determine the displacements, w_1 and w_2. Figure C.2 shows a point A lying within a contact surface of radius $\bar{\rho}$. The contact surface is considered to lie on the surface of a half space. A pressure P, resulting
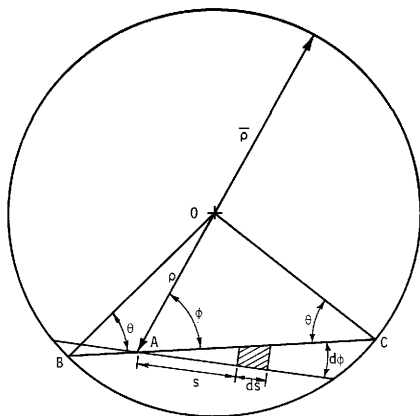
Figure C.2 -- Geometry for Distributed Load on a Halfspace.

from the compression of the two spheres acts normal to the contact surface. Employing the solution for a distributed load acting on the surface of a halfspace, the local deformations w_1 and w_2 are given by

$$w_1 = w_2 = \frac{(1-\nu^2)}{\pi E} \iint\limits_{\Omega} P(s,\phi) \, ds \, d\phi \tag{C.6}$$

where

s,ϕ = the coordinates defined in Figure C.2, and

Ω = the loaded area, corresponding to the contact surface.

Substitution of Equation C.6 into Equation C.5 yields

$$\frac{2(1-\nu^2)}{\pi E} \iint\limits_{\Omega} P(s,\phi) \, ds \, d\phi = \zeta - \frac{\rho^2}{R} \tag{C.7}$$

The problem is now to determine the pressure distribution, $P(s,\phi)$, which satisfies Equation C.7. The pressure distribution which satisfies Equation C.7 is that of an elliptical cap acting over the contact surface. Consider the chord BC appearing in Figure C.2. The pressure distribution along this chord would appear as that shown in Figure C.3. The maximum pressure along this chord is given by

$$P_o(\phi) = \frac{P_o}{a} \sqrt{\bar{\rho}^2 - \rho^2 \sin^2\phi} \quad , \quad -\frac{\pi}{2} \le \phi \le \frac{\pi}{2} \tag{C.8}$$
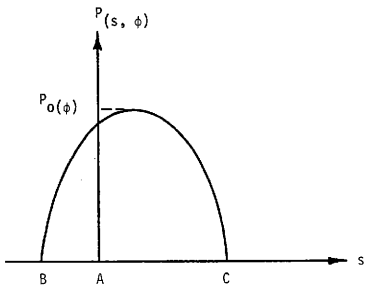
where

Figure C.3 -- Pressure Distribution Along Chord BC of
Circular Loaded Area.

P_0 = the pressure acting on the center of the contact region.

The pressure distribution along the chord BC of Figure C.3 is given by

$$P(s,\phi) = \frac{P_0(\phi)}{\bar{\rho}\cos\theta} \sqrt{\bar{\rho}^2\cos^2\theta - (s-\rho\cos\phi)^2} \tag{C.9}$$

where

$$\bar{\rho}\sin\theta = \rho\sin\phi \tag{C.10}$$

The variable s may be expressed as

$$s = \rho\cos\phi + \bar{\rho}\cos\phi\,\cos\theta, \quad 0 \leq \theta \leq \pi \tag{C.11}$$

Substitution of Equations C.8, C.9, C.10 and C.11 into Equation C.7 gives

$$\frac{-2\,(1-\nu^2)P_0}{\pi\,E\,\bar{\rho}} \iint (\bar{\rho}^2 - \rho^2\sin^2\phi)\,\sin^2\theta\,d\theta d\phi \tag{C.12}$$

$$= \zeta - \frac{\rho^2}{R}$$

Integration of Equation C.12 gives the following result.

$$\frac{2\,(1-\nu^2)\,P_0}{\bar{\rho}\,E} \left[\frac{\pi\,\bar{\rho}^2}{2} - \frac{\pi\,\rho^2}{4} \right] = \zeta - \frac{\rho^2}{R} \tag{C.13}$$

Equation C.13 shows that Equation C.7 is satisfied by an elliptical pressure distribution acting on the contact surface provided the radius of the contact surface, $\bar{\rho}$, and the displacement, ζ, are given by

$$\bar{\rho} = \frac{\pi\,(1-\nu^2)\,R\,P_0}{2E} \tag{C.14}$$

$$\zeta = \frac{\pi (1-\nu^2) \bar{\rho} P_0}{E} \qquad (C.15)$$

The constant P_0 appearing in Equations C.14 and C.15 is determined by setting the integral of the pressure distribution taken over the contact surface equal to the total compressive force, F_c. The pressure distribution over the contact surface is

$$P (\rho) = \frac{P_0}{\bar{\rho}} \sqrt{\bar{\rho}^2 - \rho^2} \qquad (C.16)$$

For equilibrium of the spheres the following condition must hold

$$\iint_{\Omega} P (\rho) \, da = \frac{2\pi P_0}{\bar{\rho}} \int_0^{\bar{\rho}} \sqrt{\bar{\rho}^2 - \rho^2} \quad \rho d\rho = F_c \qquad (C.17)$$

Integration of Equation C.17 and then solving for P_0 gives

$$P_0 = \frac{3 F_c}{2 \pi \bar{\rho}^2} \qquad (C.18)$$

Equations C.6, C.9, C.10, and C.11 may be used to determine the local deformations, w_1 and w_2, of points on the surfaces of spheres 1 and 2, contained in the contact surface. The local deformations are

$$w_1 = w_2 = \frac{\pi (1-\nu^2) P_0}{4 \bar{\rho} E} [2\bar{\rho}^2 - \rho^2] \qquad (C.19)$$

To determine the force-displacement relationship at the center of the contact surface (ρ = o), Equations C.14, C.18 and C.19 are combined to yield

$$w\big|_{\rho\,=\,o} \;=\; \left[\frac{3\,(1-\nu^2)\,F_c}{4E}\right]^{2/3}\frac{1}{R^{1/3}} \qquad\qquad (C.20)$$

Equation C.20 shows that the force-displacement relationship on the contact surface is given by a power-law.

The results for the pressure distribution resulting from two spheres in contact will now be used to determine the surface tractions which result from the contact of a single sphere with the two neighboring spheres, along an axis of symmetry. The sphere configuraton under consideration is shown in Figure C.4. The coordinates (x_1, x_2, x_3) are a Cartesian coordinate system whose origin is located at the center of the middle sphere as shown in Figure C.4. Also shown in Figure C.4 are the spherical coordinates, (z_1, z_2, z_3). The coordinates (x_1, x_2, x_3) are related to the coordinates (z_1, z_2, z_3) by the mapping

$$x_1 = z_1\,\sin(z_2)\,\cos(z_3) \qquad\qquad (C.21a)$$

$$x_2 = z_1\,\sin(z_2)\sin(z_3) \qquad\qquad (C.21b)$$

$$x_3 = z_1\,\cos(z_2) \qquad\qquad (C.21c)$$

Quantities referred to the (x_1, x_2, x_3) coordinates will be denoted by a hat ($\hat{}$) and quantities referred to the (z_1, z_2, z_3) coordinates
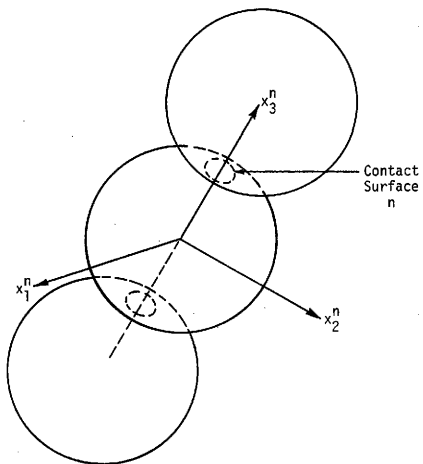
Figure C.4 -- Three Spheres in Contact Along an Axis
of Symmetry.

will be denoted by a prime. The pressure distribution on the contact surfaces of the center sphere will act along the x_3 coordinate axis. Using Equations C.14 and C.17, the surface tractions on the center sphere are given by

$$\hat{\sigma}_{33} = \begin{cases} \dfrac{2E}{\pi(1-\nu^2)R} \sqrt{\bar{\rho}^2 - x_1^2 - x_2^2} & , \ x_1^2 + x_2^2 \leq \bar{\rho}^2 \\ 0 & , \ x_1^2 + x_2^2 > \bar{\rho}^2 \end{cases} \qquad (C.22)$$

To determine the surface tractions given by Equations (C.21) in the coordinate system $(\bar{z}_1, \bar{z}_2, \bar{z}_3)$, the following relationship exists between the stresses referenced to the two coordinate systems.

$$\sigma_{11}' = \hat{\sigma}_{33} \cos^2(\bar{z}_2) \qquad (C.23)$$

$$\sigma_{12}' = \hat{\sigma}_{33} \sin(\bar{z}_2) \cos(\bar{z}_2) \qquad (C.24)$$

Using Equations C.21, C.22, C.23, and C.24, the surface tractions referred to the coordinates $(\bar{z}_1, \bar{z}_2, \bar{z}_3)$ are given by

$$\sigma'_{11} = \begin{cases} \dfrac{-2E}{\pi(1-\nu^2)} \sqrt{\cos^2(\bar{z}_2) - \cos^2(\bar{\bar{z}}_2)} \ \cos^2(\bar{z}_2), \\ \qquad 0 \leq \bar{z}_2 \leq \bar{\bar{z}}_2, \ \pi - \bar{\bar{z}}_2 \leq \bar{z}_2 \leq \pi \\ 0 \quad , \quad \bar{\bar{z}}_2 < \bar{z}_2 < \pi - \bar{\bar{z}}_2 \end{cases} \qquad (C.25)$$

$$\sigma'_{12} = \begin{cases} \dfrac{2E}{\pi \, (1-\nu^2)} \sqrt{\cos^2 (z_2) - \cos^2 (\bar{z}_2)} \quad \sin (z_2), \\ \qquad\qquad \cos(z_2), \; 0 \le z_2 \le \bar{z}_2, \; \pi - \bar{z}_2 \le z_2 \le \pi \\ 0 \qquad , \qquad\qquad\qquad\qquad \bar{z}_2 \le z_2 \le \pi - \bar{z}_2 \end{cases} \qquad (C.26)$$

where

$$z_2 = \sin^{-1} \left(\frac{\bar{\rho}}{R} \right) \qquad\qquad\qquad (C.27)$$

Equations C.25, C.26 and C.27 define the surface tractions on the center sphere of Figure C.4 referred to the spherical coordinates (z_1, z_2, z_3).

APPENDIX D

The case of a material acting as a binder between equal spheres will be considered. Figure D.1 shows two spheres being held together by a material acting as a binder. The initial position of the spheres is shown in Figure D.1a. In this position the spheres are touching. A portion of the surfaces of the spheres is covered by another material which acts as a binder. It will be assumed that the binder material has perfect cohesion with the spheres. There is no slippage between this material and the surfaces of the spheres, as the spheres are displaced relative to one another. The surface area of the spheres which is covered by the binder material is described by the angle $\bar{z}_2$. In Figure D.1b, the spheres are shown displaced relative to one another. The surfaces of the spheres which were touching are displaced a distance δ, due to the load F_b. The load displacement relationship for the binder material is assumed to be given by

$$F_b = K_b \delta \tag{D.1}$$

where

K_b = the elastic spring constant for the binder material.

The angle $\bar{z}_2$, shown in Figure D.1 remains constant as the spheres are displaced. It is assumed that the vectors that are normal to the surface of the binder material and the surfaces of the sphere, are parallel for all points located by the angle $\bar{z}_2$. The surface tractions present on the spheres when the system is displaced will

(a)   (b)
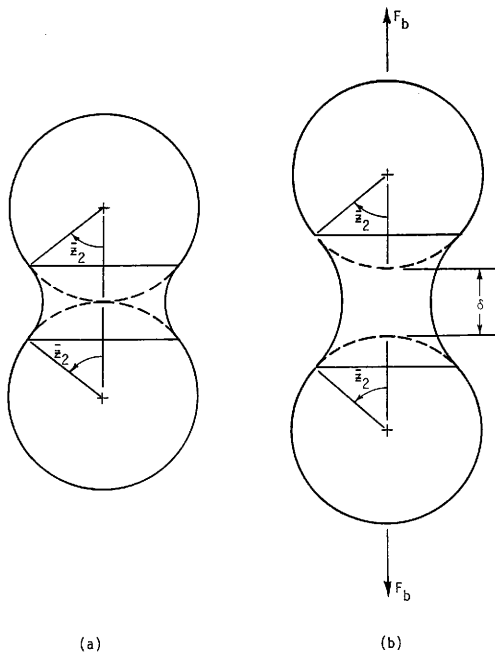
Figure D.1 -- Mixture Material Acting as a Binder
           Between Neighboring Spheres.

be determined. The surface tractions to be determined are approximate. The approximate solution will be obtained by considering a single sphere and half of the binder material as shown in Figure D.2. Appearing in Figure D.2 are the radial coordinates, ρ_b and ρ_s. These are used to describe points on the plane, $x_3 = R + \delta/2$, and the surface of the sphere. Also shown in Figure D.2 are two strips of the binder material. One strip is located at the outer edge ($\rho_s = \overline{\rho}_s$, $\rho_b = \overline{\rho}_b$) of the binder and one strip is located at the center ($\rho_b = \rho_s = 0$) of the binder. These strips have rotational symmetry about the x_3 axis. The binder material as a whole will be viewed as a collection of these strips thus forming a series of concentric rings. When the spheres are displaced as shown in Figure D.1b, the outer strip of binder material will experience a greater displacement than that at the center. The load is to be viewed as being transferred through the strips to the sphere. The force-displacement relationship for the binder material is linear. A greater portion of the load will be transferred through the outer strip since it undergoes the larger displacement. It will be assumed that the stress, $\hat{\sigma}_{33}$, occurring on the $x_3 = R + \delta/2$ plane, in the x_3 coordinate direction, varies elliptically with respect to the coordinate ρ_b. The assumed stress distribution is

$$\hat{\sigma}_{33} \ (x_3 = R + \delta/2) = \Delta\sigma \ [1 - \sqrt{1 - (\rho_b/\rho_b)^2} \ ] + \sigma_0 \qquad (D.2)$$
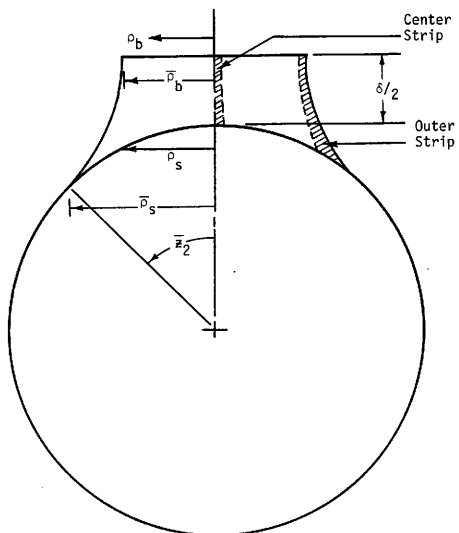
Figure D.2 -- Geometry for Determining the Surface
Tractions on a Single Sphere Due to
the Mixture Phase Acting as a Binder
Material.

The constants, $\Delta\sigma$ and σ_0, are to be interpreted as shown in Figure D.3. The constants $\Delta\sigma$ and σ_0 may be related to each other by considering the displacements of the outer and center strips of the binder material. The linear load-displacement relationship allows the following relationship.

$$\frac{\sigma_0}{d \ (\rho_b = 0)} = \frac{\sigma_0 + \Delta\sigma}{d \ (\rho_b = \overline{\rho}_b)} \tag{D.3}$$

where

    d = the displacement of the strips of the binder material.

The displacement of the binder material at the center ($\rho_b = 0$) is equal to $\delta/2$. Through geometry considerations, the displacement of the binder material at the outer edge ($\rho_b = \overline{\rho}_b$) is

$$d \ (\rho_b = \overline{\rho}_b) = 1/2 \ \delta \ (1/2\pi - \overline{z}_2) \ \sec \ (\overline{z}_2) \tag{D.4}$$

The relationship between $\Delta\sigma$ and σ_0 is given by

$$\Delta\sigma = [(1/2\pi - \overline{z}_2) \ \sec \ (\overline{z}_2) - 1] \ \sigma_0 \tag{D.5}$$

substitution of Equation D.5 into Equation D.2 yields

$$\sigma_{33}^{\wedge} \ (x_3 = R + \delta/2) = \sigma_0 \ \Big\{ [1 - (1/2\pi - \overline{z}_2) \ \sec \ (\overline{z}_2)] \ +$$

$$(1/2\pi - \overline{z}_2) \ \sec \ (\overline{z}_2) \Big\} \quad , \ \rho_b \leq \overline{\rho}_b \tag{D.6}$$

The total force, F_b, transmitted by the binder is given by
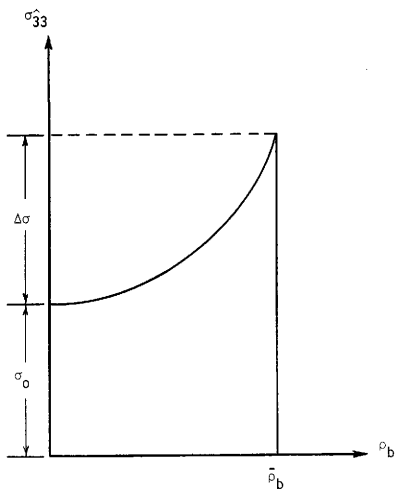
Figure D.3 -- Stress Distribution at Center of Mixture
Phase Which Acts as a Binder.

$$F_b = 2\pi \int_0^{\bar{\rho}_b} \hat{\sigma}_{33} \; (x_3 = R + \delta/2) \; \rho_s \; d \; \rho_s \qquad (D.7)$$

Integration of Equation D.7 yields the following relationship between the force F_b, and the constant σ_0

$$F_b = \pi \; \bar{\rho}_b^2 \; \sigma_0 \; [2/3 + (1/2\pi - \bar{\bar{z}}_2) \; \sec \; (\bar{\bar{z}}_2)] \qquad (D.8)$$

Through geometry considerations, the radius, $\bar{\rho}_b$, is determined to be

$$\bar{\rho}_b = [R + \delta/2] \; [\tan \; (\bar{\bar{z}}_2) - \sec \; (\bar{\bar{z}}_2)] + R \qquad (D.9)$$

Equations D.1 and D.8 may be used to relate the constant σ_0 to the relative displacement between spheres, δ.

   To determine the surface tractions which result on the surface of the sphere, the strip of the binder material shown in Figure D.4 is considered. The loads acting on the sides of the ring will be assumed to be self-equilibrating in the x_3 coordinate direction. The coordinates, ρ_b and ρ_s, define the position of the ring with respect to the x_3 axis on the plane, $x_3 = R + \delta/2$, and the surface of the sphere, respectively. The relationship between the coordinates, ρ_b and ρ_s, is

$$\frac{\rho_b}{\bar{\rho}_b} = \frac{\rho_s}{\bar{\rho}_s} \qquad (D.10)$$

where

$$\bar{\rho}_s = R \sin \; (\bar{\bar{z}}_2) \qquad (D.11)$$

and $\bar{\rho}_b$ is given by Equation D.9. The force dF_b, shown in Figure D.4 acts parallel to the x_3 coordinate axis on the plane, $x_3 = R + \delta/2$. The magnitude of dF_b is
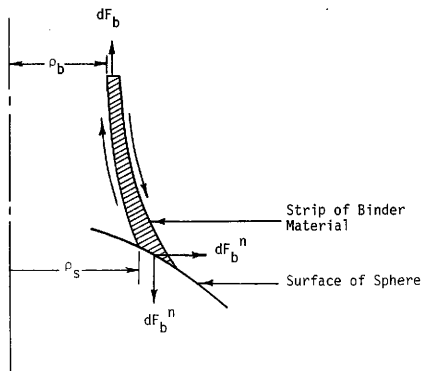
Figure D.4 -- Forces Acting on Strip of Binder Material.

$$dF_b = \hat{\sigma}_{33} \ (x_3 = R + \delta/2) \quad \rho_b \ d\rho_b \ d\theta_c \qquad (D.12)$$

where

$d\theta_c$ = an infinitesimal rotation about the x_3 coordinate axis. The vertical force, dF_s^V, acting on the strip because of cohesion of the binder to the surface of the sphere must be such that equilibrium in the x_3 coordinate direction is satisfied. Therefore, dF_s^V is given by

$$dF_s^V = dF_b = \hat{\sigma}_{33} \ (x_3 = R \sin (\bar{z}_2)\rho_s \ d\rho_s \ d\theta_c \qquad (D.13)$$

Combining Equations D.10, D.13, and D.14 give the following stress distribution acting on the surface of the sphere.

$$\hat{\sigma}_{33} \ (x_3 = R \sin (\bar{z}_2)) = \left(\frac{\bar{\rho}_b}{\bar{\rho}_s}\right)^2 \ \hat{\sigma}_{33} \ (x_3 = R + \delta/2) \qquad (D.14)$$

Combining Equations D.6, D.10 and D.14 gives the following expression for the stress, $\hat{\sigma}_{33}$, acting on the surface of the sphere.

$$\sigma_{33} \ (x_3 = R \sin (\bar{z}_2)) = \sigma_o \ \left(\frac{\bar{\rho}_b}{\bar{\rho}_b}\right)^2 \left\{ \ [1 - (1/2\pi - \bar{z}_2) \sec(\bar{z}_2)] \right.$$

$$\left. \sqrt{1 - (\rho_s/\bar{\rho}_s)^2} \ + (1/2\pi - \bar{z}_2) \sec (\bar{z}_2) \right\} \ , \ \rho_b \leq \bar{\rho}_b \qquad (D.15)$$

As shown in Figure D.3, the total force, dF_s, on the lower portion of the strip acts at an angle, θ_F, to the $x_3 = R \sin(\bar{z}_2)$, plane. The horizontal component of this force is determined as

$$F_s^{\,h} = F_s^{\,v} \cot \theta_F \tag{D.16}$$

The force $F_s^{\,h}$ will cause a compressive stress to be exerted on the sphere by the binder material. This stress will act in the ρ_s coordinate direction. This stress is given by

$$\sigma_{\rho\rho}\,(x_3 = R \sin(\bar{z}_2)) \;=\; \frac{-\,F_s^{\,h}}{\rho_s\,d\theta_c\,dx_3} \tag{D.17}$$

Combining equations D.13, D.15, D.16, and D.17 yields

$$\sigma_{\rho\rho}\,(x_3 = R \sin(\bar{z}_2)) \;=\; -\sigma_o \left(\frac{\bar{\rho}_b}{\bar{\rho}_s}\right)^2 \cot^2\theta_F \Bigg\{ \;\; [1 - (1/2\pi - \bar{z}_2)$$

$$\sqrt{1 - (\rho_s/\bar{\rho}_s)^2} + (1/2\pi - \bar{z}_2)\,\sec(\bar{z}_2) \Bigg\} \;,\; \rho_s \leq \bar{\rho}_s \tag{D.18}$$

The angle, θ_F, will vary from $\delta/2$ at $\rho_s = 0$ to $\bar{z}_2$ at $\rho_s = R \sin(\bar{z}_2)$. It will be assumed that the angle, θ_F, is closely approximated as

$$\theta_F \cong \frac{\pi}{2} - \left(\frac{\pi}{2} - \bar{z}_2\right)(\bar{z}_2/\bar{z}_2)^2 \tag{D.19}$$

The stress components given by Equations D.15 and D.18 are the surface tractions exerted on the sphere by the binder. The stress components relative to the spherical coordinate system, (z_1, z_2, z_3), as shown in Figure 3.8, will be determined. The non-zero components of the stress tensor relative to this coordinate system, which act on the surface of the sphere are

$$\sigma'_{11} \ (z_1 = R) \ = \sigma_{33} \ (x_3 = R \sin (z_2)) \cos^2 (z_2) +$$
$$\sigma_{\rho\rho} \ (x_3 = R \sin (z_2)) \sin^2 (z_2)$$
$$, \ 0 \le z_2 \le \bar{z}_2 \tag{D.20}$$

$$\sigma_{12} \ (z_1 = R) = - [\sigma_{33} \ (x_3 = R \sin (z_2)) -$$
$$\sigma_{\rho\rho} \ (x_3 = R \sin (z_2))] \sin (z_2)$$
$$\cos (z_2) \ 0 \le \bar{z}_2 \le \bar{z}_2 \tag{D.21}$$

where

σ'_{ij} = the components of the stress tensor relative to the (z_1, z_2, z_3) coordinate axes.

Combining Equations D.15, D.18, D.20 and D.21 yields the following expressions for the surface stresses on the sphere.

$$\sigma'_{11} (z_1 = R) = \sigma_0 \left(\frac{\bar{\rho}_b}{\bar{\rho}_s}\right)^2 [\cos^2(z_2) - \cot^2(\theta_f)\sin^2(z_2)]$$

$$\left\{ [1 - (\tfrac{1}{2}\pi - \bar{z}_2) \sec(\bar{z}_2)]\csc(\bar{z}_2) \sqrt{\cos^2(z_2) - \cos^2(\bar{z}_2)} \right.$$

$$\left. + (\tfrac{1}{2}\pi - \bar{z}_2) \sec(\bar{z}_2) \right\} , \ 0 \leq z_2 \leq \bar{z}_2 \qquad\qquad (D.22)$$

$$\sigma'_{12} (z_1 = R) = \sigma_0 \left(\frac{\bar{\rho}_b}{\bar{\rho}_s}\right)^2 \csc^2(\bar{z}_2) \left\{ [1 - (\tfrac{1}{2}\pi - \bar{z}_2) \right.$$

$$\sec(\bar{z}_2)] \csc(\bar{z}_2) \sqrt{\cos^2(z_2) - \cos^2(\bar{z}_2)} + (\tfrac{1}{2}\pi - \bar{z}_2) \sec(\bar{z}_2) \right\}$$

$$\sin(z_2) \cos(z_2), \ 0 \leq z_2 \leq \bar{z}_2 \qquad\qquad (D.23)$$

Equations D.22 and D.23 are the approximate solution to the non-zero components of the stress tensor, σ'_{ij}, which act on the surface of a sphere, due to the cohesion of the sphere with the binder material.

APPENDIX E

Contained is a copy of a computer program which may be used to calculate the dimensionless quantities required for the evaluation of the effective compliance and stiffness tensor.

THIS PROGRAM WILL CALCULATE INTERACTION AND NON-INTERACTION CONSTANTS
REQUIRED FOR THE EVALUATION OF THE EFFECTIVE COMPLIANCE AND
STIFFNESS TENSORS. THIS VERSION OF THE PROGRAM IS SET UP FOR CONTACT
TYPE SURFACE TRACTIONS. IT MAY BE MODIFIED TO CONSIDER BINDER
SURFACE TRACTIONS OR BINDER-CONTACT INTERACTIONS. THIS MODIFICATION
REQUIRES USE OF THE SUBROUTINE BTCON TO REPLACE SUBROUTINE DTCON OR
FOR THE CASE OF BINDER TYPE SURFACE TRACTIONS OR USE OF SUBROUTINE
BTCON IN CONJUNCTION WITH SUBROUTINE DTCON FOR BINDER-CONTACT
INTERACTIONS.

```
      IMPLICIT REAL*8(A-H,O-Z)
      REAL*8 EC1(70),DEC1(70),DDEC1(70),ZNC1(70),DNC1(70),DDNC1(70)
      REAL*8 EC(70),DEC(70),DDEC(70),ZNC(70),DNC(70),DDNC(70),ANC(68)
      REAL*8 DANC(68),DDANC(68),DBNC(68),BNC(68),DDBNC(68),CNANG1(2)
      REAL*8 CNANG2(2),TRANRR(3,3),SCORD(1728,4),TRANSR(3,3),TT(4)
      REAL*8 DTT(4),DDTT(4),T(1728,6),DT(1728,6),DDT(1728,6),E(1728,6)
      REAL*8 DE(1728,6),DDE(1728,6),EE(4),DEE(4),DDEE(4)
      DO 5 I=1,1728
      READ(1,100)(SCORD(I,J),J=1,4)
    5 CONTINUE
  100 FORMAT(1X,4(2X,E15.8))
      CNANG1(1)=0.
      CNANG1(2)=0.
      CNANG2(1)=3.14159/3.*2.
      CNANG2(2)=0.
      WRITE(2,150)CNANG1(1),CNANG1(2),CNANG2(1),CNANG2(2)
  150 FORMAT(' ','ANG(1,1) = ',F6.2,/,' ','ANG(1,2) = ',F6.2,
     /,' ','ANG(2,1) = ',F6.2,/,' ','ANG(2,2) = ',F6.2,/,/,/)
      ANG1=0.0
      DO 50 II=1,8
      ANG1=ANG1+1.
      CANG1=DCOS(ANG1*3.14159/180)
      CALL DTCON(CANG1,EC1,DEC1,DDEC1,ZNC1,DNC1,DDNC1)
      DO 40 I=1,11
      NSFLG=0
      POIS=(I-1)*.05
      IF (POIS.EQ..5) POIS=.499
      CALL COFSUP(POIS,EC1,DEC1,DDEC1,ZNC1,DNC1,DDNC1,ANC,DANC,DDANC,
      BNC,DBNC,DDBNC)
      CALL GTRANS(CNANG1,TRANRR)
      DO 10 J=1,1728
      CALL LCOORD(SCORD(J,1),SCORD(J,2),SCORD(J,3),TRANRR,SCRD1,SCRD2,
      SCRD3)
```

```
      CALL TRNSSR(SCRD1,SCRD2,SCRD3,TRANRR,TRANSR)
      CALL NONDIM(NSFLG,SCRD1,SCRD2,ANC,DANC,DDANC,BNC,DBNC,
      DDBNC,POIS,TT,DTT,DDTT)
      CALL CGLOB(J,TT,DTT,DDTT,TRANSR,TRANRR,T,DT,DDT)
   10 CONTINUE
      NSFLG=1
      ANG2=0.
      DO 30 J=1,8
      ANG2=ANG2+1.
      CANG2=DCOS(ANG2*3.14159/180)
      CALL DTCON(CANG2,EC,DEC,DDEC,ZNC,DNC,DDNC)
      CALL COFSUP(POIS,EC,DEC,DDEC,ZNC,DNC,DDNC,ANC,DANC,DDANC,BNC,DBNC,
      DDBNC)
      CALL GTRANS(CNANG2,TRANRR)
      DO 20 K=1,1728
      CALL LCOORD(SCORD(K,1),SCORD(K,2),SCORD(K,3),TRANRR,SCRD1,SCRD2,
      SCRD3)
      CALL TRNSSR(SCRD1,SCRD2,SCRD3,TRANRR,TRANSR)
      CALL NONDIM(NSFLG,SCRD1,SCRD2,ANC,DANC,DDANC,BNC,DBNC,
      DDBNC,POIS,EE,DEE,DDEE)
      CALL CGLOB(K,EE,DEE,DDEE,TRANSR,TRANRR,E,DE,DDE)
   20 CONTINUE
      CALL ENCON(J,ANG1,ANG2,POIS,SCORD,T,DT,DDT,E,DE,DDE)
   30 CONTINUE
   40 CONTINUE
   50 CONTINUE
      STOP
      END
      SUBROUTINE DTCON(CANG,EC,DEC,DDEC,ZNC,DNC,DDNC)
      IMPLICIT REAL*8(A-H,O-Z)
      REAL*8 EC(70),DEC(70),DDEC(70),ZNC(70),DNC(70),DDNC(70),XIP(80)
      REAL*8 YIP(80),TPN(140),TDPN(140),F1(80,70),F2(80,70),F3(80,70)
      REAL*8 F5(80,70),F6(80,70),PN(140),DPN(140),DDPN(140),WGT(80)
      REAL*8 F4(80,70)
C
C     ASSIGN INTEGRATION POINTS ON INTERVAL -1 TO 1. USE EIGHTY POINT
C     GAUSSIAN INTERGRATION.
C
      XIP(1)=.0195113832
      XIP(3)=.0585044371
      XIP(5)=.0974083984
      XIP(7)=.1361640228
      XIP(9)=.1747122918
      XIP(11)=.2129945028
      XIP(13)=.2509523583
      XIP(15)=.2885280548
      XIP(17)=.3256643707
      XIP(19)=.3623047534
      XIP(21)=.3983934058
      XIP(23)=.4338753708
      XIP(25)=.4686966151
      XIP(27)=.5028041118
```

```
      XIP(29)=.5361459208
      XIP(31)=.5686712681
      XIP(33)=.6003306228
      XIP(35)=.6310757730
      XIP(37)=.6608598989
      XIP(39)=.6896376443
      XIP(41)=.7173651853
      XIP(43)=.7440002975
      XIP(45)=.7695024201
      XIP(47)=.7938327175
      XIP(49)=.8169541386
      XIP(51)=.8388314735
      XIP(53)=.8594314066
      XIP(55)=.8787225676
      XIP(57)=.8966755794
      XIP(59)=.9132631025
      XIP(61)=.9284598771
      XIP(63)=.9422427613
      XIP(65)=.9545907663
      XIP(67)=.9654850890
      XIP(69)=.9749091405
      XIP(71)=.9828485727
      XIP(73)=.9892913024
      XIP(75)=.9942275409
      XIP(77)=.9976498643
      XIP(79)=.9995538226
C
C ASSIGN WEIGHT VALUES
C
      WGT(1)=.0390178136
      WGT(3)=.0389583959
      WGT(5)=.0388396510
      WGT(7)=.0386617597
      WGT(9)=.0384249930
      WGT(11)=.0381297113
      WGT(13)=.0377763643
      WGT(15)=.0373654902
      WGT(17)=.0368977146
      WGT(19)=.0363737499
      WGT(21)=.0357943939
      WGT(23)=.0351605290
      WGT(25)=.0344731204
      WGT(27)=.0337332149
      WGT(29)=.0329419393
      WGT(31)=.0321004986
      WGT(33)=.0312101741
      WGT(35)=.0302723217
      WGT(37)=.0292883695
      WGT(39)=.0282598160
      WGT(41)=.0271882275
      WGT(43)=.0260752357
      WGT(45)=.0249225357
```

```
      WGT(47)=.0237318828
      WGT(49)=.0225050902
      WGT(51)=.0212440261
      WGT(53)=.0199506108
      WGT(55)=.0186268142
      WGT(57)=.0172746520
      WGT(59)=.0158961835
      WGT(61)=.0144935080
      WGT(63)=.0130687615
      WGT(65)=.0116241141
      WGT(67)=.0101617660
      WGT(69)=.0086839452
      WGT(71)=.0071929047
      WGT(73)=.0056909224
      WGT(75)=.0041803131
      WGT(77)=.0026635335
      WGT(79)=.0011449500
C
C   ASSIGN INTEGRATION POINTS AND WEIGHTS TO EVEN ARRAY ELEMENTS
C
      DO 5 I=2,80,2
      XIP(I)=(-1)*XIP(I-1)
      WGT(I)=WGT(I-1)
    5 CONTINUE
C
C     INTERPOLATE TO DETERMINE INTEGRATION POINTS ON THE INTERVAL OF
C     INTEREST
C
      DO 10 I=1,80
      YIP(I)=(1-CANG)*XIP(I)/2.+(1+CANG)/2.
   10 CONTINUE
C
C     CALL SUBROUTINE TO DETERMINE VALUE OF LEGRENDRE POLYNOMINALS AND
C     DERIVATIVES EVALUATED AT 1.
C
      ARG=1.
      CALL POLY(ARG,TPN,TDPN)
C
C     DETERMINE INTEGRALS REQUIRED FOR EVALUATION OF THE CONSTANTS
C     RESULTING FROM THE STRESS BOUNDARY CONDITIONS FOR SPHERES IN
C     CONTACT.
C
      DO 30 I=1,80
C
C     CALL SUBROUTINE TO DETERMINE LEGRENDRE POLYNOMINALS AND DERIVATIVES
C     EVALUATED AT INTEGRATION POINT YIP(I).
C
      ARG=YIP(I)
      CALL POLY(ARG,PN,DPN)
      CALL DDPOLY(ARG,DPN,DDPN)
C
C     EVALUATE FUNCTIONS CONTAINED IN INTEGRALS.
```

```
C
      DO 20 J=1,70
      K=2*J-1
      F1(I,J)=DSQRT(YIP(I)**2-CANG**2)*YIP(I)**2*PN(K)
      F2(I,J)=DSQRT(YIP(I)**2-CANG**2)*(1-YIP(I)**2)*YIP(I)*DPN(K)
      F3(I,J)=DSQRT(YIP(I)**2-CANG**2)*(PN(K)+YIP(I)*DPN(K))
      F4(I,J)=DLOG((DSQRT(YIP(I)**2-CANG**2)+YIP(I))/CANG)*(2*
      DPN(K)+YIP(I)*DDPN(K))
      F5(I,J)=DSQRT(YIP(I)**2-CANG**2)*PN(K)
      F6(I,J)=DLOG((DSQRT(YIP(I)**2-CANG**2)+YIP(I))/CANG)*DPN(K)
   20 CONTINUE
   30 CONTINUE
C
C     ZERO OUT ARRAYS CONTAINING CONSTANTS.
C
      DO 40 I=1,70
      EC(I)=0.
      DEC(I)=0.
      DDEC(I)=0.
      ZNC(I)=0.
      DNC(I)=0.
      DDNC(I)=0.
   40 CONTINUE
C
C     DETERMINE CONSTANTS.
C
      DO 60 I=1,70
      K=2*I-1
      L=I-1
      DO 50 J=1,80
      EC(I)=EC(I)+(1-CANG)/2.*WGT(J)*F1(J,I)
      DEC(I)=DEC(I)+(1-CANG)/2.*WGT(J)*F3(J,I)
      DDEC(I)=DDEC(I)+(1-CANG)/2.*WGT(J)*F4(J,I)
      IF(I.EQ.1) GOTO 50
      ZNC(I)=ZNC(I)+(1-CANG)/2.*WGT(J)*F2(J,I)
      DNC(I)=DNC(I)+(1-CANG)/2.*WGT(J)*F5(J,I)
      DDNC(I)=DDNC(I)+(1-CANG)/2.*WGT(J)*F6(J,I)
   50 CONTINUE
      EC(I)=EC(I)*(4*L+1)*(-1)
      DEC(I)=(DEC(I)*(-1)+DSQRT(1-CANG**2))*CANG*(4*L+1)
      DDEC(I)=(DDEC(I)*(-1)-1./DSQRT(1-CANG**2)+(1+TDPN(K))*DLOG((DSQRT
      (1-CANG**2)+1.)/CANG))*(4*L+1)*CANG**2+DEC(I)/CANG
      IF(I.EQ.1) GOTO 60
      ZNC(I)=ZNC(I)*(4*L+1)/4./L/(2*L+1)
      DNC(I)=DNC(I)*(4*L+1)*CANG/2.*(-1)
      DDNC(I)=(DDNC(I)*(-1)+DLOG((DSQRT(1.-CANG**2)+1.)/CANG))*(4*L+1)*
      CANG**2/2.+DNC(I)/CANG
   60 CONTINUE
      RETURN
      END
      SUBROUTINE COFSUP(POIS,EC,DEC,DDEC,ZNC,DNC,DDNC,
      ANC,DANC,DDANC,BNC,DBNC,DDBNC)
```

```
      IMPLICIT REAL*8(A-H,O-Z)
      REAL*8 EC(70),DEC(70),DDEC(70),ZNC(70),DNC(70),DDNC(70),ANC(68)
      REAL*8 DDANC(68),BNC(68),DBNC(68),DDBNC(68),DANC(68)
C
C     DETERMINE COEFFICIENTS OF SUPERPOSITION FOR STRESS SOLUTION
C
      DO 20 I=1,68
      J=I-1
      A1=(4*I**2+4*I-1+2*POIS)/2./(2*I-1)/(4*I**2+2*I+1+(4*I+1)*POIS)
      A2=2.*(2*I+1)*(2*I**2-I-1-POIS)/2./(2*I-1)/(4*I**2+2*I+1+(4*I+1)
     *POIS)
      B1=1./2./(4*J**2+2*J+1+(4*J+1)*POIS)
      B2=2*J/2./(4*J**2+2*J+1+(4*J+1)*POIS)
      ANC(I)=A1*EC(I+1)+A2*ZNC(I+1)
      DANC(I)=A1*DEC(I+1)+A2*DNC(I+1)
      DDANC(I)=A1*DDEC(I+1)+A2*DDNC(I+1)
      BNC(I)=B1*EC(I)+B2*ZNC(I)
      DBNC(I)=B1*DEC(I)+B2*DNC(I)
   20 DDBNC(I)=B1*DDEC(I)+B2*DDNC(I)
      RETURN
      END
      SUBROUTINE GTRANS(CNANG,TRANRR)
      IMPLICIT REAL*8(A-H,O-Z)
      REAL*8 CNANG(2),TRANRR(3,3)
C
C     DETERMINE TRANSFORMATION MATRIX TO GO FROM LOCAL RECTANGULAR
C     COORDINATES TO GLOBAL RECTANGULAR COORDINATES
C
      TRANRR(1,1)=DCOS(CNANG(1))*DCOS(CNANG(2))
      TRANRR(1,2)=DCOS(CNANG(1))*DSIN(CNANG(2))
      TRANRR(1,3)=-DSIN(CNANG(1))
      TRANRR(2,1)=-DSIN(CNANG(2))
      TRANRR(2,2)=DCOS(CNANG(2))
      TRANRR(2,3)=0.
      TRANRR(3,1)=DSIN(CNANG(1))*DCOS(CNANG(2))
      TRANRR(3,2)=DSIN(CNANG(1))*DSIN(CNANG(2))
      TRANRR(3,3)=DCOS(CNANG(1))
      RETURN
      END
      SUBROUTINE TRNSSR(SC1,SC2,SC3,TRANRR,TRANSR)
      IMPLICIT REAL*8(A-H,O-Z)
      REAL*8 TRANSR(3,3),TRANRR(3,3)
C
C     DETERMINE TRANSFORMATION MATRIX TO GO FROM LOCAL SPHERICAL
C     COORDINATES TO LOCAL RECTANGULAR COORDINATES
C
   80 TRANSR(1,1)=DSIN(SC2)*DCOS(SC3)
      TRANSR(1,2)=DSIN(SC2)*DSIN(SC3)
      TRANSR(1,3)=DCOS(SC2)
      TRANSR(2,1)=DCOS(SC2)*DCOS(SC3)
      TRANSR(2,2)=DCOS(SC2)*DSIN(SC3)
      TRANSR(2,3)=-DSIN(SC2)
```

```
      TRANSR(3,1)=-DSIN(SC3)
      TRANSR(3,2)=DCOS(SC3)
      TRANSR(3,3)=0.
      RETURN
      END
      SUBROUTINE NONDIM(NSFLG,SC1,SC2,ANC,DANC,DDANC,BNC,DBNC,
      DDBNC,POIS,TE,DTE,DDTE)
      IMPLICIT REAL*8(A-H,O-Z)
      REAL*8 BT(4),BE(4),DTE(4),AE(4)
      REAL*8 ANC(68),DANC(68),DDANC(68),BNC(68),DBNC(68)
      REAL*8 DDBNC(68),TE(4)
      REAL*8 DDTE(4)
      REAL*8 AT(4),PN(140),DPN(140)
C
C     CALL SUBROUTINE TO DETERMINE LEGRENDRE POLYNOMINALS AND THEIR
C     DERIVATIVES AT INTEGRATION POINT JJ
C
      ARG=DCOS(SC2)
      CALL POLY(ARG,PN,DPN)
C
C     DETERMINE NON-DIMENSIONALIZED QUANTITIES FOR INTEGRATION POINT
C     M, AND CONTACT N.
C
      DO 18 LK=1,4
      TE(LK)=0.
      DTE(LK)=0.
      DDTE(LK)=0.
   18 CONTINUE
      DO 30 I=1,68
      J=I-1
      K=I+1
      AT(1)=2*I*(2*I-1)*PN(2*I+1)
      AT(2)=DPN(2*I)-2*I*(2*I-1)*PN(2*I+1)
      AT(3)=DPN(2*I)*(-1)
      AT(4)=(-1)*(2*I-1)*DSIN(SC2)*DPN(2*I+1)
      AE(1)=.5*AT(1)
      AE(2)=.5*AT(2)
      AE(3)=.5*AT(3)
      AE(4)=.5*AT(4)
      BT(1)=(-1)*(2*J+1)*((2*J+1)*(2*J-2)-2*POIS)*PN(2*I-1)
      BT(2)=((2*J+1)*(4*J**2+10*J+7-2*POIS)*PN(2*I-1)-(2*J+5-4*POIS)
      *DPN(2*I))
      BT(3)=(2*J+5-4*POIS)*DPN(2*I)-(4*J+3)*(2*J+1)*(1-2*POIS)*
      PN(2*I-1)
      BT(4)=(4*J**2+4*J-1+2*POIS)*DSIN(SC2)*DPN(2*I-1)
      BE(1)=(-.5)*(2*J+1)**2*(2*J-2+4*POIS)*PN(2*I-1)
      BE(2)=(-.5)*((2*J+5-4*POIS)*DPN(2*I)-(2*J+1)*((2*J+1)**2+2*
      (J+1)*(3-4*POIS))*PN(2*I-1))
      BE(3)=(-.5)*((4*J+3)*(2*J+1)*PN(2*I-1)-(2*J+5-4*POIS)*DPN(2*I))
      BE(4)=.5*BT(4)
      DO 60 L=1,4
      IF(NSFLG.EQ.1) GOTO 20
```

```
C
C   DETERMINE STRESSES IN SPHERICAL COORDINATES
C
      TE(L)=TE(L)+SC1**(2*J)*(ANC(I)*
     AT(L)+BNC(I)*BT(L))
      DTE(L)=DTE(L)+SC1**(2*J)*(DANC(I)*
     AT(L)+DBNC(I)*BT(L))
      DDTE(L)=DDTE(L)+SC1**(2*J)*(DDANC(I)*
     AT(L)+DDBNC(I)*BT(L))
      GOTO 60
C
C   DETERMINE STRAINS IN SPHERICAL COORDINATES
C
   20 TE(L)=TE(L)+SC1**(2*J)*(ANC(I)*
     AE(L)+BNC(I)*BE(L))
      DTE(L)=DTE(L)+SC1**(2*J)*(DANC(I)*
     AE(L)+DBNC(I)*BE(L))
      DDTE(L)=DDTE(L)+SC1**(2*J)*
     (DDANC(I)*AE(L)+DDBNC(I)*BE(L))
   60 CONTINUE
   30 CONTINUE
      RETURN
      END
      SUBROUTINE CGLOB(JJ,TE,DTE,DDTE,TRANSR,TRANRR,GTE,DGTE,DDGTE)
      IMPLICIT REAL*8(A-H,O-Z)
      REAL*8 TE(4),DTE(4),DDTE(4),TRANSR(3,3)
      REAL*8 TRANRR(3,3),GTE(1728,6),DGTE(1728,6)
      REAL*8 TMAT(3,3),TMAT1(3,3)
      REAL*8 TMAT2(3,3),TMAT3(3,3)
C
C   ZERO OUT TEMPORARY ARRAYS AND GLOBAL ARRAYS
C
      DO 10 I=1,3
      DO 5 J=1,3
      TMAT(I,J)=0.
      TMAT1(I,J)=0.
      TMAT2(I,J)=0.
      TMAT3(I,J)=0.
    5 CONTINUE
   10 CONTINUE
      DO 35 I=1,6
      GTE(JJ,I)=0.
      DGTE(JJ,I)=0.
      DDGTE(JJ,I)=0.
   35 CONTINUE
C
C   DETERMINE TEMPORARY ARRAY TMAT(  ) AS THE PRODUCT OF THE
C   TRANSFORMATION MATRICES.
C
      DO 50 I=1,3
      DO 45 J=1,3
      DO 40 K=1,3
```

```
   40 TMAT(I,J)=TMAT(I,J)+TRANSR(I,K)*TRANRR(K,J)
   45 CONTINUE
   50 CONTINUE
C
C     DETERMINE ARRAY TAMT4( ) TO PRE MULTIPLY STRESS AND STRAIN TENSORS
C
      DO 54 I=1,3
      DO 52 J=1,3
   52 TRANSR(J,I)=TMAT(I,J)
   54 CONTINUE
C
C     DETERMINE GLOBAL QUANTITIES
C
      DO 60 I=1,3
      TMAT1(I,1)=TRANSR(I,1)*TE(1)+TRANSR(I,2)*TE(4)
      TMAT2(I,1)=TRANSR(I,1)*DTE(1)+TRANSR(I,2)*DTE(4)
      TMAT3(I,1)=TRANSR(I,1)*DDTE(1)+TRANSR(I,2)*DDTE(4)
      TMAT1(I,2)=TRANSR(I,1)*TE(4)+TRANSR(I,2)*TE(2)
      TMAT2(I,2)=TRANSR(I,1)*DTE(4)+TRANSR(I,2)*DTE(2)
      TMAT3(I,2)=TRANSR(I,1)*DDTE(4)+TRANSR(I,2)*DDTE(2)
      TMAT1(I,3)=TRANSR(I,3)*TE(3)
      TMAT2(I,3)=TRANSR(I,3)*DTE(3)
      TMAT3(I,3)=TRANSR(I,3)*DDTE(3)
   60 CONTINUE
      GTE(JJ,1)=TMAT1(1,1)*TMAT(1,1)+TMAT1(1,2)*TMAT(2,1)+TMAT1(1,3)*
     TMAT(3,1)
      DGTE(JJ,1)=TMAT2(1,1)*TMAT(1,1)+TMAT2(1,2)*TMAT(2,1)+TMAT2(1,3)*
     TMAT(3,1)
      DDGTE(JJ,1)=TMAT3(1,1)*TMAT(1,1)+TMAT3(1,2)*TMAT(2,1)+TMAT3(1,3)*
     TMAT(3,1)
      GTE(JJ,4)=TMAT1(1,1)*TMAT(1,2)+TMAT1(1,2)*TMAT(2,2)+TMAT1(1,3)*
     TMAT(3,2)
      GTE(JJ,2)=TMAT1(2,1)*TMAT(1,2)+TMAT1(2,2)*TMAT(2,2)+TMAT1(2,3)*
     TMAT(3,2)
      DGTE(JJ,4)=TMAT2(1,1)*TMAT(1,2)+TMAT2(1,2)*TMAT(2,2)+TMAT2(1,3)*
     TMAT(3,2)
      DGTE(JJ,2)=TMAT2(2,1)*TMAT(1,2)+TMAT2(2,2)*TMAT(2,2)+TMAT2(2,3)*
     TMAT(3,2)
      DDGTE(JJ,4)=TMAT3(1,1)*TMAT(1,2)+TMAT3(1,2)*TMAT(2,2)+TMAT3(1,3)*
     TMAT(3,2)
      DDGTE(JJ,2)=TMAT3(2,1)*TMAT(1,2)+TMAT3(2,2)*TMAT(2,2)+TMAT3(2,3)*
     TMAT(3,2)
      GTE(JJ,5)=TMAT1(1,1)*TMAT(1,3)+TMAT1(1,2)*TMAT(2,3)+TMAT1(1,3)*
     TMAT(3,3)
      GTE(JJ,6)=TMAT1(2,1)*TMAT(1,3)+TMAT1(2,2)*TMAT(2,3)+TMAT1(2,3)*
     TMAT(3,3)
      GTE(JJ,3)=TMAT1(3,1)*TMAT(1,3)+TMAT1(3,2)*TMAT(2,3)+TMAT1(3,3)*
     TMAT(3,3)
      DGTE(JJ,5)=TMAT2(1,1)*TMAT(1,3)+TMAT2(1,2)*TMAT(2,3)+TMAT2(1,3)*
     TMAT(3,3)
      DGTE(JJ,6)=TMAT2(2,1)*TMAT(1,3)+TMAT2(2,2)*TMAT(2,3)+TMAT2(2,3)*
     TMAT(3,3)
```

```
      DGTE(JJ,3)=TMAT2(3,1)*TMAT(1,3)+TMAT2(3,2)*TMAT(2,3)+TMAT2(3,3)*
     TMAT(3,3)
      DDGTE(JJ,5)=TMAT3(1,1)*TMAT(1,3)+TMAT3(1,2)*TMAT(2,3)+TMAT3(1,3)*
     TMAT(3,3)
      DDGTE(JJ,6)=TMAT3(2,1)*TMAT(1,3)+TMAT3(2,2)*TMAT(2,3)+TMAT3(2,3)*
     TMAT(3,3)
      DDGTE(JJ,3)=TMAT3(3,1)*TMAT(1,3)+TMAT3(3,2)*TMAT(2,3)+TMAT3(3,3)*
     TMAT(3,3)
      RETURN
      END
      SUBROUTINE ENCON(JJ,ANG1,ANG2,POIS,SCORD,T,DT,DDT,E,DE,DDE)
      IMPLICIT REAL*8(A-H,O-Z)
      REAL*8 SCORD(1728,4),T(1728,6),DT(1728,6),DDT(1728,6),E(1728,6)
      REAL*8 DE(1728,6),DDE(1728,6)
      U=0.
      DU1=0.
      DU2=0.
      DDU1=0.
      DDU12=0.
      DDU2=0.
      DO 20 I=1,1728
      TEMP=.5*SCORD(I,4)*3./4./3.14159
      DO 10 J=1,6
      IF(J.EQ.4) TEMP=TEMP*2
      U=U+T(I,J)*E(I,J)*TEMP
      DU1=DU1+DT(I,J)*E(I,J)*TEMP
      DU2=DU2+T(I,J)*DE(I,J)*TEMP
      DDU1=DDU1+DDT(I,J)*E(I,J)*TEMP
      DDU12=DDU12+DT(I,J)*DE(I,J)*TEMP
      DDU2=DDU2+T(I,J)*DDE(I,J)*TEMP
   10 CONTINUE
   20 CONTINUE
      IF(JJ.NE.1) GOTO 30
      WRITE(2,100)
      WRITE(2,200)ANG1,POIS
      WRITE(2,300)
   30 CONTINUE
      WRITE(2,400)ANG2,U,DU1,DU2,DDU1,DDU12,DDU2
  100 FORMAT('1',T10,'INTERACTION ENERGY CONSTANTS')
  200 FORMAT(' ',T10,'ANGLE 1:',F5.2,/,' ',T10,'POISSOINS RATIO:',F5.3)
  300 FORMAT('0',T34,'DU',T48,'DU',T61,'DDU',T75,'DDU',T91,'DDU',/,' ',
     T2,'ANGLE 2',T21,'U',T33,'DC1',T47,'DC2',T61,'DC1',T75,'DC12',
     T91,'DC2')
  400 FORMAT(' ',T3,F5.2,T10,6(2X,E12.5))
      RETURN
      END
      SUBROUTINE POLY(ARG,PN,DPN)
      IMPLICIT REAL*8(A-H,O-Z)
      REAL*8 PN(140),DPN(140)
C
C     DETERMINE LEGRENDRE POLYNOMINALS
C
```

```
      PN(1)=1.
      PN(2)=ARG
      DO 10 I=3,140
      J=I-1
   10 PN(I)=((2*J-1)*ARG*PN(J)-(J-1)*PN(J-1))/J
C
C      DETERMINE DERIVATIVES OF LEGRENDRE POLYNOMINALS
C
      DPN(1)=0.
      DPN(2)=1.
      DO 20 I=3,140
      J=I-1
   20 DPN(I)=((2*J-1)*(PN(J)+ARG*DPN(J))-(J-1)*DPN(J-1))/J
      RETURN
      END
      SUBROUTINE DDPOLY(ARG,DPN,DDPN)
      IMPLICIT REAL*8(A-H,O-Z)
      REAL*8 DPN(140),DDPN(140)
      DDPN(1)=0.
      DDPN(2)=0.
      DO 10 I=3,140
      J=I-1
      DDPN(I)=((2*J-1)*(2*DPN(J)+ARG*DDPN(J))-(J-1)*DDPN(J-1))/J
   10 CONTINUE
      RETURN
      END
      SUBROUTINE LCOORD(SC1,SC2,SC3,TRANRR,SCRD1,SCRD2,SCRD3)
      IMPLICIT REAL*8 (A-H,O-Z)
      REAL*8 TRANRR(3,3)
C
C  DETERMINE GLOBAL RECTANGULAR COORDINATES
C
      X1=SC1*DSIN(SC2)*DCOS(SC3)
      X2=SC1*DSIN(SC2)*DSIN(SC3)
      X3=SC1*DCOS(SC2)
C
C  DETERMINE LOCAL RECTANGULAR COORDINATES
C
      Z1=X1*TRANRR(1,1)+X2*TRANRR(1,2)+X3*TRANRR(1,3)
      Z2=X1*TRANRR(2,1)+X2*TRANRR(2,2)+X3*TRANRR(2,3)
      Z3=X1*TRANRR(3,1)+X2*TRANRR(3,2)+X3*TRANRR(3,3)
C
C  DETERMINE LOCAL SPHERICAL COORDINATES
C
      SCRD1=DSQRT(Z1**2+Z2**2+Z3**2)
      SCRD2=DARCOS(Z3/SCRD1)
      SCRD3=DATAN2(Z2,Z1)
      RETURN
      END
```

BELOW IS A LISTING OF SUBROUTINE BTCON. THIS SUBROUTINE IS
USED WHEN DETERMINING NON-DIMENSIONALIZED QUANTITIES FOR
BINDER TYPE SURFACE TRACTIONS. THIS SUBROUTINE REPLACES
SUBROUTINE DTCON WHEN ONLY BINDER TYPE SURFACE TRACTIONS ARE
CONSIDERED. THIS SUBROUTINE IS USED IN CONJUNCTION WITH
SUBROUTINE DTCON WHEN BINDER-CONTACT INTERACTIONS ARE BEING
CONSIDERED.

```
      SUBROUTINE BTCON(CANG,EC,DEC,DDEC,ZNC,DNC,DDNC)
      IMPLICIT REAL*8(A-H,O-Z)
      REAL*8 EC(70),DEC(70),DDEC(70),ZNC(70),DNC(70),DDNC(70),XIP(80)
      REAL*8 YIP(80),TPN(140),TDPN(140),F1(80,70),F2(80,70),F3(80,70)
      REAL*8 F5(80,70),F6(80,70),PN(140),DPN(140),DDPN(140),WGT(80)
      REAL*8 F4(80,70)
C
C     ASSIGN INTEGRATION POINTS ON INTERVAL -1 TO 1. USE EIGHTY POINT
C     GAUSSIAN INTERGRATION.
C
      XIP(1)=.0195113832
      XIP(3)=.0585044371
      XIP(5)=.0974083984
      XIP(7)=.1361640228
      XIP(9)=.1747122918
      XIP(11)=.2129945028
      XIP(13)=.2509523583
      XIP(15)=.2885280548
      XIP(17)=.3256643707
      XIP(19)=.3623047534
      XIP(21)=.3983934058
      XIP(23)=.4338753708
      XIP(25)=.4686966151
      XIP(27)=.5028041118
      XIP(29)=.5361459208
      XIP(31)=.5686712681
      XIP(33)=.6003306228
      XIP(35)=.6310757730
      XIP(37)=.6608598989
      XIP(39)=.6896376443
      XIP(41)=.7173651853
      XIP(43)=.7440002975
      XIP(45)=.7695024201
      XIP(47)=.7938327175
      XIP(49)=.8169541386
```

```
      XIP(51)=.8388314735
      XIP(53)=.8594314066
      XIP(55)=.8787225676
      XIP(57)=.8966755794
      XIP(59)=.9132631025
      XIP(61)=.9284598771
      XIP(63)=.9422427613
      XIP(65)=.9545907663
      XIP(67)=.9654850890
      XIP(69)=.9749091405
      XIP(71)=.9828485727
      XIP(73)=.9892913024
      XIP(75)=.9942275409
      XIP(77)=.9976498643
      XIP(79)=.9995538226
C
C ASSIGN WEIGHT VALUES
C
      WGT(1)=.0390178136
      WGT(3)=.0389583959
      WGT(5)=.0388396510
      WGT(7)=.0386617597
      WGT(9)=.0384249930
      WGT(11)=.0381297113
      WGT(13)=.0377763643
      WGT(15)=.0373654902
      WGT(17)=.0368977146
      WGT(19)=.0363737499
      WGT(21)=.0357943939
      WGT(23)=.0351605290
      WGT(25)=.0344731204
      WGT(27)=.0337332149
      WGT(29)=.0329419393
      WGT(31)=.0321004986
      WGT(33)=.0312101741
      WGT(35)=.0302723217
      WGT(37)=.0292883695
      WGT(39)=.0282598160
      WGT(41)=.0271882275
      WGT(43)=.0260752357
      WGT(45)=.0249225357
      WGT(47)=.0237318828
      WGT(49)=.0225050902
      WGT(51)=.0212440261
      WGT(53)=.0199506108
      WGT(55)=.0186268142
      WGT(57)=.0172746520
      WGT(59)=.0158961835
      WGT(61)=.0144935080
      WGT(63)=.0130687615
      WGT(65)=.0116241141
      WGT(67)=.0101617660
```

```
      WGT(69)=.0086839452
      WGT(71)=.0071929047
      WGT(73)=.0056909224
      WGT(75)=.0041803131
      WGT(77)=.0026635335
      WGT(79)=.0011449500
C
C ASSIGN INTEGRATION POINTS AND WEIGHTS TO EVEN ARRAY ELEMENTS
C
      DO 5 I=2,80,2
      XIP(I)=(-1)*XIP(I-1)
      WGT(I)=WGT(I-1)
    5 CONTINUE
C
C     INTERPOLATE TO DETERMINE INTEGRATION POINTS ON THE INTERVAL OF
C     INTEREST
C
      DO 10 I=1,80
      YIP(I)=(1-CANG)*XIP(I)/2.+(1+CANG)/2.
   10 CONTINUE
C
C     CALL SUBROUTINE TO DETERMINE VALUE OF LEGRENDRE POLYNOMINALS AND
C     DERIVATIVES EVALUATED AT 1.
C
      ARG=1.
      CALL POLY(ARG,TPN,TDPN)
C
C     DETERMINE INTEGRALS REQUIRED FOR EVALUATION OF THE CONSTANTS
C     RESULTING FROM THE STRESS BOUNDARY CONDITIONS FOR SPHERES IN
C     CONTACT.
C
      DO 30 I=1,80
C
C     CALL SUBROUTINE TO DETERMINE LEGRENDRE POLYNOMINALS AND DERIVATIVES
C     EVALUATED AT INTEGRATION POINT YIP(I).
C
      ARG=YIP(I)
      CALL POLY(ARG,PN,DPN)
      CALL DDPOLY(ARG,DPN,DDPN)
C
C     EVALUATE FUNCTIONS CONTAINED IN INTEGRALS.
C
      DO 20 J=1,70
      K=2*J-1
      DIANG=DARCOS(CANG)
      KB=1./(1.-CANG**2)/(2./3.+(3.14159/2-DIANG)/CANG)
      HSARG=3.14159/2-(3.14159/2-DIANG)*(DARCOS(YIP(I))/DIANG)**2
      HS=1./(DTAN(HSARG))**2
      F1(I,J)=((1.+HS)*YIP(I)**2-HS)*((3.14159/2-DIANG)/CANG+1-
      DSQRT(YIP(I)**2-CANG**2))*PN(K)*KB
      F2(I,J)=(-1)*(1+HS)*((3.14159/2-DIANG)/CANG+1-DSQRT(YIP(I)**2-
      CANG**2))*(1.-YIP(I)**2)*YIP(I)*DPN(K)*KB
```

```
      F3(I,J)=F1(I,J)
      F4(I,J)=F1(I,J)
      F5(I,J)=F2(I,J)
      F6(I,J)=F2(I,J)
   20 CONTINUE
   30 CONTINUE
C
C     ZERO OUT ARRAYS CONTAINING CONSTANTS.
C
      DO 40 I=1,70
      EC(I)=0.
      DEC(I)=0.
      DDEC(I)=0.
      ZNC(I)=0.
      DNC(I)=0.
      DDNC(I)=0.
   40 CONTINUE
C
C     DETERMINE CONSTANTS.
C
      DO 60 I=1,70
      K=2*I-1
      L=I-1
      DO 50 J=1,80
      EC(I)=EC(I)+(1-CANG)/2.*WGT(J)*F1(J,I)
      DEC(I)=DEC(I)+(1-CANG)/2.*WGT(J)*F3(J,I)
      DDEC(I)=DDEC(I)+(1-CANG)/2.*WGT(J)*F4(J,I)
      IF(I.EQ.1) GOTO 50
      ZNC(I)=ZNC(I)+(1-CANG)/2.*WGT(J)*F2(J,I)
      DNC(I)=DNC(I)+(1-CANG)/2.*WGT(J)*F5(J,I)
      DDNC(I)=DDNC(I)+(1-CANG)/2.*WGT(J)*F6(J,I)
   50 CONTINUE
      EC(I)=EC(I)*(4*L+1)
      DEC(I)=DEC(I)*(4*L+1)
      DDEC(I)=DDEC(I)*(4*L+1)
      IF(I.EQ.1) GOTO 60
      ZNC(I)=ZNC(I)*(4*L+1)/4./L/(2*L+1)
      DNC(I)=DNC(I)*(4*L+1)/4./L/(2*L+1)
      DDNC(I)=DDNC(I)*(4*L+1)/4./L/(2*L+1)
   60 CONTINUE
      RETURN
      END
```

VITA

Mark Jackson Lamborn was born August 5, 1955 in Warren, Ohio. He graduated from Richard Montgomery High School, Rockville, Maryland in June of 1973. He entered Montgomery College, Rockville, Maryland in January 1976. He graduated in May 1978 with an Associate of Arts Degree in Civil Engineering Technology. Mark entered Texas A&M University, College Station, Texas in September 1978. He graduated in December 1981 with a Bachelor of Science Degree in Civil Engineering. He entered the graduate college of Texas A&M University in January of 1982. Mark is to receive his Master of Science Degree in Civil Engineering in December 1986.

Permanent Mailing Address:

5450 Township Rd. 103

Mount Gilead, Ohio 43338